Establishment of Functional Cannabinoid Receptor Test Systems and Evaluation of Ligands Derived from *Echinacea pallida*

Dissertation

zur Erlangung des Doktorgrades der Naturwissenschaften (Dr. rer. nat.)
der Naturwissenschaftlichen Fakultät IV – Chemie und Pharmazie –
der Universität Regensburg

vorgelegt von
Kathrin Nickl
aus Bayreuth

2008

Die vorliegende Arbeit entstand in der Zeit von Januar 2005 bis April 2008 unter der Leitung von Herrn Prof. Dr. J. Heilmann und Herrn Prof. Dr. R. Seifert am Institut für Pharmazie der Naturwissenschaftlichen Fakultät IV - Chemie und Pharmazie - der Universität Regensburg.

Das Promotionsgesuch wurde eingereicht im April 2008.

Tag der mündlichen Prüfung: 23. Mai 2008

Prüfungsausschuss:
Prof. Dr. J. Schlossmann (Vorsitzender)
Prof. Dr. J. Heilmann (Erstgutachter)
Prof. Dr. R. Seifert (Zweitgutachter)
Prof. Dr. B. König (Drittprüfer)

La prueba del pudín consiste en comer.

(Miguel de Cervantes: Don Quijote de la Mancha)

Danksagungen

An dieser Stelle möchte ich mich bedanken bei:

Prof. Dr. Jörg Heilmann für die Gelegenheit, an einem so interessanten und vielseitigen Projekt arbeiten zu dürfen, für seine wissenschaftlichen Anregungen sowie für seine ehrliche und freundliche Art und seine hilfreiche konstruktive Kritik beim Verfassen der phytochemischen Teile dieser Arbeit,

Prof. Dr. Roland Seifert für die Möglichkeit zur Durchführung der molekularpharmakologischen Untersuchungen, für seine kompetente fachliche Anleitung, wissenschaftliche Anregungen sowie für die hilfreiche konstruktive Kritik beim Verfassen der pharmakologischen Teile dieser Arbeit,

Prof. Dr. Sigurd Elz für die Bereitstellung eines Büro-Arbeitsplatzes,

Dr. Erich Schneider, Dr. Hendrik Preuss und David Schnell für ihre Hilfe bei pharmakologischen Problemstellungen und die [γ-^{32}P]GTP-Herstellung,

besonders Kerstin Fisch für ihre Hilfe bei zahlreichen Experimenten, insbesondere bei der Durchführung der GTPase Assays und bei dem Mahlen zahlreicher Wurzeldrogen,

Gertraud Wilberg für die Anfertigung von Western Blots und ihre Unterstützung auf dem Gebiet der Sf9-Zellkultur,

Astrid Seefeld für ihre Hilfe bei der Durchführung von AC Assays,

Gabriele Brunner für ihre stetige Hilfsbereitschaft bei Problemen jeder Art,

Sarah Geiger für ihre tatkräftige Unterstützung bei phytochemischen und pharmakologischen Arbeiten,

Eric Gardner für seine Unterstützung am Institut für Pharmakologie und Toxikologie,

Patrina Pellett und Michael Egger für die Synthese der Naturstoffe und die Hilfe bei chemischen Fragestellungen,

Gesine Bradacs, für ihre Hilfsbereitschaft und ihr offenes Ohr in allen Lebens- und Laborlagen,

Susanne Ohmayer, nicht nur für einige sehr wichtige Mausklicks,

meinen Kolleginnen und meinem Kollegen aus der Dom-Apotheke für viele schöne Stunden,

allen Freunden, die mich in den letzten Jahren unterstützt haben und deren Aufzählung hier den Rahmen sprengen würde,

allen bisher nicht namentlich erwähnten Mitgliedern der Lehrstühle Pharmazeutische Biologie und Pharmakologie und Toxikologie,

ganz besonders meinen Eltern und meiner Schwester, für ihre Unterstützung und Hilfe sowie

allen, die mit zum Gelingen dieser Arbeit beigetragen haben.

TABLE OF CONTENTS

Abbreviations

2-AG	2-arachidonoyl glycerol
AA	amino acid
AC	adenylyl cyclase
ACN	acetonitrile
AEA	anandamide
AM 251	6-iodopravadoline
AM 281	1-(2,4-dichlorophenyl)-5-(4-iodophenyl)-4-methyl-N-4-morpholinyl-1*H*-pyrazole-3-carboxamide
AM 630	(6-iodo-2-methyl-1-[2-4(morpholinyl)-ethyl]-[1*H*-indol-3-yl]-(4-methoxyphenyl)methanone)
ATP	adenosine 5`-triphosphate
β_2AR	β_2-adrenoceptor
bp	base pair(s)
BSA	bovine serum albumin
cAMP	cyclic 3`:5`-adenosine monophosphate
cDNA	copy-DNA
CNS	central nervous system
CP 55,940	[(-)-*cis*-3-[2-hydroxy-4-(1,1-dimethylheptyl)phenyl]-*trans*-4-(3-hydroxypropyl)cyclohexanol]
hCB_1R	human cannabinoid receptor subtype 1
hCB_2R	human cannabinoid receptor subtype 2
DCM	dichloromethane
DEPC	diethyl pyrocarbonate
DMSO	dimethyl sulfoxide
EC_{50}	agonist concentration which induces 50% of the maximum effect
EC	endocannabinoid
ECS	endocannabinoid system
EDTA	ethylenediaminetetraacetic acid (Ca^{2+} - chelator)
E_{max}	efficacy (maximal response)
EtOAc	ethyl acetate
FACS	fluorescence activated cell sorter
FLAG	octapeptide epitope for the labeling of proteins (mostly DYKDDDDK)
GAP	GTPase-activating protein
GDP	guanosinediphosphate
GIT	gastrointestinal tract
GPCR	G-protein-coupled receptor
GTP	guanosine 5`-triphosphate
GTPγS	guanosine 5`-[γ-thio]triphosphate
h	hour(s)
HPLC	high performance liquid chromatography
IC_{50}	antagonist concentration which suppresses 50% of an agonist induced effect
IP_3	inositoltrisphosphate
K_i	dissociation constant (competition binding assay)
MAPK	mitogen-acitivated protein kinase
MeOH	methanol

NMR	nuclear magnetic resonance
PAGE	polyacrylamide gel electrophoresis
PBS	phosphate buffered saline
PCR	polymerase chain reaction
P_i	inorganic phosphate
PIP_2	phosphatidylinositolbisphosphate
PLC	phospholipase C
Rimonabant	5-(4-chlorphenyl)-1-(2,4-dichlorphenyl)-4-methyl-N-piperidinopyrazol-3-carbamide
RGS	regulator of G-protein signaling
RNA	ribonucleic acid
RP	reverse phase
rpm	revolutions per minute
RT	reverse transcription
RT-PCR	combined reverse transcription and polymerase chain reaction
S.D.	standard deviation
SDS-PAGE	sodiumdodecylsulfate-polyacrylamide gel electrophoresis
Sf9	insect cell line of *Spodoptera frugiperda*
Taranabant (MK-0364)	N-[(1S,2S)-3-(4-chlorophenyl)-2-(3-cyanophenyl)-1-methyl-propyl]-2-methyl-2-[[5-(trifluoromethyl)pyridin-2-yl]oxy]-propanamide
Δ^9-THC	Δ^9-tetrahydrocannabinol
TMD	transmembrane domain
Tris	tris(hydroxymethyl)aminomethan
WIN 55,212-2	(*R*)-(+)-[2,3-dihydro-5-methyl-3-(4-morpholinylmethyl)pyrrolo[1,2,3-de]-1,4-benzoxazin-6-yl]-1-naphthalenylmethanone mesylate

1 Introduction

1.1 Cannabinoid receptors

Cannabinoid receptors have been of high interest since their discovery in the early 1990`s. In 1990, the first cannabinoid receptor mainly expressed in the central nervous system, named CB_1R, was cloned (Matsuda et al., 1990). The CB_1R is primarily located on presynaptic axon terminals in neurons and has an especially high density in the brain compared to other GPCRs. Apart from neurons, the CB_1R is also present in the adrenal gland, bone marrow, heart, lung, prostate and testicles (Pertwee, 1997). Shortly after the discovery of CB_1R, a second receptor, named CB_2R, less highly expressed than the CB_1R and mainly found in the periphery on immune cells and tissues was described (Munro et al., 1993). Particular high CB_2R expression levels are found on B cells and natural killer cells (Howlett et al., 2002). Recently, CB_2R have also been detected on neurons, but to a much lesser extent than the CB_1R (Van Sickle et al., 2005; Gong et al., 2006).

In 2006, an orphan receptor named GPR55 was highlighted as a putative CBR having similar signal transductory ways (Baker et al., 2006). GPR55 is activated by several cannabinoid receptor ligands. However, amino acid sequence homology to CB_1R and CB_2R is very low (Johns et al., 2007; Ryberg et al., 2007). Up to now it remains elusive, if there are more receptors belonging to the cannabinoid receptor group.

Cannabinoid receptors belong to the family A of GPCRs with 7 transmembrane domains (TMD) and are $G\alpha_{i/o}$ protein-coupled. CBRs activate mitogen-activated protein kinases (MAPK), inhibit adenylyl cyclase activity after activation and are sensititve to pertussis toxin (Howlett, 2005). CB_1R is also capable of inhibiting N-, P/Q- and L-type calcium channels in neurons and modulating potassium channels (Mackie et al., 1995; Twitchell et al., 1997).

Aligning the amino acid sequence of both CBRs, they share only a 44% protein homology which increases to 68% compairing the TMDs (www.iuphar-db.org). The sequence identity in the TMDs is high enough that agonists, such as CP 55,940, anandamide and 2-AG, do bind to both subtypes (see Fig. 1 in Chapter 1.2.1). This may be explained by a similarity of their orthosteric ligand binding sites (Munro et al.,

1993). The low overall sequence identity suggests the evolution of the different receptors very long ago in the past (McPartland and Glass, 2003).

1.2 Cannabinoid receptor ligands

1.2.1 Cannabinoid receptor agonists

CBR agonists have very different chemical structures. Hence, they are often divided in 4 structural classes (see Fig. 1). First, the classic cannabinoids, e.g. Δ^9-THC isolated from *Cannabis sativa* L. (var. *indica*), Cannabaceae. Second, the non-classic cannabinoids, e.g. CP 55,940, a Pfizer compound derived from Δ^9-THC. In the third class are the endogenous cannabinoids, e.g. anandamide and 2-AG. The fourth class comprises the aminoalkylindoles, e.g. WIN 55,212-2.

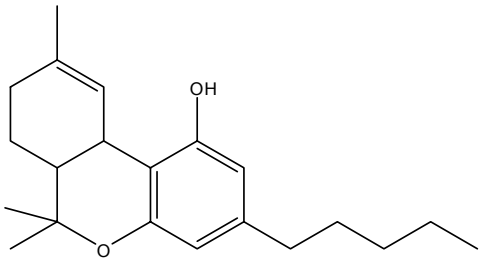

Δ^9-THC

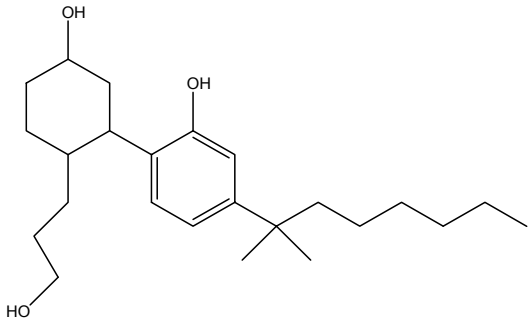

CP 55,940

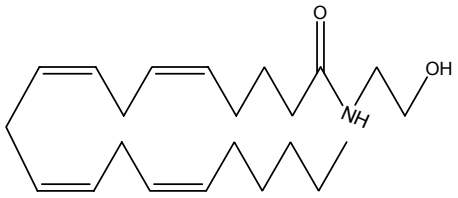

Anandamide

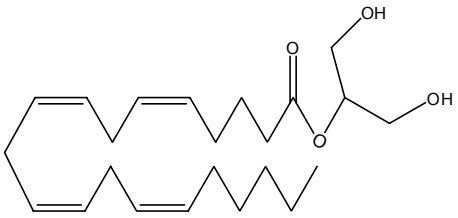

2-AG

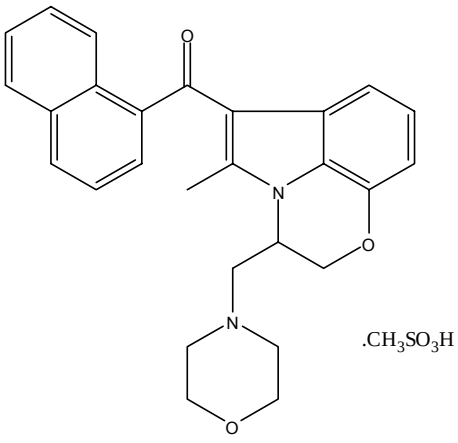

WIN 55,212-2 mesylate

Fig. 1: Examples for cannabinoid receptor agonists.

1.2.2 Cannabinoid receptor antagonists/inverse agonists

In general, CBR antagonists are not neutral antagonists, but inverse agonists. Those ligands can also be divided in different structural classes (see Fig. 2). CB_1R antagonists/inverse agonists, e.g. AM 251 and AM 281, belong to the class of biarylpyrazoles. The CB_2R antagonist/inverse agonist AM 630 belongs to the class of aminoalkylindoles.

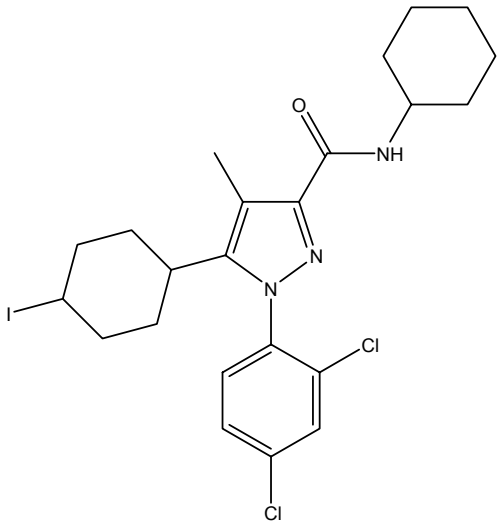

AM 251

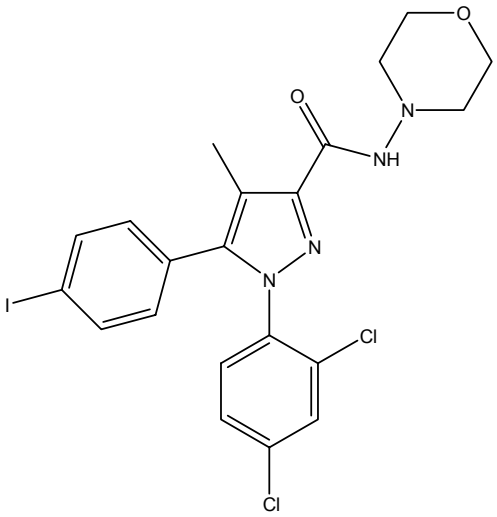

AM 281

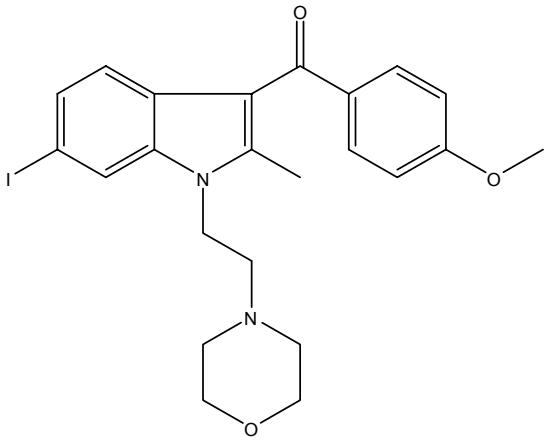

AM 630

Fig. 2: Examples for cannabinoid receptor antagonists/inverse agonists.

1.3 Endogenous ligands and endocannabinoid system

Endogenous ligands for cannabinoid receptors, named endocannabinoids, have also been discovered. Up to now, two main endocannabinoids (EC) have been reported, anandamide (AEA), derived from the sanskrit word ananda for bliss, and 2-arachidonoyl glycerol (2-AG), for structures see Fig. 1 in Chapter 1.2.1 (Devane et al., 1992; Mechoulam et al., 1995; Sugiura et al., 1995). Those ligands are agonists at both receptors. However, AEA and 2-AG possess a 3 – 4 times higher affinity for the CB_1R (Felder and Glass, 1998). Anandamide is also described as a partial agonist at both CBRs and can activate TRPV1 (vanilloid) receptors (Zygmunt et al., 1999; Smart et al., 2000). The concentrations of endocannabinoids in the brain differ, 2-AG is present in 50 – 500 fold higher concentrations than AEA (Felder et al., 1996; Sugiura et al., 2006).

The endocannabinoid system (ECS) itself regulates many functions throughout the body, such as movement, memory, immune regulation, appetite and pain (De Petrocellis et al., 2004; Di Marzo et al., 2004). In general, imbalances in the ECS and the interaction of AEA and 2-AG result in various diseases, e.g. inflammation. Currently, neuroinflammatory disorders, such as Alzheimer`s disease, amyotrophic lateral sclerosis, multiple sclerosis, parkinson`s disease, are associated with malfunction of CBRs, because neurodegeneration is often linked to inflammatory processes (Centonze et al., 2007).

Also, animal models of obese mice and Zucker rats showed elevated hypothalamic endocannabinoid levels. Endocannabinoid production was also increased in peripheral tissues, adipocytes, hepatocytes and pancreatic cells (Bensaid et al., 2003; Cota et al., 2003; Pagotto et al., 2006). Targeting this overactivity of the ECS in obese animals led to the development of the first CB_1R antagonist/inverse agonist SR141716A by Sanofi-Aventis (Meschler et al., 2000), named rimonabant (Acomplia®). Rimonabant was launched on the US and European market in 2005. However, severe neuronal side effects due to the blockade of CB_1R in the brain, such as an increased risk for suicide, depression and fear, led to the withdrawal of the drug by the FDA in 2006. In Europe, the drug is still on the market, available for patients with a BMI > 30 or a BMI > 27 and other risk factors, such as diabetes type 2. However, intensive monitoring of these patients has to be performed and

patients with severe depressions are excluded from the treatment with rimonabant (www.emea.europa.eu).

Just very recently, Merck developed taranabant (MK-0364), also a selective inverse agonist at CB_1R. Taranabant is currently investigated in a phase III clinical study with 2400 obese patients (Fong et al., 2007; Addy et al., 2008; Addy et al., 2008a).

While CB_1R antagonists are currently linked to the treatment of obesity, a drug already on the market and a second drug in the clinical stage, the development of clinically useful CB_2R antagonists is still ongoing. However, CB_2R antagonists are thought to be antiinflammatory and antiallergic drugs due to their localization on cells and tissues of the immune system.

Agonists for cannabinoid receptors are also of high interest and intensive research is performed. After activation of CB_1R by endogenous or exogenous agonists anticonvulsive effects and neuroprotective effects have been observed during ischemia and after traumatic brain injury (Panikashvili et al., 2001; Marsicano et al., 2003). The connection of cannabinoids and pain is currently investigated (Lever and Rice, 2007). Stimulation of CB_1R by exogenous cannabinoids on nociceptive neurons results in analgesia. Also, during stress, neuropathic conditions and inflammation, endocannabinoids are released modulating pain and nociception (Jhaveri et al., 2007).

Yet, continuous administration of CB_1R agonists always led to tolerance and addiction in animals and humans (Maldonado, 2002; Justinova et al., 2005).

Interestingly, activation of CB_2R also had analgesic and antinociceptive effects (Ibrahim et al., 2003; Malan et al., 2003). The treatment of pain by CB_2R and not CB_1R agonists would result in less severe or even no neuronal side effects due to the much lower expression of CB_2R in the CNS.

1.4 Activation of GPCRs

If a ligand binds to the receptor binding site, the conformation of the GPCR changes and G-protein (inactive state) couples to the receptor. The inactive G-protein heterodimer consists of a Gα-subunit, a Gβγ heterodimer and GDP bound to the Gα-subunit. After binding and activation of the receptor by an agonist, the receptor binds to the heterotrimeric G-protein. GDP is then released from the Gα-protein and a ternary complex consisting of the agonist-occupied receptor and the nucleotide-free Gα forms. Subsequently, GTP binds to Gα. This GDP/GTP exchange causes a decrease in affinity of the Gα-subunit to the Gβγ heterodimer and the ternary complex is disrupted by disscociation in Gα-GTP and Gβγ. The separated Gα- and Gβγ-subunits can interact with effector proteins and continue the signal cascade. Due to the intrinsic GTPase activity of the Gα-subunit, GTP is hydrolysed to GDP and P_i. After the cleavage of P_i, the Gα- and Gβγ-subunit reassociate and the heterotrimer is ready to interact with another activated receptor. For illustration see Fig. 3.

The intrinsic GTPase activity of the Gα-subunit, that means the hydrolysis of GTP bound to Gα to GDP and P_i, can be accelerated by RGS-proteins (regulators of G-protein signaling). Hence, the reassociation of Gα/GDP- and Gβγ-subunits occurs faster, terminating the activation. This standard model of GPCR activation assumes that the lifetime of Gα-GTP and the hydrolysis of GTP is the rate-determining step of the signaling process.

In the steady-state GTPase assay, a radioactively labeled GTP derivative is used. [γ-^{32}P]GTP binds to the Gα-subunit and is then hydrolysed to GDP and radioactive $^{32}P_i$ by the intrinsic GTPase activity of Gα. The amount of released $^{32}P_i$ is measured under steady-state conditions (usually 20 min) and can be determined by liquid scintillation counting.

The GTPγS binding assay kinetically determines the GDP/GTP exchange at the Gα-subunit. In contrast to [γ-^{32}P]GTP, [^{35}S]GTPγS cannot be hydrolysed by the Gα-subunit and the heterotrimeric G-protein accumulates. This assay can be performed as a filtration assay through glass-fibre filters, as the Gα-subunit/[^{35}S]GTPγS complex remains membrane-associated and is not filtrated. [^{35}S]GTPγS on the filters can also be determined by liquid scintillation counting (Harrison and Traynor, 2003).

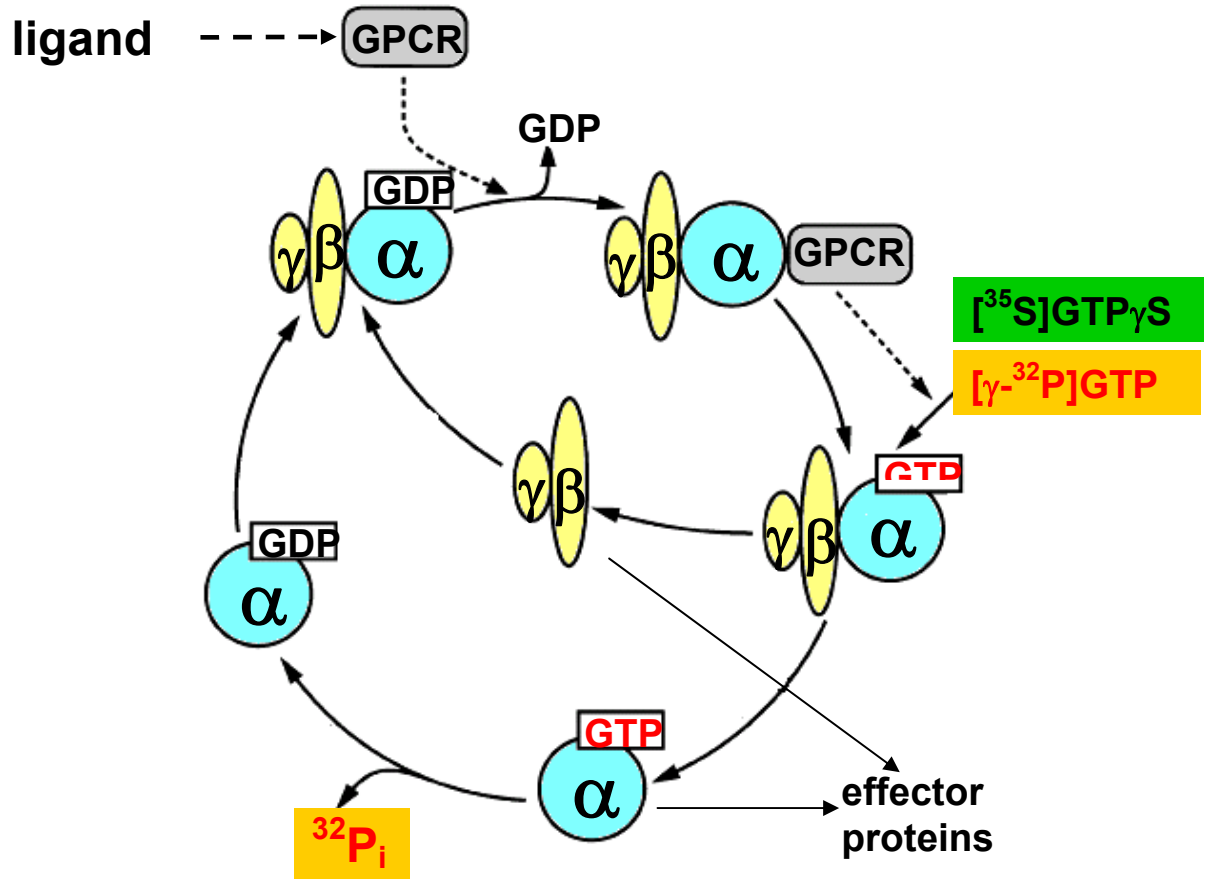

Fig. 3: Mechanism of G-protein activation of GPCRs by ligands and possible methods to analyse GPCRs by radioactively labeled GTP derivatives (Seifert and Wenzel-Seifert, 2003).

1.5 Two-state activation model of GPCRs

According to the two-state model of GPCR activation (Leff, 1995), a receptor can exist in two states, the active state R* and the inactive state R. Both states, R* and R, are in equilibrium. R* can bind G-proteins, as described in Chapter 1.4, whereas R does not interact with G-proteins, and no GDP/GTP exchange will happen.
Depending on the pharmacological profile of ligands, the different states of the receptor will be stabilized and hence the equilibrium can be shifted to one side (see Fig. 4). Agonists stabilize the active conformation R* of the receptor, whereas inverse agonists stabilize the inactive form R of the receptor. Neutral antagonists do not alter the equilibrium between R* and R, but occupy the binding site of other ligands at the GPCR. Actually, many neutral antagonists are inverse agonists. Though inverse agonists stabilize the inactive state R, some of the receptors remain in the active state R* with no agonist bound due to the present equilibrium. This fact is called constitutive activity. Constitutive activity is often observed among GPCRs, e.g. the formyl peptide receptor (Seifert and Wenzel-Seifert, 2003) and might also be related to diseases (Seifert and Wenzel-Seifert, 2002).

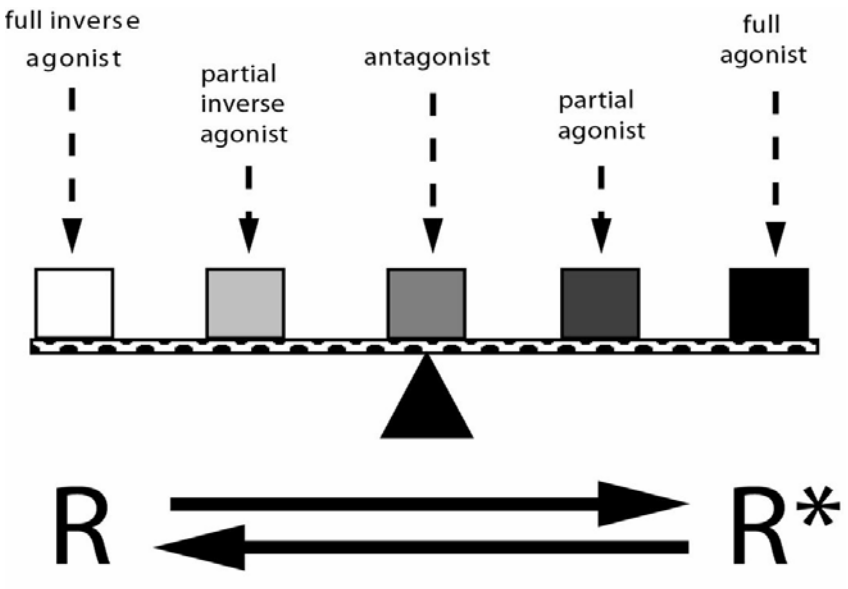

Fig. 4: Two-state activation model of GPCRs. Agonists stabilize the active conformation R*, inverse agonists the inactive conformation R and antagonists do not alter the equilibrium between the two states of the receptor (Seifert and Wenzel-Seifert, 2002).

According to the model, full agonists generate full receptor activation and a maximal response (E_{max} = 100%). Partial agonists result in a sub-maximal response due to a lower intrinsic efficacy. They also might attenuate a maximal response produced by a full agonist. Antagonists result in no physiological response at all.

1.6 Plant-derived ligands at CBRs

Decades before the two cannabinoid receptors CB_1R and CB_2R were cloned, Δ^9-THC and other cannabinoids were isolated of *C. sativa* L. and their structures were elucidated (Mechoulam and Gaoni, 1965). Most of the compounds do bind to CBRs, e.g. Δ^9-THC, Δ^8-THC and cannabinol. Others, e.g. cannabidiol, do not (Ashton, 2001). All above noted compounds are depicted in Fig. 5.

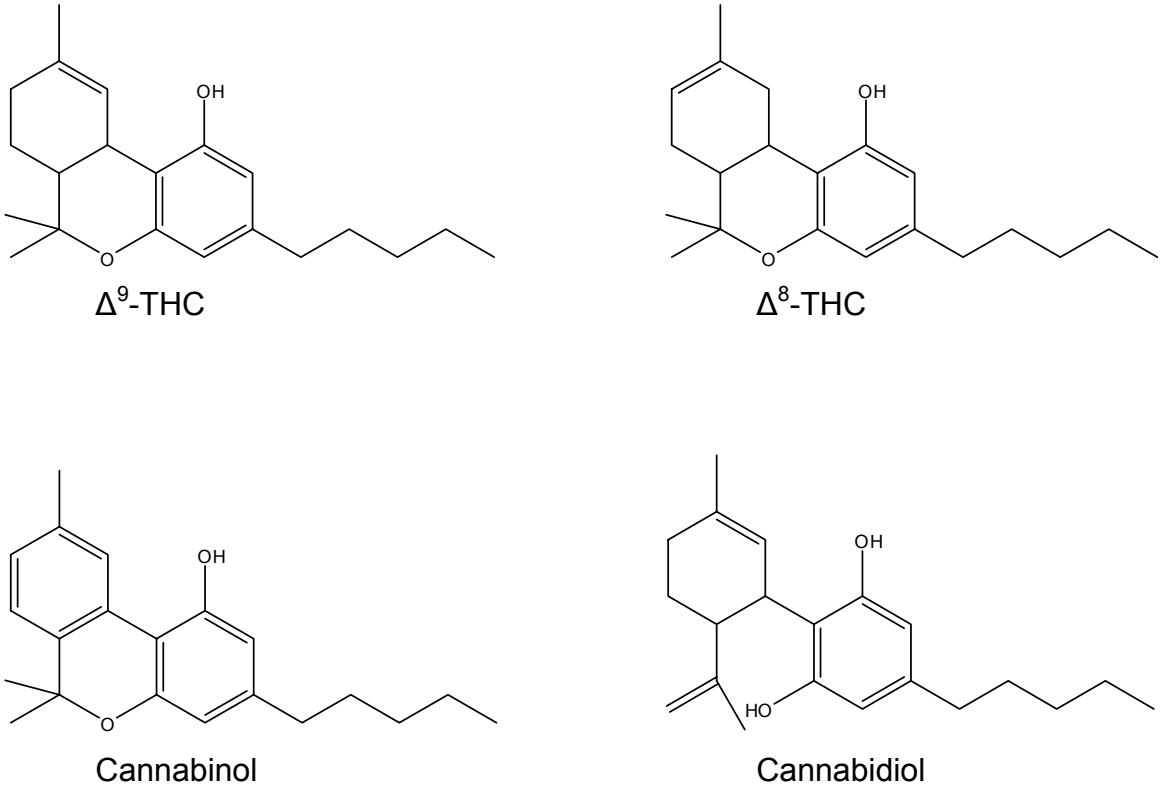

Fig. 5: Structures of compounds isolated from *C. sativa*.

Just recently, the immunomodulatory effects of *Echinacea* species have been linked to cannabinoid receptors, indicating the first natural ligands at CBRs not derived from *C. sativa* (Gertsch et al., 2004; Woelkart et al., 2005).

It has been reported that an extract of *Echinacea purpurea* (Echinaforce®) showed an induction of the *de novo* synthesis of TNFα mRNA, but not TNFα protein, in human monocytes and macrophages. Lipophilic compounds with a high structural similarity to the known endogenous cannabinoid receptor ligands anandamide and 2-AG have

been proposed to be responsible for the TNFα mRNA synthesis (Gertsch et al., 2004). This class of plant compounds is named alkamides, a shorter version of the name alkylamides. CB_2R are mainly found in the periphery and are expressed on immune cells, such as monocytes and macrophages (Klein et al., 2003), and the endogenous CBR agonists anandamide and 2-AG inhibit the release of TNFα by immune cells (Chang et al., 2001). Hence, Gertsch et al. reported that alkamides may activate cannabinoid receptors. They showed that the induction of TNFα mRNA synthesis was blocked only by selective CB_2R antagonists and not by selective CB_1R antagonists (Gertsch et al., 2004).

The compounds which have been described as CB_2R agonists are the isomer pair dodeca-2*E*,4*E*,8*Z*,10*E*-tetraenoic acid isobutylamide and dodeca-2*E*,4*E*,8*Z*,10*Z*-tetraenoic acid isobutylamide, dodeca-2*E*,4*E*,8*Z*-trienoic acid isobutylamide and dodeca-2*E*,4*E*-dienoic acid isobutylamide (see Fig. 6).

Dodeca-2*E*,4*E*,8*Z*,10*Z*-tetraenoic acid isobutylamide and dodeca-2*E*,4*E*-dienoic acid isobutylamide interacted with the CB_2R in a homology model based on the crystal structure of bovine rhodopsin. The amphiphilic property of these alkamides allowed docking in the predicted binding pocket of the CB_2R. Both alkamides showed even higher affinity at the human CB_2R than anandamide in radioligand displacement studies (Raduner et al., 2006).

Alkamides isolated from the roots of *E. angustifolia* also have been screened for rat CB_1R and mouse CB_2R affinity in a [^{3}H]CP 55,940 competition binding assay (Woelkart et al., 2005). Several alkamides showed affinities for cannabinoid receptors in the micromolar range, but none of the depicted compounds by Gertsch et al. (Fig. 6) showed selectivity for either CB_1R or CB_2R (Woelkart et al., 2005). Contradictory results as pointed out above have been linked to the history of *Echinacea* since research in this field started.

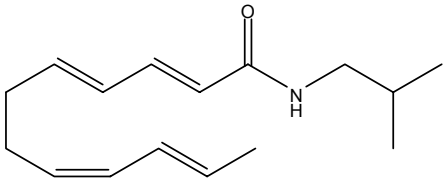

Dodeca-2*E*,4*E*,8*Z*,10*E*-tetraenoic acid isobutylamide

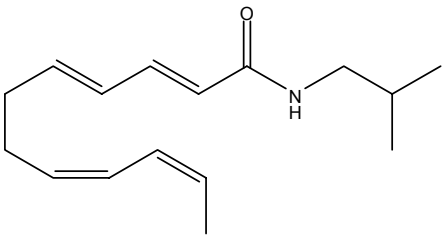

Dodeca-2*E*,4*E*,8*Z*,10*Z*-tetraenoic acid isobutylamide

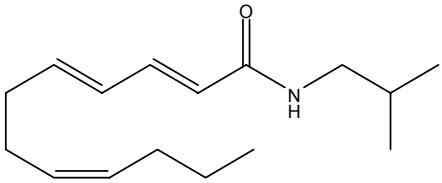

Dodeca-2*E*,4*E*,8*Z*-trienoic acid isobutylamide

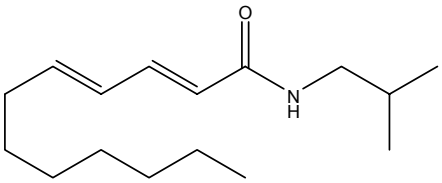

Dodeca-2*E*,4*E*-dienoic acid isobutylamide

Fig. 6: Alkamides isolated from *E. purpurea* described as CB_2R agonists (Gertsch et al., 2004).

1.7 Use of *Echinacea*

Echinacea has been already used in the 18th and 19th century by the Indians of North America for the treatment of wounds, burns, toothache and common cold. Several classes of compounds, such as caffeic acid derivatives, flavonoids, polyacetylenes, alkamides, pyrrolizidine alkaloids, polysaccharides and glycoproteins have been isolated from *Echinacea* species (Bauer and Wagner, 1990; Hostettmann, 2003). The genus *Echinacea* Moench (Heliantheae: Asteraceae) consist of four species, which probably belong to eight varieties. Three different taxa are cultivated and used for medical purposes: *E. purpurea* (L.) MOENCH, *E. pallida* var. *angustifolia* (DC.) CRONQ. and *E. pallida* var. *pallida* (Nutt.) CRONQ. (Binns et al., 2002a). Apart from the above described class of alkamides, other more hydrophilic compounds have been reported being responsible for the immunomodulatory effects, such as the caffeic acid derivates (see Fig. 7) or polysaccharides/glycoproteins (Bauer, 1999; Classen et al., 2004).

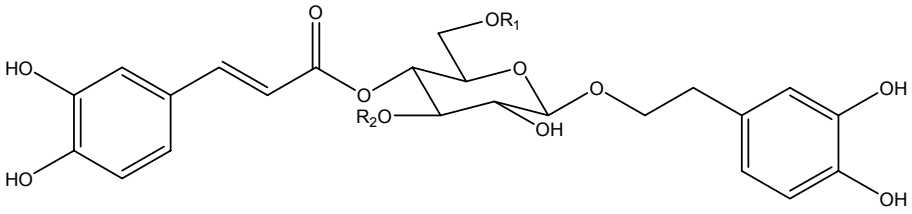

Echinacoside (R_1 = β-D-Glucose, R_2 = α-L-Rhamnose)

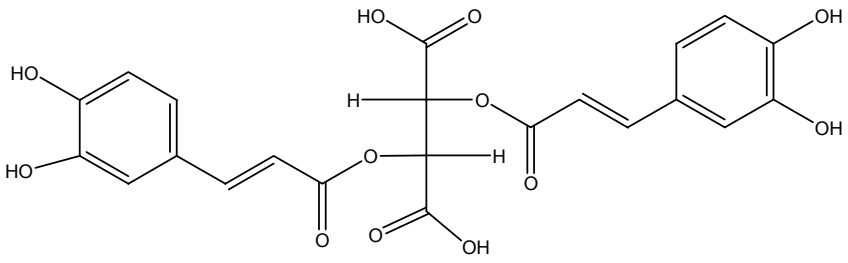

Cichoric acid

Fig. 7: Examples for hydrophilic caffeic acid derivates in *Echinacea*.

Caffeic acid derivates are mainly considered to be responsible for the antioxidative effects of *Echinacea* preparations (Xiong et al., 1996; Heilmann et al., 2000). However, echinacoside also decreased the NO concentration in rat macrophages which may contribute for the antiinflammatory effects of *Echinacea* (Xiong et al., 2000). Several polysaccharides and glycoproteins isolated from *E. purpurea* and *E. angustifolia* showed immunomodulatory effects, e.g. an increased phagocytotic activity (Wagner et al., 1985) or a proliferative effect on rat spleen cells (Beuscher et al., 1995).

Interestingly, alkamides are not present in all *Echinacea* species, e.g. in *E. pallida*. However, *E. pallida* roots contain another class of lipophilic compounds which can only be found in this *Echinacea* species (see Fig. 8). Those ketoalkenes and ketoalkynes are present in the whole plant. They are also components of the essential oil of the roots of *E. pallida*. Approximately half of the essential oil consists of only two compounds, pentadec-8*Z*-en-2-one and pentadeca-1,8*Z*-dien. Although ketoalkenes and ketoalkynes show structural similarity to the endocannabinoid anandamide, those compounds and *E. pallida* in general have never been analysed for their immunological activity.

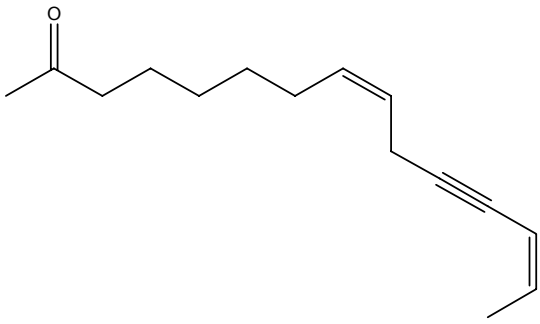

Pentadeca-8*Z*,13*Z*-dien-11-yn-2-one

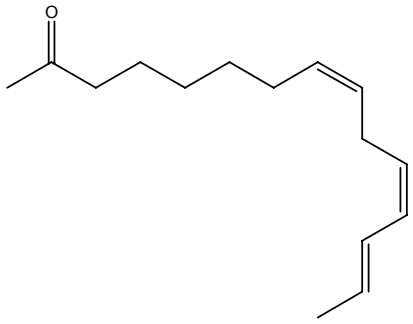

Pentadeca-8*Z*,11Z,13E-trien-2-one

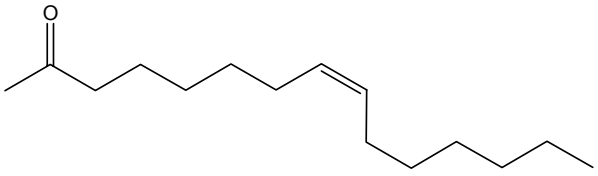

Pentadec-8*Z*-en-2-one

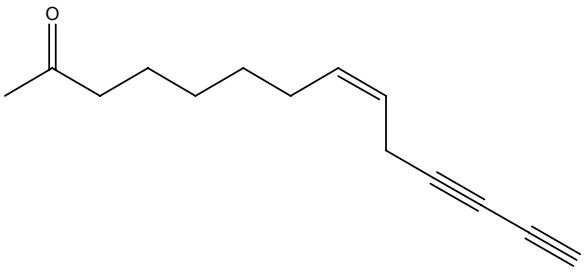

Tetradeca-8*Z*-en-11,13-diyn-2-one

Fig. 8: Overview of ketoalkenes and ketoalkynes present in *E. pallida* roots.

The use of *Echinacea* for the treatment of common cold has been topic of many clinical trials and scientific publications, often with contradictory outcome. It is known that different manufacturers and different batches of the same plant extract lead to large differences in the concentrations of active or adjuvant compounds (Osowski et al., 2000). This reflects the main disadvantage of especially older studies, no quantification of the potentially active compounds was made and sometimes not even the investigated species or plant material were defined correctly. Some clinical trials were not performed according to GCP guidelines, e.g. patient population was inhomogenous, only a small number of patients was included or the dosage scheme did not meet actual standards (Melchart et al., 1995; Melchart et al., 1998; Schwarz et al., 2005).

Until now, the following species and plant parts have been used for clinical trials on *Echinacea*-containing drugs: preparations of *E. purpurea* herb, roots and herb with roots, *E. pallida* and *E. angustifolia* roots. Of 13 randomized double-blind studies treating infections of the upper respiratory tract, 6 studies showed a significantly better outcome when patients used an *Echinacea*-containing drug. However, the drugs used in the 3 latter studies had a relatively low or not detectable alkamide or cichoric acid content (Osowski et al., 2000). Most of the modern clinical studies according to GCP guidelines prove the efficacy using *Echinacea* to reduce the incidence and duration of the common cold (Goel et al., 2004; Shah et al., 2007).

On the molecular pharmacological level, the antiinflammatory and antifungal activity of *Echinacea* species has been widely investigated (Müller-Jakic et al., 1994). Regarding the antiviral activity against herpes simplex virus (HSV-1), lipophilic *n*-hexane root extracts containing alkamides were more active than more hydrophilic ethyl acetate extracts containing caffeic acids (Binns et al., 2002).

Despite the popularity of *Echinacea* containing herbal products, especially on the U.S. market, the underlying molecular mechanisms remain unclear and poorly understood.

2 Scope and Objectives

G-protein coupled receptors (GPCRs) represent the largest group of transmembrane receptors. GPCRs are often related to diseases and have therefore been of high interest for the last decades. About 50% of the drugs on the market target GPCRs and among all top-selling drugs more than one third are ligands of GPCRs (Nambi and Aiyar, 2003). Hence, it is not only very important for pharmacological but also interesting for financial reasons for pharmaceutical companies to find new ligands for GPCRs, especially for those which are only known for a short time, such as cannabinoid receptors.

It is also necessary to evaluate the efficacies and pharmacological profiles of GPCR ligands. Competition binding assays with a radiolabeled ligand and increasing concentrations of the investigated compound are often applied. However, this assay does not allow the differentiation of full or partial agonists, inverse agonists and antagonists. Other test systems measure the effects at a very distal point of the signal cascade via second messengers, e.g. the increase of intracellular Ca^{2+} levels by FACS or the measurement of cAMP concentrations. These second messengers are often influenced by receptor-independent effects. Therefore, determination of the release of $^{32}P_i$ in the GTPase assay or the GDP/GTP exchange in the GTPγS binding assay is more suitable.

Only a few years ago, alkamides of *E. purpurea* have been proposed to be ligands at CB_2R (Gertsch et al., 2004; Woelkart et al., 2005). However, alkamides have only been characterized as ligands in competition binding assays. The fact that a compound binds to a receptor or is able to compete with another compound bound to a receptor does not automatically demonstrate pharmacological activity. Also, *Echinacea* preparations that are efficient treating common cold do not always contain *E. purpurea*, but also *E. pallida*. The latter possesses ketoalkenes and ketoalkynes, which are very lipophilic compounds and are only present in *E. pallida*. Those compounds have neither been discussed as possible ligands nor been tested for CBR affinity at all.

Therefore, our interest was to establish several functional assays to study cannabinoid receptors and their ligands at a proximal point of the signal cascade, such as the steady-state GTPase assay and the GTPγS binding assay. We also wished to optimize [^{3}H]CP 55,940 competition binding assay to complete pharmacological investigations characterizing cannabinoid receptor ligands. The effects of different Gα-subunits, RGS-proteins and solvents should be investigated. We were further interested if differences in the coupling and activation of CBR via Gα-proteins exist.

In summary, the aim of this thesis was to establish several highly sensitive and efficient test systems to fully characterize cannabinoid receptors, to detect pharmacological properties of commercially available ligands and to analyse isolated natural and synthesized ligands derived from *Echinacea* species by functional test systems.

3 Materials and Methods

3.1 Pharmacological materials

The cDNA for hCB_1R and hCB_2R in pcDNA 3.1 was obtained from the cDNA bank of the University of Missouri (Rolla, MO, USA). All restriction enzymes and T4 ligase were from New England Biolabs (Beverley, MA, USA). Cloned *Pfu* DNA polymerase was from Stratagene (La Jolla, CA, USA). The anti-FLAG Ig (M1 monoclonal antibody) was from Sigma (St. Louis, MO, USA). The anti-$G\alpha_{i\ common}$ Ig, anti-$G\beta_{common}$ Ig, purified $G\alpha_i$- and $G\beta_1\gamma_2$-protein were a kind gift from Dr. Dr. B. Nürnberg (Department of Biochemistry, University of Düsseldorf, Germany). The anti-CB Igs and the anti-$G\alpha_o$ Ig were from Calbiochem (La Jolla, CA, USA). Antibodies for RGS- and GAIP-protein were obtained by Santa Cruz Biotechnology Inc. (Santa Cruz, CA, USA). Baculovirus encoding for $G\alpha_o$ was a kind gift by Dr. J. Garrison (University of North Carolina, Chapel Hill, NC, USA). Baculovirus encoding $G\alpha_{i2}$ was generously provided by Dr. A. G. Gilman (Department of Pharmacology, University of Texas Southwestern Medical Center, Dallas, TX, USA). Baculovirus encoding $G\beta_1\gamma_2$ was a kind gift from Dr. P. Gierschik (Department of Pharmacology, University of Ulm, Germany). Baculoviruses encoding for RGS4 and GAIP were a kind gift from Dr. E. Ross (University of Texas Southwestern Medical Center, Dallas, TX, USA). Phenylmethylsulfonylfluoride and leupeptine hemisulfate were from Calbiochem (La Jolla, CA, USA). Benzamidine 99% was from Sigma-Aldrich (St. Louis, MO, USA). Adenylyl imidophosphate (AppNHp) was obtained from Roche (Mannheim, Germany). Boric acid p.A. was from Merck (Darmstadt, Germany).

[^{3}H]CP 55,940 (160 Ci/mmol), [^{35}S]GTPγS (1,100 Ci/mmol) and [α-^{32}P]ATP (3,000 Ci/mmol) were from PerkinElmer Life Sciences (Boston, MA, USA). [γ-^{32}P]GTP was synthesized through enzymatic phosphorylation of GDP and [^{32}P]orthophosphoric acid (8,000 Ci/mmol, PerkinElmer Life Sciences, Boston, MA, USA) as described previously (Walseth and Johnson, 1979). Mono(cyclohexyl)-ammoniumphosphoenolpyruvate, pyruvate kinase and myokinase were from Sigma (St. Louis, MO, USA).

Unlabeled GTPγS, all nucleotides, creatine kinase, creatine phosphate, polyethyleneimine solution (50% (w/v) in water), glucose and salts (highest purity

available) were purchased either from Roche (Mannheim, Germany) or Sigma (St. Louis, MO, USA). Forskolin was purchased from LC laboratories (Woburn, MA, USA). Dimethyl sulfoxide and glycerol were from Merck (Darmstadt, Germany). Tris base was purchased from USB (Cleveland, OH, USA). GF/C filters were from Brandel (Gaithersburg, MD, USA). Agarose was purchased from Biozym Scientific (Oldendorf, Germany). Ethidium bromide (10 mg/ml) was from Sigma (St. Louis, MO, USA). Ampicillin was from Fisher BioReagents (Fisher Scientific, Schwerten, Germany).

The CBR ligands CP 55,940, anandamide, 2-AG, WIN 55,212-2, AM 251 and AM 630 were purchased from Tocris Cookson (Ballwin, MO, USA). Δ^9-THC was obtained by THC Pharm (Frankfurt/Main, Germany).

3.2 Buffers and media

For the preparation of buffers and solutions Millipore water was used, unless otherwise stated. DEPC water was prepared by adding 1 ml DEPC ad 1 l Millipore water and autoclaving the solution the following morning.

For Sf9 cell culture, SF 900 II medium (Invitrogen, Carlsbad, CA, USA) was supplemented with fetal calf serum (Pan-Biotech, Aidenbach, Germany) to 5% (v/v) and gentamicin sulfate (BioWhittaker, Walkersville, MD, USA) to 0.1 mg/ml.

LB medium (pH = 7.0)
10 g NaCl
10 g tryptone (Difco, Detroit, USA)
5 g yeast extract (Roth, Karlsruhe, Germany)
ad 1000 ml Millipore water (pH=7.0)

selective LB medium
add 100 mg/l ampicillin to sterilized LB medium

selective agar plates
add 20 g Agar (Roth, Karlsruhe, Germany) per l of LB medium
sterilize, let medium cool down to 55 – 60°C, add 100 mg/l ampicillin
store agar plates at 4°C

SOC medium

add to LB medium

2.5 mM KCl

10 mM $MgCl_2$

10 mM Mg_2SO_4

add 20 mM glucose after sterilization

PBS buffer (pH = 7.4)

137 mM NaCl

2.6 mM KCl

0.5 mM $MgCl_2$

0.9 mM $CaCl_2$

1.5 mM KH_2PO_4

0.8 mM Na_2HPO_4

Lysis buffer (pH = 7.4)

10 mM Tris/HCl

1 mM EDTA

0.2 mM phenylmethylsulfonylfluoride

10 μg/ml benzamidine

10 μg/ml leupeptin

Binding buffer (pH = 7.4)

75 mM Tris/HCl

1 mM EDTA

12.5 mM $MgCl_2$

TBE buffer

89 mM Tris-base

89 mM boric acid

2 mM EDTA

3.3 Pharmacological methods

3.3.1 Sf9 cell/baculovirus expression system

Sf9 cells, derived from *Spodoptera frugiperda* pupal ovarian tissue, are commonly used for baculovirus expression. Insect cells do not possess mammalian GPCRs or G-proteins; hence by coinfection of baculoviruses encoding for a certain GPCR and for the needed G-proteins functional studies of GPCRs can be performed (Wenzel-Seifert and Seifert, 2003). Insect cells can be grown rather easily and do not require a CO_2 atmosphere. The Sf9 cell/baculovirus expression system itself offers several advantages, such as high GPCR expression (up to 30 pmol/mg), high G-protein expression (up to 500 pmol/mg), large yields of protein and easy reconstitution of GPCRs and G-proteins. Possible disadvantages of this system could be misfolding or proteolysis of expressed proteins. Also, the N-glycosylation of GPCRs by insect cells is different from mammalian cells.

3.3.2 Transformation of CB_1 and CB_2 receptor DNA in *E. coli*

100 µl of competent *E. coli* (JM109) were thawed on ice and 2 ng of the DNA (in 10 mM Tris/HCl, pH 8.5) were added and very gently mixed. After 30 min of incubation on ice the suspension was heated to 42°C for 60 sec and placed on ice for 3 min. 900 µl of SOC medium was added and the mixture was incubated for 60 min at 37°C under shaking at 200 rpm in an incubation shaker (New Brunswick Scientific, model C24KC, Edison, NJ, USA). Then, 100 µl of the incubated suspension was plated on selective agar containing 0.01% (m/v) ampicillin. The plates were incubated overnight at 37°C to grow ampicillin-resistant colonies. The next morning, 2 - 6 colonies were picked, placed in selective LB medium (2.5 ml for MiniPrep, 100 ml for MaxiPrep). Small amounts of DNA (up to 20 µg) were isolated for analytical purposes (MiniPrep), whereas larger amounts of DNA (up to 500 µg) were isolated for transfection (MaxiPrep). For both preparations the Qiagen Plasmid Purification Kit (Qiagen, Hilden, Germany) was used according to the instructions of the manufacturer. Glycerol stocks of MaxiPrep cultures were prepared (700 µl bacterial suspension and 300 µl glycerol 50%) and stored at -80°C.

3.3.3 DNA analytics

3.3.3.1 Electrophoretic separation of DNA on agarose gels

Agarose gels were prepared by dissolving 1 – 2% (w/v) agarose in TBE buffer under heating. 4 µl ethidium bromide solution (10 mg/ml) was added to the warm mixture before pouring it in the gel chamber. After cooling down, gels were covered with TBE buffer. DNA samples were mixed with loading dye, pipetted in the pockets of the gel and separated by applying a voltage of 150 V for 30 min. An appropriate DNA molecular weight standard was used (GeneRuler^{TM}, Fermentas, St. Leon-Rot, Germany). Due to intercalation of the DNA with ethidiumbromide gels could be analysed at UV-light radiation at 254 nm (BDA Digital, Biometra, Göttingen, Germany).

For preparative electrophoresis or purifying PCR-products with subsequent extraction of DNA, 1% (w/v) agarose gels were used. After separation, DNA fragments were cut out of the gel at a higher wavelength (366 nm) to avoid mutations or strand breaks. To elute the DNA of the agarose gel the Qiagen PCR Purification Kit (Qiagen, Hilden, Germany) was used according to the instructions of the manufacturers. DNA concentrations were determined (DC protein assay kit, BioRad, Hercules, CA, USA) and DNA was stored at -20°C until use.

3.3.3.2 Restriction analysis of DNA and gene sequencing

Various enzymes (New England BioLabs, Frankfurt, Germany) were used for restriction analysis of the DNA (see Chapter 3.3.4). Usually, double digests were carried out by mixing 1 µg of DNA with 1 µl of each restriction enzyme and 1.5 µl of the according buffer. Millipore water and, if necessary, BSA solution were added to a final volume of 15 µl. After incubation at 37°C for 90 min, an inactivation step was carried out by heating the mixture to 65°C for 15 min. Electrophoretic analysis of the DNA was performed after adding loading buffer to each sample as described above.

Sequences were determined by Entelechon (Regensburg, Germany) using fluorescence dye-labeled stop nucleotides. Gene sequences were analysed with pDRAW 3.2 (AcaClone software) and Gene Runner 3.05 software (Hastings Software, New York, USA).

3.3.4 Construction of FLAG epitope- and hexahistidine-tagged hCB_1R and hCB_2R

The cDNA for hCB_1R and hCB_2R in pcDNA 3.1 was obtained from the cDNA bank of the University of Missouri (Rolla, MO, USA) on filter paper. The plasmid was reconstituted by elution for 4 h at 4°C with 50 µl 10 mM Tris/HCl, pH 8.5. After centrifugation for 1 min at 18.000 x g, the supernatant containing the eluted DNA was collected and used directly for the transformation of competent *E. coli* (JM109). The concentration of isolated DNA by MaxiPrep was determined and then analysed on agarose gels.

hCBR constructs were generated by analogy to the previously described strategy (Wenzel-Seifert et al., 1999; Wenzel-Seifert and Seifert, 2000; Seifert and Wenzel-Seifert, 2001). By sequential overlap-extension PCR, a DNA sequence encoding the cleavable signal peptide from influenza hemagglutinin to direct the receptor protein to the cell membrane, followed by the FLAG epitope, which is recognized by the M1 monoclonal antibody, was placed 5` of the start codon of the cDNA of the hCBRs. 3` of the cDNA a hexahistidine (6xHIS) epitope to allow further purification was introduced.

In PCR 1A with pGEM-3Z-$SFhH_4R$ as template, a DNA fragment consisting of a *SacI* restriction site, the signal peptide (S) and the FLAG epitope (F) was amplified (see Fig. 9). The sense primer F1 annealed prior to the 5` end of SF of pGEM-3Z, containing a *SacI* restriction site. The antisense primer C3 encoded 5`-CATGGCGTCATCATCGTC-3` annealing at the 3` end of the FLAG epitope sequence. All primers were synthesized by MWG-Biotech (Ebersberg, Germany), for sequences see Table 1. PCR was performed with a T1-Thermocycler (Biometra, Göttingen, Germany). The PCR 1A and 1B tubes were prepared by mixing 5 µl 1 mM dNTP-mix (Promega, Madison, WI, USA), 10 µl *Pfu* reaction buffer, 1 µl *Pfu* DNA polymerase solution (2.5 U/µl), 10 µl DMSO, 5 µl of sense and antisense primer (10 µM), 1 µl DNA (0.1 µg/µl) and 63 µl DEPC-water.

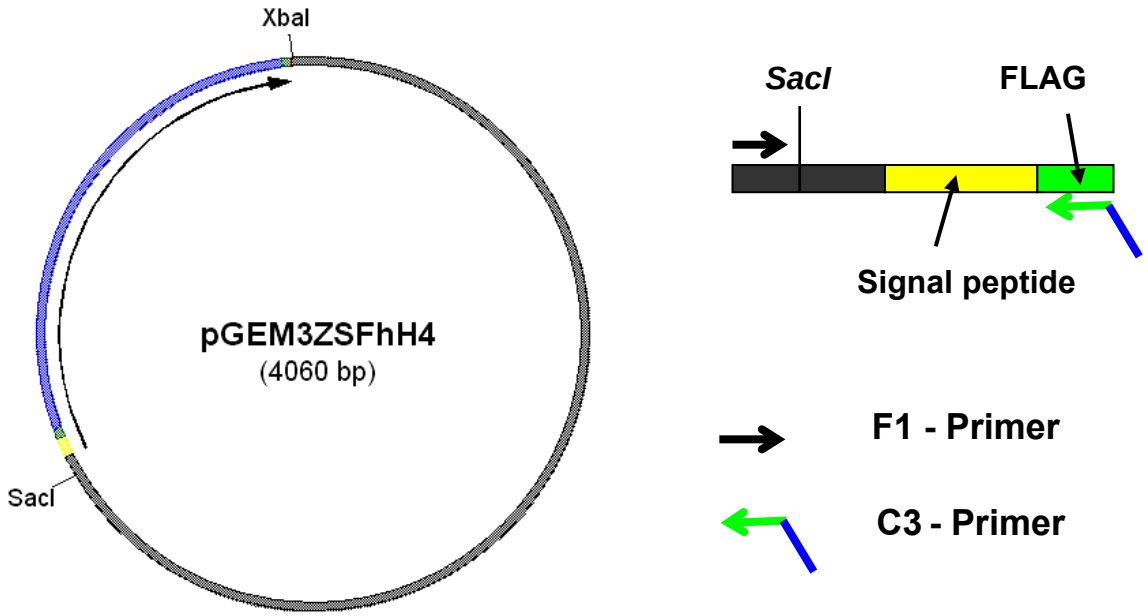

Fig. 9: Generation of the PCR 1A product.

In PCR 1B, a part of the FLAG epitope, the DNA sequence of hCB_1R or hCB_2R and a hexahistidine tag was generated (see Fig. 10). The sense primer encoded the sequence 5`GACGATGATGACGCCATGAAGTCGATCCTAGATGG-3`(hCB_1R) or 5`-ACGATGATGACGCCATGGAGGAATGCTGGGTG-3` (hCB_2R). The antisense primer annealed with the cDNA encoding the 5 C-terminal amino acid residues of hCB_1R/hCB_2R, the stop codon and an *XbaI* site (hCB_1R) or a *PstI* site (hCB_2R).

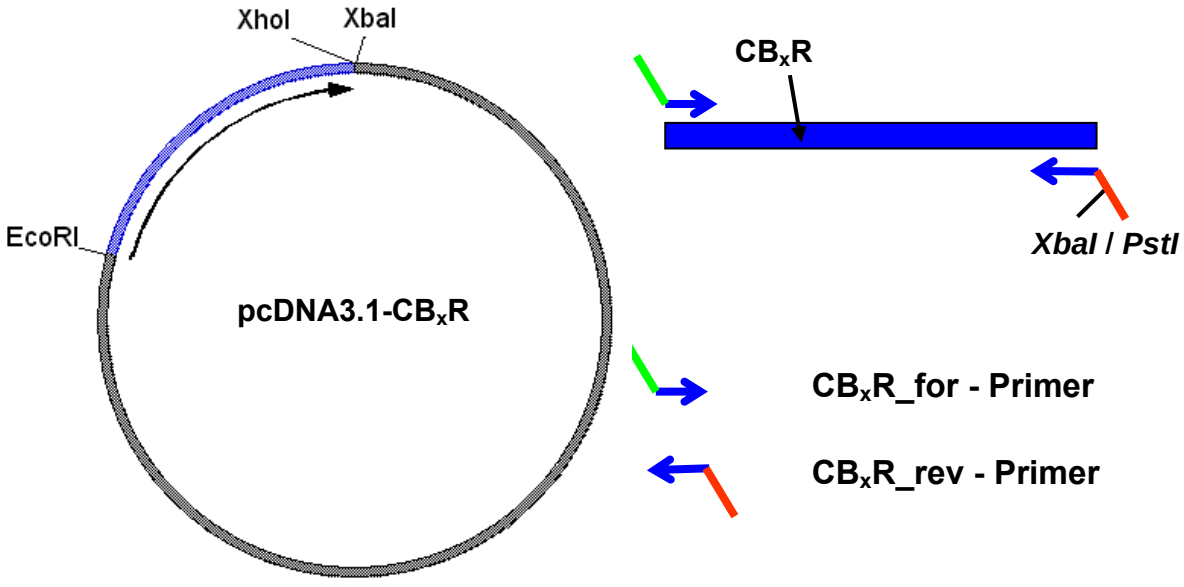

Fig. 10: Generation of the PCR 1B product.

PCR 1A and 1B were performed using the following program:

1.	5 min	95°C
2.	1 min	95°C
3.	1 min	53°C
4.	1 min (PCR 1A)	72°C
	2 min (PCR 1B)	72°C
5.	10 min	72°C
6.	hold	4°C

Steps 2. – 4. were repeated 25 times.

In PCR 2, the products of PCR 1A and 1B annealed in the region of the FLAG epitope using the primers F1 and CB_xR_rev, the respective reverse primer (see Fig. 11).

The PCR 2 tube was prepared by mixing 5 µl 1 mM dNTP-mix (Promega, Madison, WI, USA), 10 µl *Pfu* reaction buffer, 1 µl *Pfu* DNA polymerase solution (2.5 U/µl), 10 µl DMSO, 5 µl of sense and antisense primer (10 µM), 1.5 µl PCR 1A and 1.5 µl PCR 1B product and 61 µl DEPC-water. Polymerase chain reaction was performed using the same program as described above.

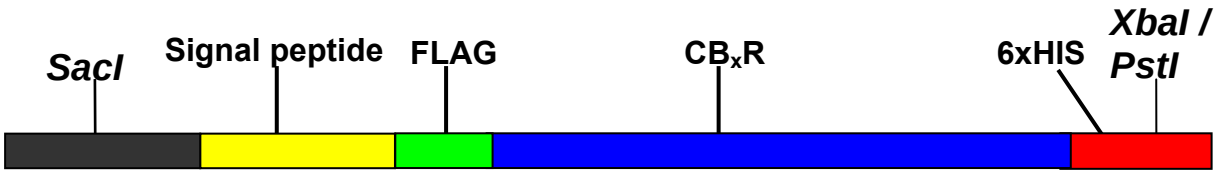

Fig. 11: Structure of the hCB_xR construct after PCR 2.

The product of PCR 2 and pGEM-3Z-$SFhH_4R$ were digested with *SacI* and *XbaI* (hCB_1R) or *SacI* and *PstI* (hCB_2R). Both double digested mixtures were electrophoretically separated on a preparative agarose gel. The expected bands were cut out of the gel and purified by the Qiagen PCR Purification Kit (Qiagen, Hilden, Germany). For the ligation of the hCBxR construct and the pGEM-3Z-$SFhH_4R$

vector, an insert to vector ratio of 3:1 was used. cDNAs for FLAG- and hexahistidine-tagged hCB_1R and hCB_2R were then cloned into the baculovirus transfer vector pVL1392 for transfection of Sf9 insect cells. PCR-generated DNA sequences were confirmed by extensive restriction enzyme analysis and enzymatic sequencing.

Table 1: Primer sequences used for overlap-extension PCR.

Primer	Sequence
F1 (sense)	5`-GCT CAC TCA TTA GGC ACC-3`
C3 (antisense)	5`-CAT GGC GTC ATC ATC GTC-3`
CB1_for (sense)	5`-GAC GAT GAT GAC GCC ATG AAG TCG ATC CTA GAT GG-3`
CB1_rev (antisense)	5`-AAT TCT CTA GAG GTC ACA GAG CCT CGG CAG ACG-3`
CB2_for (sense)	5`-GAC GAT GAT GAC GCC ATG GAG GAA TGC TGG GTG-3`
CB2_rev (antisense)	5`-TGG GCT GCA GTC AGT GAT GGT GAT GAT GGT GGC AAT CAG AGA G-3`

3.3.5 Generation of recombinant baculoviruses, cell culture and membrane preparation

Recombinant baculoviruses encoding FLAG- and hexahistidine-tagged hCB_1R and hCB_2R were generated in Sf9 cells using the BaculoGOLD transfection kit (BD PharMingen, San Diego, CA, USA) (Wenzel-Seifert et al., 1999; Wenzel-Seifert and Seifert, 2000; Seifert and Wenzel-Seifert, 2001). After initial transfection, high-titer virus stocks were generated by two sequential virus amplifications. In the first amplification, cells are seeded at 2.0 x 10^6 cells/ml and infected with a 1:100 dilution of the supernatant of the culture following initial transfection. 7 days after the transfection, all cultured cells died releasing virus to the medium. Efficient transfections can be observed visually because infected cells change their morphology from round cells forming a confluent monolayer to enlarged or lysed cells (see Fig. 12). The virus containing supernatant of the first amplification, was harvested by centrifugation for 10 min at 3,000 x g. The obtained supernatant was used in a 1:20 dilution for the second amplification, where cells are seeded at 3.0 x 10^6 cells/ml. After 48 h, the supernatant was harvested as described above. Cells showed signs of infection but not all cells were lysed after 48 h. The supernatant of the second amplification was used for all further transfections and membrane preparations. All supernatants containing baculoviruses were stored at 4°C and, if protected from light, can be kept for up to 5 years without loss of potency.

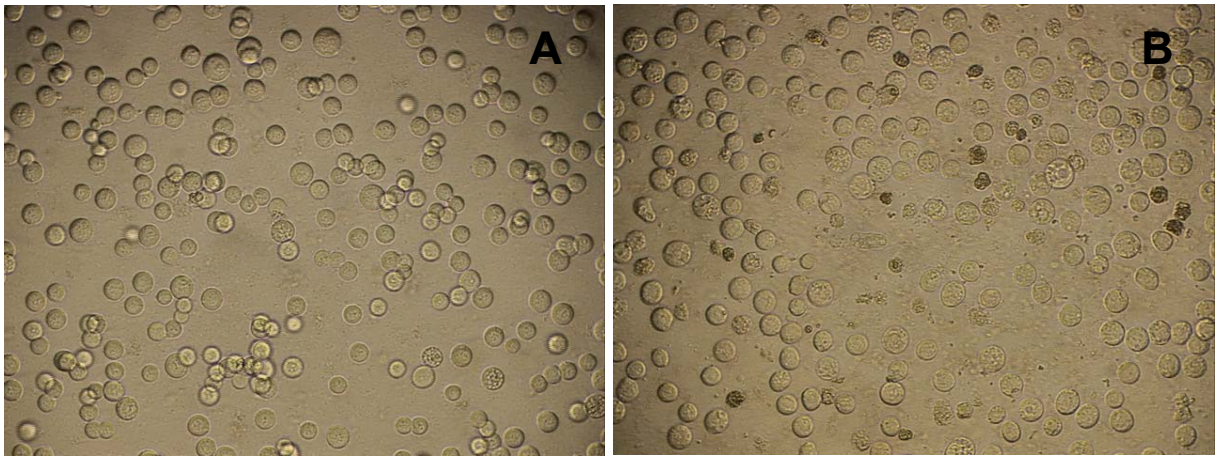

Fig. 12: Uninfected Sf9 cells (A) and Sf9 cells after transfection with recombinant baculoviruses (B), (adapted from Dr. A. Gille).

Generally, Sf9 cells were cultured in 250 ml disposable Erlenmeyer flasks at 28°C shaking at 125 rpm in an incubation shaker (New Brunswick Scientific, model C24KC, Edison, NJ, USA) in SF 900 II medium supplemented with fetal calf serum to 5% (v/v) and gentamicin sulfate to 0.1 mg/ml. Supplementation of fetal calf serum is not absolutely necessary, but cells grow better and show higher GPCR expression levels if serum is added. Sf9 cells were maintained at a density of 0.5 to 6.0 x 10^6 cells/ml. For transfection, cells were seeded at 3.0 x 10^6 cells/ml and infected with a 1:100 dilution of high-titer baculovirus stocks encoding either hCB_1R or hCB_2R as well as $G\alpha_o$- or $G\alpha_{i2}$- and $G\beta_1\gamma_2$-protein. In some transfections, RGS4 or GAIP were additionally coexpressed. Cells were cultured for 48 h and checked for signs of infection before membrane preparation. Sf9 membranes were prepared as described previously (Wenzel-Seifert and Seifert, 2000). All membrane preparation steps were conducted at 4°C in 50 ml Falcon tubes. Briefly, cells were washed once by centrifuging for 10 min at 170 x g, discarding the supernatant and resuspending the cell pellet in 50 ml PBS-buffer. After repeating the centrifugation step, the supernatant was discarded and the pellet was suspended in 15 ml lysis buffer and homogenized in a 15 ml Dounce homogenizer with 25 strokes. After centrifugation at 40 x g for 5 min the pellet contained the nuclei and unbroken cells and the supernatant contained the membranes. Therefore, the supernatant was carefully transferred to a plastic Sorvall tube and spun down by 38,500 x g for 20 min in a Sorvall centrifuge. The pellet containing the membranes was resuspended in 20 ml lysis buffer and again centrifuged as described above. The resulting membrane pellet was suspended in 25 ml binding buffer and homogenized by a syringe with 20 strokes. Protein concentrations were determined using the DC protein assay kit (BioRad, Hercules, CA, USA) according to the instructions of the manufacturer. This assay allows the protein determination in presence of reducing agents or detergents and is based on a colorimetric reaction according to the Lowry method.

The membrane suspension was aliquoted into 25 tubes at 1 ml each for storage at -80°C until use. At -80°C, GPCRs and G-proteins are functionally and structurally stable for up to 4 years. By SDS-PAGE and immunoblotting with specific antibodies the expression of FLAG-tagged cannabinoid receptors, G-protein subunits and RGS-proteins was confirmed (see Chapter 4.1.1).

3.3.6 SDS-PAGE and immunoblot analysis

Membrane proteins were separated on 0.1% (m/v) SDS polyacrylamide gels containing 12% (w/v) acrylamide at 110 V for 150 min (Wenzel-Seifert et al. 1999; Wenzel-Seifert and Seifert 2000; Seifert and Wenzel-Seifert 2001). Proteins were transferred onto Immobilon-P membranes (Millipore, Bedford, MA, USA) at 0.15 A for 120 min at 4°C. Non-specific binding sites were blocked for 2 h before proteins reacted with specific antibodies, M1 antibody (1:1,000), CB_1R or CB_2R antibody (both 1:1,000), anti-$G\alpha_o$, anti-$G\alpha_{i\ common}$, anti-RGS4, anti-GAIP Ig (all 1:500) or anti-$G\beta_{common}$ (1:2,000). Immunoreactive protein bands were visualized by enhanced chemoluminescence (Pierce, Rockford, IL, USA) using goat anti-mouse IgG for the M1 antibody, donkey anti-rabbit IgG for CB_1R/CB_2R, anti-$G\alpha$ and anti-Gβ Igs; and donkey anti-goat IgG for anti-RGS4 and anti-GAIP Igs coupled to peroxidase.

3.3.7 Handling of cannabinoid receptor ligands

Almost all commercially available CBR ligands are highly lipophilic. Their solubility in water is very low, which implies dissolving them in aequous solutions, such as binding buffer, is not possible at all. However, solubility in DMSO or ethanol is sufficient to prepare at least 1 mM stock solutions. Ethanol has several disadvantages relative to DMSO. Firstly, ethanol evaporates easily, making it difficult to ensure accurate concentrations present in either stored stock solutions or dilutions. Secondly, ethanol is toxic for cell proteins, whereas DMSO can be used in concentrations up to 5% (v/v) in Sf9 cell membranes without affecting receptor protein function.

Therefore, stock solutions of CBR ligands (10 mM each) were prepared in dimethyl sulfoxide and stored at -20°C for up to 3 months without loss of pharmacological activity. Dilutions of ligands were prepared in such a way that the dimethyl sulfoxide concentration was 30% (v/v) and that the final dimethyl sulfoxide concentration in all assay tubes was 3% (v/v). A final volume percentage of 3% DMSO assured accurate and stable solutions without affecting the receptor protein. Lowering the DMSO concentration to 1% (v/v) resulted in cloudy suspensions when diluting ligands.

Some CBR ligands, such as anandamide or Δ^9-THC are oily and therefore presolved in ethanol. Therefore, ethanol was completely removed and compounds were subsequently dissolved in DMSO to obtain 10 mM stock solutions.

3.3.8 [^{3}H]CP 55,940 competition binding assay

Membranes were thawed, sedimented by centrifugation at 18,000 x g for 10 min at 4°C, and carefully resuspended in 10 mM Tris/HCl, pH 7.4. Assay tubes contained Sf9 membranes expressing either hCB_1R and hCB_2R (5 - 30 µg protein/tube), 0.2% (m/v) bovine serum albumin, 3% (v/v) dimethyl sulfoxide, 1 nM [^{3}H]CP 55,940, and varying concentrations of unlabeled CP 55,940 in 500 µl binding buffer (12.5 mM $MgCl_2$, 1 mM EDTA, and 75 mM Tris/HCl, pH 7.4). For saturation binding assays and determination of B_{max} values 10 nM [^{3}H]CP 55,940 was used. Bovine serum albumin was added to prevent absorption of membrane protein to assay tubes. Non-specific binding was determined in the presence of 1 µM unlabeled CP 55,940. Incubations were conducted for 90 min at 25°C and shaking at 250 rpm on a platform shaker (Innova™ 2000, New Brunswick Scientific, Edison, NJ, USA). Assays were stopped by filtration through GF/C filters soaked in 0.05% (m/v) polyethyleneimine, followed by three washes with 2 ml of ice-cold (4°C) binding buffer. Filter-bound [^{3}H]CP 55,940 was determined by liquid scintillation with Rotiszint® eco plus cocktail (Roth Chemie, Karlsruhe, Germany) after at least 4 hours of equilibration at room temperature. Non-specific binding amounted to ~10% of total binding.

Absolute agonist binding (pmoles of CP 55,940 bound per mg of membrane protein) was calculated as follows:

$$\frac{pmol}{mg} = \frac{(cpm\ total - cpm\ nonspecific) \times pmol\ [^3H]CP}{cpm\ added \times mg\ \ protein}$$

Equation 1

Explanations:

cpm total:	filter-bound radioactivity of [^{3}H]CP 55,940 from assay tubes, except from those tubes containing 1 µM CP 55,940
cpm non-specific:	filter-bound radioactivity of [^{3}H]CP 55,940 from assay tubes containing 1 µM CP 55,940
pmol [^{3}H]CP:	absolute amount of [^{3}H]CP 55,940 present in the assay tubes (0.5 pmoles in competition binding assays, 5.0 pmoles in saturation binding assays)
cpm total added:	the radioactivity of [^{3}H]CP 55,940 added to each tube (no filtration)
mg protein:	absolute amount of membrane protein added per tube (0.005 – 0.030 mg)

3.3.9 GTPγS binding assay

The GTPγS binding assay was performed as described previously (Wenzel-Seifert et al., 1999; Wenzel-Seifert and Seifert, 2000; Seifert and Wenzel-Seifert, 2001). Briefly, membranes were thawed, sedimented by centrifugation at 18,000 x g for 10 min at 4°C, and carefully resuspended in 10 mM Tris/HCl, pH 7.4. In GTPγS saturation binding experiments, assay tubes contained 0.2% (m/v) bovine serum albumin, 3% (v/v) dimethyl sulfoxide, 15 µg of membrane protein, 0.4 nM [^{35}S]GTPγS, unlabeled GTPγS at various concentrations and 1 µM GDP in 500 µl binding buffer (12.5 mM $MgCl_2$, 1 mM EDTA, and 75 mM Tris/HCl, pH 7.4) in the presence and absence of CBR ligands.

For time course studies, Sf9 membranes (15 µg of protein/tube) were suspended in binding buffer supplemented with 0.2% (m/v) BSA, 3% (v/v) DMSO, 0.6 nM [^{35}S]GTPγS plus 4.4 nM unlabeled GTPγS and 1 µM GDP in the presence and absence of CBR ligands (10 µM each). Aliquots of 200 µl were withdrawn at several time points.

In GDP competition binding assays, the affinity of $G\alpha_{i2}$ for GDP was determined in the presence of 0.2 nM [^{35}S]GTPγS and varying concentrations of GDP ranging from 1 nM to 10 µM in the absence or presence of 10 µM CP 55,940. Non-specific binding was taken as total binding in the presence of 10 µM unlabeled GDP and amounted to

less than 1% of total binding. Reactions were stopped by filtration through GF/C filters equilibrated with binding buffer. After filtration, filters were washed three times with 2 ml of ice-cold (4°C) binding buffer. Filter-bound radioactivity was determined by liquid scintillation counting in Rotiszint® eco plus cocktail after at least 4 hours of equilibration.

Absolute ligand binding (pmoles of [^{35}S]GTPγS bound per mg of membrane protein) was calculated as follows:

$$\frac{pmol}{mg} = \frac{(cpm\ total - cpm\ nonspecific) \times pmol\left[^{35}S\right]GTP\gamma S}{cpm\ added \times mg\ \ protein}$$

Equation 2

Explanations:

cpm total:	filter-bound radioactivity of [^{35}S]GTPγS from assay tubes, except from those tubes containing 10 µM GTPγS
cpm non-specific:	filter-bound radioactivity of [^{35}S]GTPγS from assay tubes containing 10 µM GTPγS
pmol [^{35}S]GTPγS:	absolute amount of [^{35}S]GTPγS present in the assay tubes, including any unlabeled GTPγS (0.2 pmoles in saturation binding assays, 2.5 pmoles in time course studies)
cpm total added:	the radioactivity of [^{35}S]GTPγS added to each tube (no filtration)
mg protein:	absolute amount of membrane protein added per tube (0.015 mg)

3.3.10 Steady-state GTPase assay

The steady-state GTPase assay is an established approach to study G-protein coupling of GPCRs at a very proximal point of the signal transduction cascade. The GTPase assay was performed as described previously (Wenzel-Seifert et al., 1999). Membranes were thawed, sedimented by centrifugation at 18,000 x g for 10 min at 4°C, and carefully resuspended in 10 mM Tris/HCl, pH 7.4. Assay tubes contained Sf9 membranes (15 µg of protein/tube), 1.0 mM $MgCl_2$, 0.1 mM EDTA, 0.1 mM ATP, 100 nM GTP, 0.1 mM adenylyl imidodiphosphate, 5 mM creatine phosphate, 40 µg of creatine kinase, 0.2% (w/v) bovine serum albumin in 50 mM Tris/HCl, pH 7.4, and CB_1R and CB_2R ligands at various concentrations. To determine the constitutive activity of hCBRs half of the assay tubes additionally contained 150 mM NaCl. Reaction mixtures (80 µl) were incubated for 2 min at 25°C before the addition of 20 µl of [γ-^{32}P]GTP (0.1 µCi/tube). All stock and work dilutions of [γ-^{32}P]GTP were prepared in 20 mM Tris/HCl, pH 7.4. Reactions were conducted for 20 min at 25°C. Reactions were terminated by the addition of 900 µl of slurry consisting of 5% (w/v) activated charcoal and 50 mM NaH_2PO_4, pH 2.0. Charcoal absorbs nucleotides but not $^{32}P_i$. Charcoal-quenched reaction mixtures were centrifuged for 7 min at room temperature at 15,000 x g. Sixhundred µl supernatant fluid of reaction mixtures was removed, and $^{32}P_i$ was determined by Čerenkov radiation in 3 ml water. Enzyme activities were corrected for spontaneous degradation of [γ-^{32}P]GTP. Spontaneous [γ-^{32}P]GTP degradation was determined in tubes containing all of the above described components plus a high concentration of unlabeled GTP (1 mM) that, by competition with [γ-^{32}P]GTP, prevents [γ-^{32}P]GTP hydrolysis by enzymatic activities present in Sf9 membranes. Spontaneous [γ-^{32}P]GTP degradation amounted to <1% of the total amount of radioactivity added. The experimental conditions chosen ensured that not more than 10% of the total amount of [γ-^{32}P]GTP added was converted to $^{32}P_i$.

GTPase activity (pmoles of P_i released per mg of membrane protein per min) was calculated as follows:

$$\frac{pmol}{mg \times min} = \frac{(cpm\ total - cpm\ GTP) \times pmol\ GTP\ unlabeled \times 1.67}{cpm\ added \times min\ incubation \times mg\ \ protein}$$

Equation 3

Explanations:

cpm total:	radioactivity of [γ-^{32}P]GTP counted in the 600 µl aliquot taken from all assay tubes except those containing 1 mM GTP
cpm GTP:	radioactivity of [γ-^{32}P]GTP counted in the 600 µl aliquot taken from the assay tubes containing 1 mM GTP
pmol GTP unlabeled:	absolute amount of substrate present in the assay tubes; i.e. with 100 nM GTP, 10 pmoles of GTP were present in the 100 µl reaction mixture
1.67:	factor correcting the fact that only 600 µl out of 1000 µl in the assay tubes were counted
cpm total added:	the radioactivity of [γ-^{32}P]GTP added to each tube (no charcoal addition)
min incubation:	assays were routinely conducted for 20 min
mg protein:	absolute amount of membrane protein added per tube (0.015 mg)

3.3.11 AC assay

AC assays were performed in order to determine the next step of the signaling cascade, after measuring the activation of Gα-subunits by steady-state GTPase and GTPγS binding assays. The AC assay was performed as described previously (Seifert et al., 1998). Briefly, Sf9 cell membranes coexpressing CBRs were thawed, sedimented by centrifugation at 18,000 x g for 10 min at 4°C, and resuspended in assay buffer (12.5 mM $MgCl_2$ and 1 mM EDTA in 75 mM Tris/HCl, pH 7.4). Assay tubes contained Sf9 membranes (50 - 60 µg) and 10 µM GTP to activate $G\alpha_{i2}$. Prestimulation of $G\alpha_{i2}$ was obtained by addition of 10 µM or 100 µM forskolin. AC activity was determined under basal conditions (3% (v/v) DMSO served as control) or in the presence of CB_1R and CB_2R ligands (dissolved in 3% (v/v) DMSO). The final sample volume was 50 µl. Every assay tube contained 5 µl of ligand (10 µM final) or control and 5 µl of forskolin (10 µM or 100 µM final). To every tube 20 µl of a concentrated reaction mixture (2.5x) was added to obtain the following final concentrations: 0.2 – 0.3 µCi/tube of [α-^{32}P]ATP, 40 µM of unlabeled ATP, 0.1 mM cAMP, 2.9 mM of mono(cyclohexyl)ammoniumphosphoenolpyruvate, 0.214 IU pyruvate kinase and 0.67 IU myokinase. Tubes were incubated for 2 min at 37°C, before starting the reactions by adding 20 µl homogenized membrane solutions in binding buffer. Reactions were carried out in hexaplicates at 37°C for 20 min and terminated by addition of 20 µl 2.2 N HCl. Denatured membrane protein was sedimented by a 1 min centrifugation step at room temperature and 15,000 x g. [^{32}P]cAMP was separated from [α-^{32}P]ATP by column chromatography. Columns were filled with 1.4 g of neutral alumina (MP Biomedicals, Eschwege, Germany). [^{32}P]cAMP was eluted into 20 ml scintillation counting tubes by addition of 4 ml 0.1 M ammonium acetate solution, pH 7.0. [^{32}P]cAMP was determined by Čerenkov radiation in water. Blank values were <0.01% of the total amount of [α-^{32}P]ATP added and less than 0.1% of the total amount of [α-^{32}P]ATP was converted to [^{32}P]cAMP.

AC activity (pmoles of cAMP formed per mg of membrane protein per min) was calculated as follows:

$$\frac{pmol}{mg \times min} = \frac{(cpm\ total - cpm\ blank) \times pmol\ ATP\ unlabeled \times 1.17}{cpm\ added \times min\ incubation \times mg\ protein}$$

Equation 4

Explanations:

cpm total:	radioactivity of [^{32}P]cAMP counted in the 50 µl aliquot analysed by column chromatography from all tubes except blank tubes
cpm blank:	radioactivity of [^{32}P]cAMP counted in the 50 µl aliquot analysed by column chromatography from tubes containing no membranes
pmol ATP unlabeled:	absolute amount of substrate present in the assay tubes; i.e. with 40 µM ATP, 2000 pmoles of ATP were present in the 50 µl reaction mixture
1.17:	factor correcting the fact that only 60 µl out of 70 µl in the assay tubes were counted
cpm total added:	the radioactivity of [α-^{32}P]ATP added to each tube (no processing through alumina column)
min incubation:	assays were routinely conducted for 20 min
mg protein:	absolute amount of membrane protein added per tube (0.05 – 0.06 mg)

3.3.12 Miscellaneous

Experimental data were analysed by non-linear regression using the Prism 4.02 program (GraphPad Software, San Diego, CA, USA). [^{3}H]Dihydroalprenolol saturation binding was determined as described (Wenzel-Seifert and Seifert, 2000). Expression levels of recombinant proteins were determined using the BioRad GS-710 Calibrated Imaging Densitometer and the BioRad software tool Quantity One Version 4.0.3.

3.4 Phytochemical materials and methods

3.4.1 Phytochemical materials

Echinacea pallida roots were a kind gift by Martin Bauer (type nr.: 119966). Drug material was milled to powder (Retsch ZM1, Retsch, Haan, Germany) with a particle size smaller than 1.5 mm before extracting. All solvents for the extraction of the plant material were pure grade or purified by distillation prior to use.

TLC analysis was done with Silica gel 60 RP-18 F_{254}s aluminium sheets (Merck, Darmstadt, Germany). Bands were first detected by fluorescence extinction using an UV lamp at 254 nm, then by spraying 1% (m/v) vanillin in EtOH (96%) and 2% (v/v) H_2SO_4 (95-97%) and heating the plates at 110°C for 5 min. For vacuum liquid chromatography (VLC) Geduran Si 60 (63 – 200 µM) and for RP-18 column chromatography LiChroprep RP18 (40 – 63 µM) column material was used (Merck, Darmstadt, Germany).

Dodeca-2*E*,4*E*-dienoic acid isobutylamide (2 mM (m/v) in DMSO) and *Echinacea purpurea n*-hexane root extract (10 mg/ml in DMSO) were a kind gift of Dr. J. Gertsch, ETH Zurich, Switzerland.

Synthesized compounds were provided by M. Egger and P. Pellett, Institute for Organic Chemistry, Prof. B. König, University of Regensburg, Germany (for structure and name of the compounds see Table 2 and Fig. 13 and 14).

Table 2: Names of synthesized compounds tested in the GTPase assay.

Compound	Name
1	**Pentadec-8*Z*-en-2-one**
2	**Pentadeca-8*Z*,11*Z*-dien-2-one**
3	Tridec-8*Z*-en-12-yn-2-one
4	Undec-8*Z*-en-10-yn-2-one
5	Henicosa-6*Z*,9*Z*,12*Z*,15*Z*-tetraen-2-one
6	8-Hydroxy-9,9-dimethyldecan-2-one
7	2-Methyl-2-(tridec-6*Z*-enyl)-1,3-dioxolane
8	2-Methyl-2-(trideca-6*Z*,9*Z*-dienyl-1,3- dioxolane
9	2-Methyl-2-(pentadeca-6*Z*,9*Z*-dienyl-1,3-dioxolane
10	2-Methyl-2-(non-6*Z*-ene-8-ynyl)-1,3-dioxolane
11	Trimethyl(9-(2-methyl-1,3-dioxolan-2-yl)non-3*Z*-en-1-ynyl)silane
12	2-Methyl-2-(9-phenylnon-6*Z*-en-8-ynyl)-1,3-dioxolane
13	2-Methyl-2-(10-(2-methyl-1,3-dioxolan-2-yl)dec-4*Z*-en-6-ynyl)-1,3-dioxolane
14	11-Phenylundec-8*Z*-en-10-yn-2-one

Bold names represent plant-derived compounds of *E. pallida* roots.

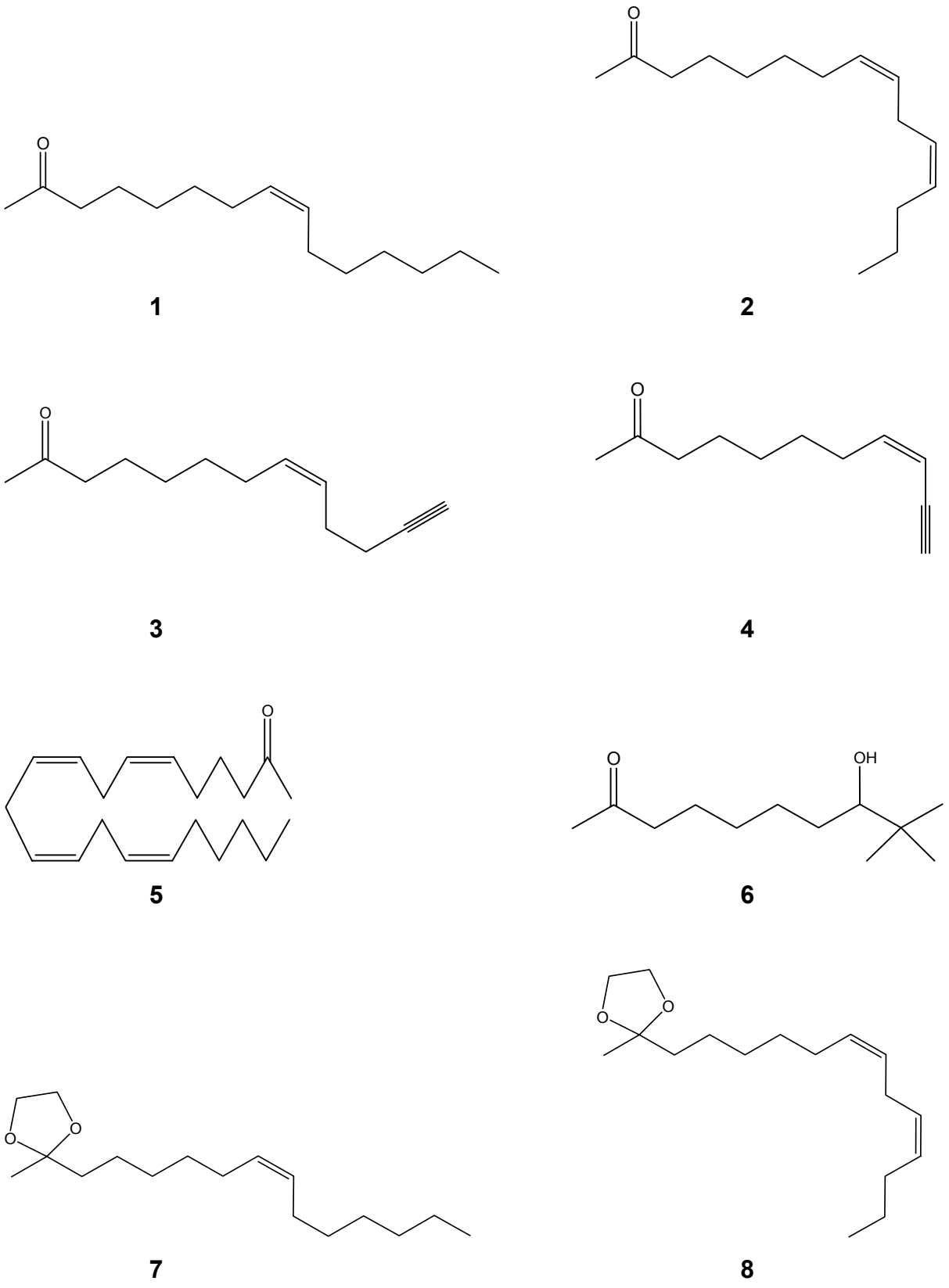

Fig. 13: Structures of synthesized compounds (1 - 8) tested in the GTPase assay.

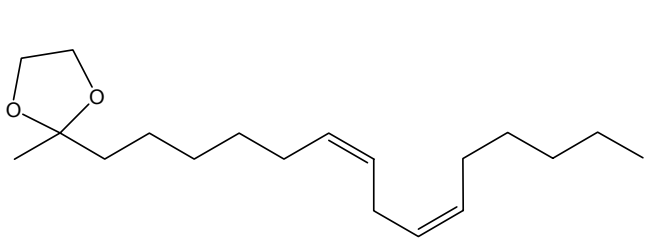

9

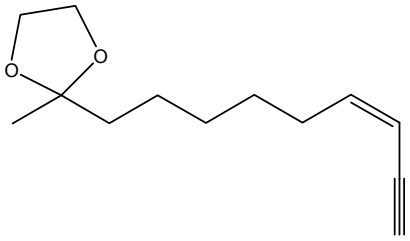

10

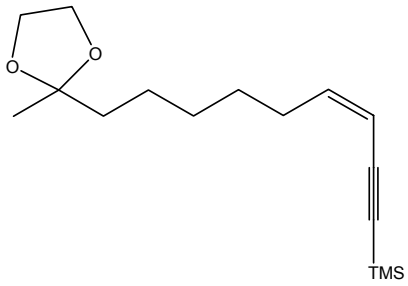

11

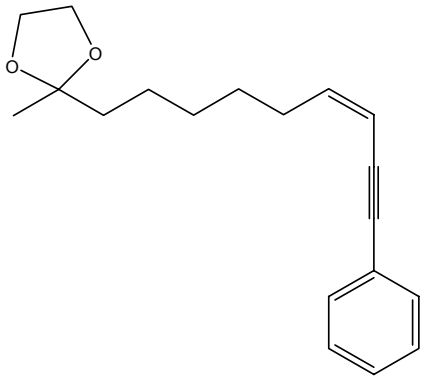

12

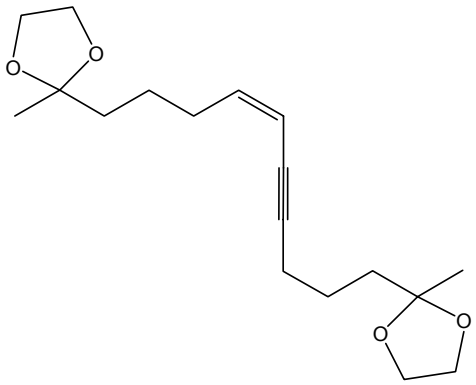

13

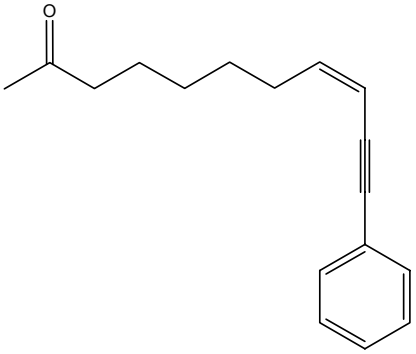

14

Fig. 14: Structures of synthesized compounds (9 - 14) tested in the GTPase assay.

3.4.2 Phytochemical methods

300 g of milled *E. pallida* roots were extracted by accelerated solvent extraction (ASE 100, Dionex, Idstein, Germany) with *n*-hexane yielding in 1.5 g *n*-hexane extract (0.5% (m/m) yield). The ratio of milled *E. pallida* roots to sea sand was 4:1. Extraction was performed at 50°C in 50 ml cells. Two static circles were done, flush volume was 60%, purge time was 200 seconds and static time was 5 min.

1.4 g of the *n*-hexane extract was subjected to vacuum liquid chromatography (VLC) on silica gel. The ratio of *n*-hexane extract to stationary phase was 1:90 (column length: 29.0 cm, diameter: 4.5 cm, height of the stationary phase: 17.0 cm). Seven different mobile phases (2 x 200 ml) with decreasing lipophilic properties were used to obtain a rough separation of the *n*-hexane extract (**A:** DCM, **B:** DCM : EtOAc 2:1, **C:** DCM : EtOAc 1:2, **D:** EtOAc, **E:** DCM : MeOH 2:1, **F:** DCM : MeOH 1:2, **G:** MeOH). The resulting 14 fractions after VLC (A1, A2, B1, etc.) were analysed by thin layer chromatography (TLC) and fractions with the same TLC profile were merged. Further separation of fractions containing alkenes or alkynes was done by RP-18 column chromatography (CC) with a ratio of VLC fraction to stationary phase of 1:400 (column length: 70.0 cm, diameter: 2.0 cm, height of the stationary phase: 34.5 cm). Fractions **C**, **D**, **G** obtained with DCM : EtOAc (1:2), EtOAc and MeOH did not contain alkenes or alkynes. Fraction **A2** (DCM) was further separated by a mobile phase of ACN, MeOH and H_2O in a ratio of 6:3:1. Fraction **B** (DCM : EtOAc 2:1), **E** (DCM : MeOH 2 : 1) and **F** (DCM : MeOH 1:2) were separated by a mobile phase of ACN, MeOH and H_2O in a ratio of 2:1:1. The resulting fractions were analysed by TLC and fractions containing the same compounds were combined. Fractions containing multiple compounds were analysed by NMR spectroscopy for the presence of ketoalkenes or ketoalkynes. Those NMR spectra, which showed the functionalities of those compounds, were analysed in the functional GTPase assay. However, none of the fractions showed any activity in the GTPase assay, hence no further separation by HPLC was performed.

3.4.3 NMR spectroscopy and mass spectrometry

All ^{1}H NMR experiments were recorded in $CDCl_3$ (Deutero, purity 99.8%) on a Bruker Avance 300 (operating at 300.13 MHz for ^{1}H) at 300.0 K and referenced against residual non deuterated solvent. The ^{13}C and 2D spectra for pentadec-8*Z*-en-2-one were measured on a Bruker Avance 400 (operating at 400.13 MHz for ^{1}H and 100.61 MHz for ^{13}C) at 300.0 K in the same solvent. Coupling constants (*J*) were given in Hz. LREIMS (70 eV) was measured on a MAT 710A.

3.4.4 Characterization of pentadec-8Z-en-2-one

Colourless oil (31 mg). TLC (ACN : MeOH : H_20 6 : 3 : 1.25) R_f = 0.26; ^{1}H NMR ($CDCl_3$, 300 MHz) δ 0.90 (3H, t, *J* = 6.0, C*H*$_3$), 1.30 (12H, m overlapping signals, 6 x C*H*$_2$), 1.55 (2H, m overlapping signals, C*H*$_2$), 2.05 (4H, m overlapping signals, 2 x C*H*$_2$), 2.12 (3H, s, COC*H*$_3$), 2.47 (2H, t, *J* = 7.3, C*H*$_2$CO), 5.34 (2H, m overlapping signals, *H*C=C*H*); ^{13}C NMR ($CDCl_3$, 75 MHz) 212.2 (*C*O), 131.1 (=*C*H), 130.6 (=*C*H), 44.3 (*C*H$_2$CO), 32.9 (*C*H$_2$), 30.8 (*C*H$_2$), 30.6 (*C*H$_2$) 30.0 (*C*H$_3$CO), 29.8 (*C*H$_2$), 29.8 (*C*H$_2$), 28.1 (*C*H$_2$), 28.0 (*C*H$_2$), 24.8 (*C*H$_2$), 23.7 (*C*H$_2$), 14.4 (*C*H$_3$); EI-MS (pos. mode) *m/z* 224 $[M]^+$ (<1), 125 $[M\text{-}C_7H_{15}]^+$ (10), 97 (13), 82 (16), 71 (29), 55 (33), 43 (100).

4 Results and Discussion

4.1 Establishment of the steady-state GTPase assay as a functional test system for cannabinoid receptors

4.1.1 Western blot analysis of cannabinoid receptors in Sf9 cell membranes

To establish a functional test system for CBRs, Sf9 cells were transfected with baculoviruses encoding the CB_1R or the CB_2R. As Sf9 insect cells do not express mammalian G-proteins, baculoviruses encoding for Gα- and Gβγ-protein were used for cotransfection of CBR cell cultures. As we were interested in the most effective coexpression system, some CBR cultures were transfected additionally with baculoviruses encoding RGS4 or GAIP.

All transfected cell cultures were harvested after 48 h incubation, the membranes expressing the receptor protein were prepared and hence analysed by immunoblotting. A representative immunoblot for the detection of CB_1R-, CB_2R-, $G\alpha_{i2}$-, RGS4- and GAIP- protein is shown in Fig. 15. Membranes used in assays were generally analysed by immunoblots to ensure correct transfection. For further analysis of CBR membranes and expression levels see Chapter 4.3.1.

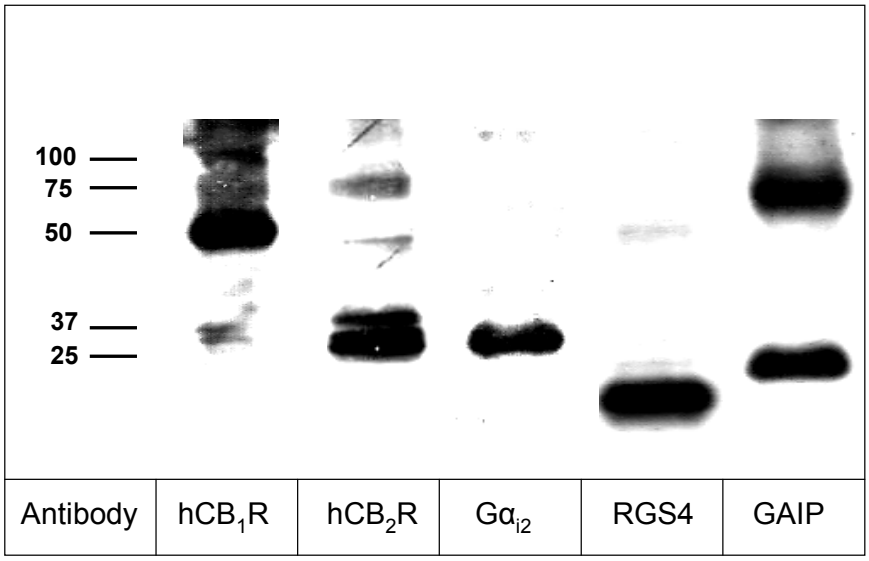

Fig. 15: Detection of expressed proteins in Sf9 cell membranes after transfection with baculoviruses encoding for CB_1R, CB_2R, $G\alpha_{i2}$, RGS4 and GAIP. Numbers on the left indicate the apparent molecular mass of marker proteins in kDa. Each lane represents 10 µg of protein.

4.1.2 Solubility of cannabinoid receptor ligands

Cannabinoid receptor ligands are highly lipophilic. Therefore, it is very important to dissolve them correctly. Commercially available stock solutions of CBR ligands are mostly prepared in 100% DMSO. The solvent DMSO can be used in concentrations up to 5% (v/v) without affecting receptor protein in Sf9 insect cell membranes. Initially, we prepared ligand solutions to achieve final DMSO concentration of 1% (v/v) in the experiments. However, in GTPase assays with ligand solutions containing 1% (v/v) DMSO final, the obtained results were not consistent. This was due to solubility problems of the lipophilic compounds. By increasing the final DMSO content from 1% (v/v) to 3% (v/v) final in the assays, clear solutions as well as reliable and consistent GTPase activation could be observed (data not shown).
Anandamide and Δ^9-THC are presolved in ethanol because they are oily and no solid compounds. Evaporating the ethanol and dissolving the oily residue in DMSO to obtain 10 mM stock solutions is necessary for stability.

4.1.3 Effect of different solvents on the solubility of CBR ligands assessed in the GTPase assay

It was described that cannabinoid receptor ligand solutions should contain at least 1 mg/ml BSA final to obtain stable solutions (Breivogel, 2006). Therefore, we compared the outcome of either 1 mg/ml BSA or 3% (v/v) DMSO in the functional GTPase assay.
As our test system should be capable of detecting predominantly CB_2R agonists, we compared 3 different agonists at both cannabinoid receptors (see Table 3 and Table 4).

For anandamide no differences could be found. Both solvents were equally effective on GTPase activation and $logEC_{50}$ values were not affected. Regarding the agonist CP 55,940 the $logEC_{50}$ value at CB_1R was higher in BSA solutions (-8.36 ± 0.19 vs. -7.93 ± 0.06, $p < 0.01$). The GTPase stimulation was higher in solutions containing 1 mg/ml BSA at CB_2R (114 ± 5% vs. 94 ± 4%, $p = 0.025$). For WIN 55,212-2, the $logEC_{50}$ value at CB_1R was higher in solutions containing 3% (v/v) DMSO (-7.38 ± 0.08 vs. -6.91 ± 0.05, $p = 0.01$).

Taken these results together, both 3% (v/v) DMSO and 1 mg/ml BSA were suitable for the preparation of cannabinoid receptor ligand solutions and neither of them resulted in a pharmacological difference. GTPase stimulation as measured in the GTPase assay was reliable and reproducible for both solvents. Also, all obtained $logEC_{50}$ values in this test system were in accordance with the values described in the literature.

However, the addition of BSA causes foamy solutions after mixing, which may result in inaccuracies when small volumes are pipetted (e.g. 10 µl in the GTPase assay). Also, BSA tends to adsorb to plastic, which might decrease the actual BSA concentration in the solutions.

The above described properties of BSA and the fact that most of the commercially available stock solutions are prepared in DMSO, led to the use of DMSO in a final concentration of 3% (v/v) DMSO for further experiments.

Table 3: Comparison of two solvents (1 mg/ml BSA and 3% (v/v) DMSO final) on GTPase activity of CB_1R.

Ligand	$CB_1R + G\alpha_{i2} + G\beta_1\gamma_2$ + RGS4	GTPase stimul. [%]	$logEC_{50}$	$logEC_{50}$ (literature)
Anandamide	**DMSO**	80 ± 8	-6.80 ± 0.10	-7.10
	BSA	73 ± 1	-6.64 ± 0.19	
CP 55,940	**DMSO**	63 ± 8	-7.93 ± 0.06**	-8.30
	BSA	71 ± 8	-8.36 ± 0.19**	
WIN 55,212-2	**DMSO**	69 ± 7	-7.38 ± 0.08*	-7.20
	BSA	87 ± 4	-6.91 ± 0.05*	

Shown is the stimulation of GTPase activity by 10 µM agonist compared to basal (3% (v/v) DMSO) GTPase activity. Data were analysed by nonlinear regression and best fit to sigmoidal concentration/response curves. The results are expressed as percentages of mean values ± S.D. and represent 3 independent experiments performed in triplicates with different membrane preparations (* $p = 0.01$, ** $p < 0.01$). Literature data was published by Tocris Cookson (www.tocris.com).

Table 4: Comparison of two solvents (1 mg/ml BSA and 3% (v/v) DMSO final) on GTPase activity of CB_2R.

Ligand	$CB_2R + G\alpha_{i2} + G\beta_1\gamma_2$ + RGS4	GTPase stimul. [%]	$logEC_{50}$	$logEC_{50}$ (literature)
Anandamide	**DMSO**	49 ± 6	-6.36 ± 0.44	-6.40
n = 5	**BSA**	51 ± 6	-5.92 ± 0.16	
CP 55,940	**DMSO**	94 ± 4*	-8.38 ± 0.10	-8.60
n = 3	**BSA**	114 ± 5*	-8.48 ± 0.09	
WIN 55,212-2	**DMSO**	95 ± 9	-8.59 ± 0.15	-8.50
n = 3	**BSA**	89 ± 8	-8.37 ± 0.06	

Shown is the stimulation of GTPase activity by 10 µM agonist compared to basal (3% (v/v) DMSO) GTPase activity. Data were analysed by nonlinear regression and best fit to sigmoidal concentration/response curves. The results are expressed as percentages of mean values ± S.D. and represent n = 3 - 5 independent experiments performed in triplicates with different membrane preparations (* $p = 0.025$). Literature data was published by Tocris Cookson (www.tocris.com).

4.1.4 Evaluation of the influence of Gα-subunits ($G\alpha_o$, $G\alpha_{i2}$) and GTPase-activating proteins (GAPs) on the GTPase activation of hCB_1R and hCB_2R

As cannabinoid receptors are $G_{i/o}$-protein-coupled GPCRs, we compared the coexpression of $G\alpha_o$- and $G\alpha_{i2}$-subunits in Sf9 insect cells. We were further interested in the potential effects of GTPase-activating proteins (GAPs) on the GTPase activity stimulated by cannabinoid receptors. We chose to investigate the effect of two different GAPs, also named RGS-proteins (regulators of G-protein signaling-proteins), RGS4 and RGS19 (GAIP).

Expression of the $G\alpha_o$-subunit resulted in a low GTPase activation by 10 µM CP 55,940 (20 ± 6% for hCB_1R and 27 ± 4% for hCB_2R). The expression of $G\alpha_{i2}$ increased the GTPase activity to 53 ± 13% for hCB_1R and 68 ± 5% for hCB_2R (see Table 5).

The effect of GTPase-activating proteins on GTPase activation was dependent of the coexpressed RGS-protein. Coexpression of CBRs and RGS4 was beneficial for all six constructs, with the highest increase in GTPase activity for membranes coexpressing $G\alpha_{i2}$ and RGS4 (hCB_1R: 70 ± 5%, hCB_2R: 84 ± 7%). This increase in GTPase activation was statistically significant for the CB_2R, comparing the $G\alpha_o/G\alpha_{i2}$ + $G\beta_1\gamma_2$ + RGS4 construct ($p = 0.01$).

GAIP, the other investigated RGS-protein, only resulted in a stimulation of GTPase activity for the CB_1R + $G\alpha_o$ + $G\beta_1\gamma_2$ construct (20 ± 6% vs. 49 ± 3%). For the other five constructs, the GTPase activation stayed at the same level as without RGS-protein.

$logEC_{50}$ values were not statistically different for the CB_1R analysing the 6 different membrane constructs. For the CB_2R the $logEC_{50}$ value for the $G\alpha_o$ + $G\beta_1\gamma_2$ construct was higher ($p < 0.05$) compared to the other membranes.

Table 5: Effect of Gα-subunits and RGS-proteins on GTPase activity.

	hCB_1R		hCB_2R	
	CP 55,940		**CP 55,940**	
Membrane	**10 µM [%]**	**$logEC_{50}$**	**10 µM [%]**	**$logEC_{50}$**
$G\alpha_o$	20 ± 6	-7.45 ± 0.64	27 ± 4	-8.73 ± 0.14*
	n=3		n=4	
$G\alpha_o$ + RGS4	67 ± 15	-7.81 ± 0.30	54 ± 8**	-8.38 ± 0.22
	n=3		n=6	
$G\alpha_o$ + GAIP	49 ± 3	-7.74 ± 0.19	31 ± 5	-7.86 ± 0.17
	n=3		n=7	
$G\alpha_{i2}$	53 ± 13	-8.07 ± 0.05	68 ± 5	-8.29 ± 0.11
	n=3		n=10	
$G\alpha_{i2}$ + RGS4	70 ± 5	-8.01 ± 0.41	84 ± 7**	-8.11 ± 0.12
	n=3		n=11	
$G\alpha_{i2}$ + GAIP	55 ± 6	-8.02 ± 0.20	63 ± 5	-7.92 ± 0.29
	n=3		n=8	

Shown is the stimulation of GTPase activity by CP 55,940 (10 µM) compared to basal (3% (v/v) DMSO) GTPase activity. Each membrane preparation contained additionally $G\beta_1\gamma_2$-protein. Data were analysed by nonlinear regression and best fit to sigmoidal concentration/response curves. The results are expressed as percentages of mean values ± S.D. and represent n = 3 experiments for CB_1R and n = 4 - 11 experiments for CB_2R performed in triplicates with different membrane infections (* $p < 0.05$ for the $logEC_{50}$ value $CB_2R + G\alpha_o + G\beta_1\gamma_2$ compared to the other five constructs, ** $p = 0.01$ for the GTPase activation by $CB_2R + G\alpha_o/G\alpha_{i2} + G\beta_1\gamma_2$ + RGS4).

At least 25 proteins with RGS domain are known, but they are highly diverse in their structure, expression levels and functions, e.g. not all RGS-proteins activate the GTPase function of Gα-subunits. RGS-proteins mainly interact with G_i- and G_o-proteins and accelerate the GTPase activity of Gα of the heterotrimeric G-protein by enhancing the cleavage of P_i. RGS4 and RGS19 (GAIP), which were used in our assays, belong to different classes of RGS-proteins. RGS4 is a small protein with no further functionalities than the RGS domain. GAIP also contains a cysteine string motif which may be palmitoylated and may improve membrane anchoring (Berman et al., 1996; Srinivasa et al., 1998; Traynor and Neubig, 2005). In general, RGS-proteins act as "allosteric activators" at the Gα-GTP complex by facilitating the hydrolysis of GTP to GDP. If GTP is hydrolyzed the signal process is terminated. Hence, RGS-proteins increase the signal cascade by increasing the hydrolysis of GTP to GDP and P_i at the Gα-protein (Berman and Gilman, 1998).

For cannabinoid receptors coexpressed with $G\alpha_o$-protein, GTP hydrolysis apparently was the rate-limiting factor as coexpression of RGS4 increased the GTPase activity up to 3.5 fold at the $G\alpha_o$-protein (CB_1R: 20 ± 6%→ 67 ± 15%, CB_2R: 27 ± 4%→ 54 ± 8%). The effect was even more pronounced when CBRs were coexpressed with $G\alpha_{i2}$ and RGS4 compared to $G\alpha_o$ without RGS4 (CB_1R: 20 ± 6%→ 70 ± 5%, CB_2R: 27 ± 4%→ 84 ± 7%), see Table 5.

GAIP strongly activates $G\alpha_{i3}$ and only weakly $G\alpha_{i2}$ proteins (De Vries et al., 1995). This is in accordance to our findings in Table 5, where GAIP had no effect on $G\alpha_{i2}$ systems. It is known that a posttranslational processing and hence activation is necessary for GAIP. Sf9 insect cells may only perform an incomplete posttranslational processing, which was sufficient for activation of the CB_1R + $G\alpha_o$ + $G\beta_1\gamma_2$ system but not for the CB_2R + $G\alpha_o$ + $G\beta_1\gamma_2$ system.

We did not observe a statistically significant effect of RGS-proteins on $logEC_{50}$ values, except for a higher $logEC_{50}$ value coexpressing CB_2R and $G\alpha_o$ without RGS-proteins. Generally, RGS-proteins should not affect $logEC_{50}$ values, because they only increase the intrinsic GTPase activity of Gα-subunits, but not the affinity of ligands for the receptor itself (Berman and Gilman, 1998).

4.2 Analysis of potencies and efficacies of agonists and antagonists/inverse agonists by steady-state GTPase assay

The comparison of different Gα-proteins and different RGS-proteins showed that coexpression of $G\alpha_{i2}$, $G\beta_1\gamma_2$ and RGS4 increased GTPase activity catalyzed by CBRs most efficiently (see Chapter 4.1.4). Hence, we chose this combination for further analysis of cannabinoid receptor ligands to assess the suitability of our test system.

We compared a plant-derived agonist (Δ^9-THC), endogenous agonists (anandamide, 2-AG), synthetic agonists (CP 55,940, WIN 55,212-2), as well as synthetic antagonists at CB_1R (AM 251, AM 281) and at CB_2R (AM 630), for results see Table 6.

2-AG, the most abundant endogenous agonist, acted as a full agonist with similar potency at both CBRs. E_{max} values of all other ligands were related to the GTPase activation by 2-AG (E_{max} set 100%).

Δ^9-THC acted as a partial agonist at CBRs, but had a higher efficacy at CB_1R than CB_2R (CB_1R: 71 ± 5%, CB_2R: 51 ± 11%). This finding was in accordance to literature (Felder and Glass, 1998; McPartland and Glass, 2003; Pertwee, 2008).

Interestingly, AEA acted as a “superagonist” at CB_1R (116 ± 19%) and as a partial agonist at CB_2R (66 ± 15%). This higher efficacy of AEA at CB_1R was statistically significant ($p = 0.02$) and in contrast to existing literature, where AEA behaved as a partial agonist at both CBRs (Zygmunt et al., 1999; Smart et al., 2000). Superagonism, a higher efficacy ($E_{max} > 100\%$) than the endogenous most abundant ligand, has been already described for amthamine at canine H_2R (Preuss et al., 2007).

At CB_1R, CP 55,940 and WIN 55,212-2 were full agonists (91 ± 21% and 100 ± 17%) with EC_{50} values in the low nM range, which is in accordance to literature (Felder et al., 1995; Griffin et al., 1998). At CB_2R, both CP 55,940 and WIN 55,212-2 were superagonists compared to 2-AG (118 ± 19% and 129 ± 21%). This result is in contrast to literature, where mostly no different efficacy of those ligands at CBRs was described (Rinaldi-Carmona et al., 1994; Felder et al., 1995). However, Song et al. showed that WIN 55,212-2 was more efficacious at CB_2R and explained this finding by an amino acid residue change from valine in CB_1R to phenylalanine in CB_2R at position 46 in transmembrane helix 5 (Song et al., 1999).

AM 251 and AM 281 were described as selective CB_1R antagonists with strong inverse agonist properties (Cosenza et al., 2000; Howlett et al., 2002). This finding was also demonstrated in our system, as AM 251 reduced GTPase acitivity by -83 ± 3% and AM 281 by -58 ± 2%. As AM 251 acted as a stronger inverse agonist at CBRs than AM 281, the E_{max} of GTPase inhibition by AM 251 was set -100%. Hence, AM 281 acted as a strong partial inverse agonist at CB_1R (Emax -70 ± 2%).
AM 630 behaved as a selective CB_2R antagonist with only weak inverse agonistic behaviour by an inhibition of GTPase activity of only -25 ± 6%. The E_{max} value for AM 630 was also small with -30 ± 7% when related to the efficacy of AM 251. This finding is in accordance with the literature (Ross et al., 1999; Howlett et al., 2002).

In summary, we compared agonists from 4 different classes of CBR ligands (classic: Δ^9-THC, non-classic: CP 55,940, aminoalkylindoles: WIN 55,212-2, eicosanoids: anandamide and 2-AG) as well as antagonists/inverse agonists at either CB_1 or CB_2 receptors in the functional steady-state GTPase assay. In general, our findings agree with literature data. We revealed partial agonism at CBRs (Δ^9-THC), superagonism at CB_1R (AEA), superagonism at CB_2R (CP 55,940, WIN 55,212-2) as well as inverse agonism (AM 251, AM 281, AM 630).

Table 6: Analysis of different CBR ligands in the GTPase assay.

Ligand	$G\alpha_{i2}$ + $G\beta_1\gamma_2$ + RGS4	GTPase stimulation / inhibition [%]	E_{max} [%]	$logEC_{50}$ / $logIC_{50}$	$logEC_{50}$ / $logIC_{50}$ (literature)
Δ^9-THC	**hCB_1R**	49 ± 3	71 ± 5	-7.13 ± 0.14	-7.80
	hCB_2R	38 ± 5	51 ± 11	-6.77 ± 0.08	-6.50
Anandamide	**hCB_1R**	80 ± 8*	116 ± 19	-6.80 ± 0.10	-7.05
	hCB_2R	49 ± 6*	66 ± 15	-6.36 ± 0.44	-6.40
2-AG	**hCB_1R**	69 ± 6	100	-6.60 ± 0.12	-6.30
	hCB_2R	74 ± 25	100	-6.53 ± 0.51	-5.85
CP 55,940	**hCB_1R**	63 ± 8	91 ± 21	-7.93 ± 0.06	-8.30
	hCB_2R	87 ± 7	118 ± 19	-8.38 ± 0.11	-8.60
WIN 55,212-2	**hCB_1R**	69 ± 7	100 ± 17	-7.38 ± 0.08	-7.20
	hCB_2R	95 ± 9	129 ± 21	-8.59 ± 0.15	-8.50
AM 251	**hCB_1R**	-83 ± 3	- 100	-7.11 ± 0.17	-8.10
AM 281	**hCB_1R**	-58 ± 2	- 70 ± 2	-7.16 ± 0.11	-7.50
AM 630	**hCB_2R**	-25 ± 6	- 30 ± 7	-7.86 ± 0.68	-7.50

Depicted is the stimulation by agonists or inhibition by antagonists of GTPase activity compared to basal GTPase activity, assessed by 3% (v/v) DMSO as control. E_{max} values represent the stimulation or inhibition relative to the endogenous agonist 2-AG (defined as 100% response). Reaction mixtures contained CBR ligands at various concentrations (1 nM - 10 µM). Data were analysed by nonlinear regression and best fit to sigmoidal concentration/response curves. The results are expressed as mean values ± S.D. and represent 3 independent experiments performed with different membrane preparations. The efficacy of antagonists was determined in the presence of 3 nM CP 55,940. Data shown are the means ± S.D. of 3 independent experiments performed in triplicates. Anandamide had a higher efficacy at the CB_1R (* $p = 0.02$). Literature data was published by Tocris Cookson (www.tocris.com).

4.3 Differences of CB_1 and CB_2 receptors

4.3.1 Analysis of expression levels of hCBRs, $G\alpha_{i2}$ and $G\beta_1\gamma_2$ in Sf9 membranes

The predicted molecular mass of hCB_1R is 55 kDa (Andersson et al., 2003; Xu et al., 2005). Due to a shorter N-terminus the expected molecular mass for the hCB_2R is only 40 kDa (Andersson et al., 2003; Filppula et al., 2004). We tagged hCBRs with an N-terminal FLAG epitope and a C-terminal hexahistidine epitope to facilitate immunological detection of GPCRs (Wenzel-Seifert et al., 1999; Wenzel-Seifert and Seifert, 2000; Seifert and Wenzel-Seifert, 2001). As expected, the M1 antibody, reacting with the FLAG epitope, detected a strong band at ~55 kDa for hCB_1R and two bands at ~40 kDa for hCB_2R (Fig. 16). The two hCB_2R bands may reflect different glycosylation states. For hCB_1R, additional weak bands at ~85 kDa and ~140 kDa were detected by the M1 antibody. Those bands may reflect oligomeric forms of hCB_1R.

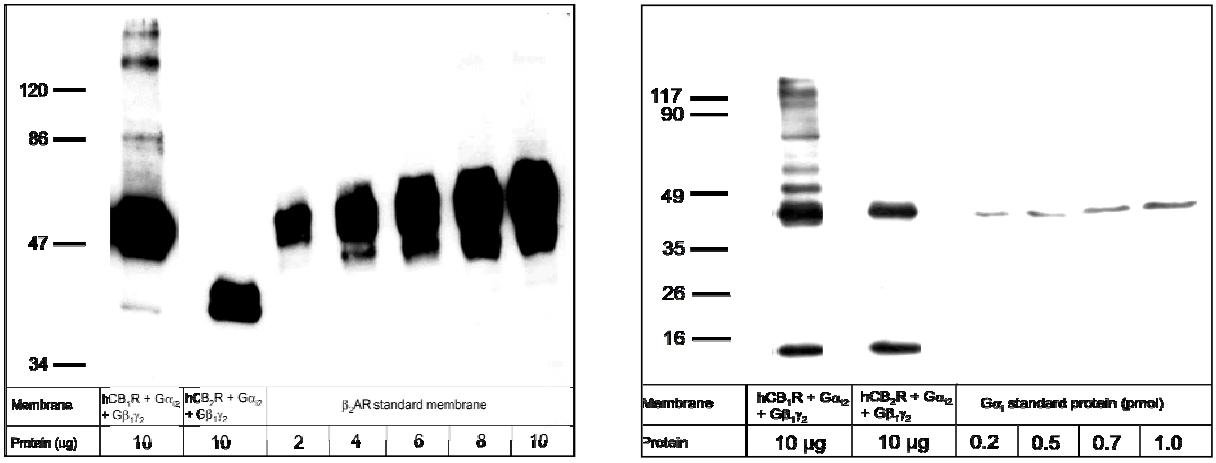

Fig. 16: Immunoblot analysis of hCBRs and $G\alpha_{i2}$ in Sf9 cell membranes. For immunological detection and determination of the expression levels of receptors the M1 antibody was used and for detection of $G\alpha_{i2}$ the anti-$G\alpha_{i\ common}$ Ig was used.

To estimate the expression levels of hCBRs, a FLAG epitope-tagged β_2AR expressed at 7.5 pmol/mg as assessed by [^{3}H]dihydroalprenolol antagonist saturation binding was used (Wenzel-Seifert et al., 1999; Wenzel-Seifert and Seifert, 2000; Seifert and Wenzel-Seifert, 2001). Densitometric analysis revealed that in all membrane preparations studied, hCB_1R was expressed at higher levels than hCB_2R (Fig. 16 and Table 7). The overall hCBR expression levels in Sf9 membranes ranged between 3 – 7 pmol/mg and are comparable with the expression levels of other GPCRs in Sf9 membranes (Wenzel-Seifert et al., 1999; Wenzel-Seifert and Seifert, 2000; Seifert and Wenzel-Seifert, 2001).

In physiological systems, G_i-proteins are expressed at a 10 - 100-fold molar excess relative to GPCRs (Wenzel-Seifert et al., 1999; Wenzel-Seifert and Seifert, 2000; Seifert and Wenzel-Seifert, 2001). Therefore, in order to properly assess hCBR-coupling to $G\alpha_{i2}\beta_1\gamma_2$, it was important to ensure an appropriate GPCR/G-protein stoichiometry in Sf9 membranes. Purified $G\alpha_i$ protein with a molecular mass of ~42 kDa (0.2-1.0 pmol/lane) was loaded onto gels, and the intensity of the bands was compared with the intensity of the $G\alpha_{i2}$ bands in Sf9 membranes using the $G\alpha_{i\ common}$ antibody (Fig. 16). In fact, $G\alpha_{i2}$ was highly expressed in Sf9 membranes, with levels ranging between ~200 – 350 pmol/mg protein (Table 7). Thus, $G\alpha_{i2}$ expression levels exceeded hCBR expression levels by ~ 60-fold, ensuring a stoichiometry comparable to physiological systems.

However, for activation of GPCRs and forming the ternary complex $G\beta_1\gamma_2$-subunits have to be present. Therefore, to ensure that enough $G\beta_1\gamma_2$-subunits are available in Sf9 cell membranes, we determined the expression levels of $G\beta_1\gamma_2$ by loading purified $G\beta_1\gamma_2$ protein onto gels. Under blotting conditions, $G\gamma_2$ is uncoupled of $G\beta_1$, hence we expect a molecular mass of ~ 36 kDa ($G\beta_1$) on the gels (Sutkowski and Catterall, 1990). After detecting the bands with the $G\beta_{common}$ antibody (Fig. 17) the intensity of the bands in Sf9 cells was compared. Surprisingly, $G\beta_1\gamma_2$ was expressed at much lower levels than $G\alpha_{i2}$ ranging between ~ 4 – 6 pmol/mg protein (Table 7). However, we show that the CBR/$G\beta_1\gamma_2$ ratio is approximately 1:1 ensuring a proper GPCR activation.

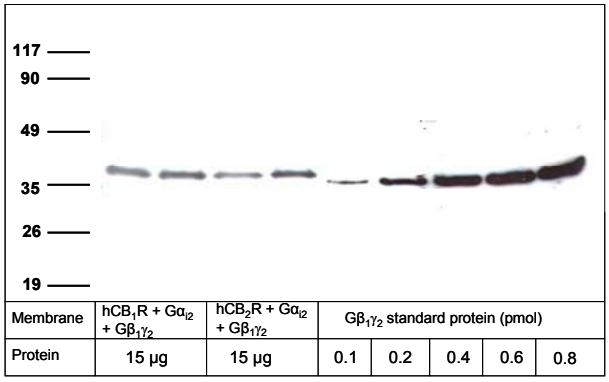

Membrane	$hCB_1R + G\alpha_{i2} + G\beta_1\gamma_2$	$hCB_2R + G\alpha_{i2} + G\beta_1\gamma_2$	$G\beta_1\gamma_2$ standard protein (pmol)				
Protein	15 µg	15 µg	0.1	0.2	0.4	0.6	0.8

Fig. 17: Immunoblot analysis of $G\beta_1\gamma_2$ in Sf9 cell membranes. For immunological detection and determination of expression levels of $G\beta_1\gamma_2$ the anti-$G\beta_{common}$ Ig was used.

Table 7. Expression levels of hCBRs, $G\alpha_{i2}$ and $G\beta_1\gamma_2$ in Sf9 membranes and stoichiometry of receptor/G-protein coupling.

Parameter	**$hCB_1R + G\alpha_{i2} + G\beta_1\gamma_2$**	**$hCB_2R + G\alpha_{i2} + G\beta_1\gamma_2$**
Receptor expression level (pmol/mg)	6.6 ± 0.9	3.4 ± 1.7
$G\alpha_{i2}$ expression level (pmol/mg)	370 ± 150	210 ± 140
$G\beta_1\gamma_2$ expression level (pmol/mg)	5.8 ± 1.2	4.3 ± 1.5
GPCR/$G\alpha_{i2}$ ratio	1 : 56	1 : 62
GPCR/$G\beta_1\gamma_2$ ratio	1 : 1	1 : 0.8
B_{max} values (pmol/mg)	16.4 ± 9.0	1.7 ± 0.9
Ligand-regulated GTPγS binding (pmol/mg)	5.3 ± 0.7	2.4 ± 1.1

Expression levels for hCB_1R and hCB_2R were determined densitometrically as shown in Fig. 16 and Fig. 17 using FLAG epitope-tagged β_2AR, purified $G\alpha_{i2}$ and purified $G\beta_1\gamma_2$ protein as standard. B_{max} values were determined by [^{3}H]CP 55,940 saturation binding as described under Materials and Methods. Ligand-regulated GTPγS was determined as shown in Fig. 21 in Chapter 4.3.3.3. Data shown are the means ± S.D. of experiments with 4 independent membrane preparations.

4.3.2 [^{3}H]CP 55,940 competition and saturation binding

Radioligand binding studies with the agonist [^{3}H]CP 55,940 (Ross et al., 1999) were performed to confirm functional integrity of hCBRs. Using 1 nM [^{3}H]CP 55,940 as tracer, unlabeled CP 55,940 inhibited radioligand binding to hCB_1R with an IC_{50} of 0.8 nM (95% confidence interval 0.6-1.0 nM) and to hCB_2R with an IC_{50} of 0.8 nM as well (95% confidence interval 0.5-1.2 nM) (Fig. 18). These values fit very well to previously published data for hCBRs and confirm functional integrity of GPCRs (MacLennan et al., 1998; Filppula et al., 2004; Xu et al., 2005).

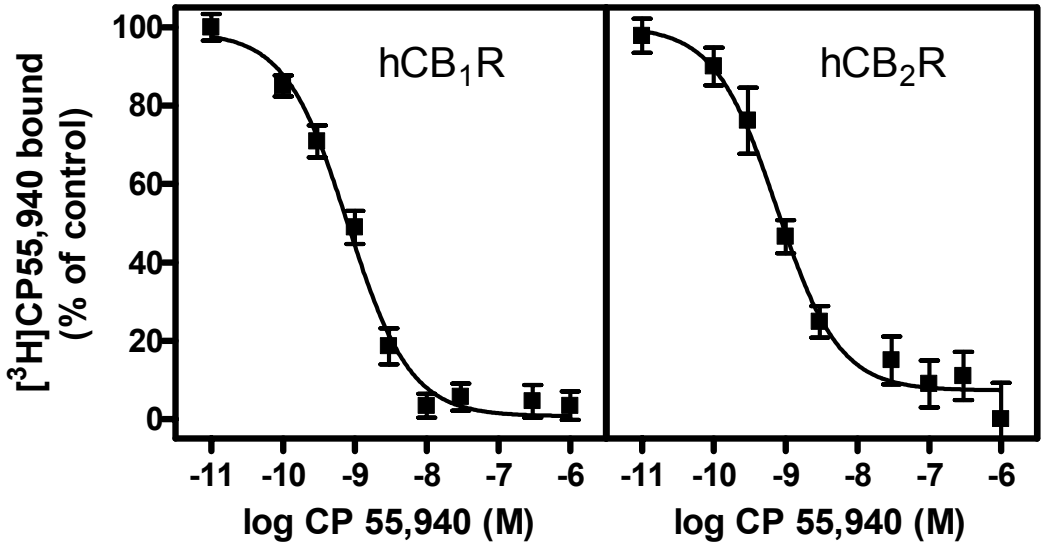

Fig. 18: [^{3}H]CP 55,940 competition binding. Competition binding experiments were performed in Sf9 cell membranes expressing either hCB_1R or hCB_2R in presence of 1 nM [^{3}H]CP 55,940. Total binding of [^{3}H]CP 55,940 amounted to 2.3 ± 1.7 pmol/mg for hCB_1R and to 0.5 ± 0.3 pmol/mg for hCB_2R. Data were normalized, analysed by non-linear regression and best fit to a one-site (monophasic) competition curve. Data shown are the means ± S.D. of 6 experiments performed in triplicates with 3 different membrane preparations.

Saturation binding with 10 nM of the labeled agonist [^{3}H]CP 55,940 was performed to determine the B_{max} values of CBRs in Sf9 cells (see Table 7). B_{max} values of the CB_1R were much higher than estimated by densitometric analysis (16.4 ± 9.0 pmol/mg protein vs. 6.6 ± 0.9 pmol/mg protein). It was the opposite for the CB_2R, B_{max} values assessed by saturation binding were lower than assumed by immunoblots (1.7 ± 0.9 pmol/mg protein vs. 3.4 ± 1.7 pmol/mg protein). These findings suggest, that for the CB_1R high-affinity binding is possible without G-protein. In contrast, approximately half of the CB_2R protein detected by immunoblots seems to be misfolded or misfunctioned.

To address the question, if high-affinity binding without G-proteins exists for the CB_1R, saturation binding assays in presence of 10 nM [^{3}H]CP 55,940 and 10 µM GTPγS were performed. GTPγS binds to Gα, but can not be hydrolysed by the intrinsic GTPase activity of the Gα-subunit and leads to uncoupling of the receptor from the G-protein. Hence, B_{max} values should be lower in presence of GTPγS.

This was true for the CB_2R, the presence of 10 µM GTPγS resulted in lower B_{max} values (56.9 ± 20.1% of control). Just the opposite was true for the CB_1R, the presence of 10 µM GTPγS resulted in B_{max} values comparable to those without GTPγS (97.4 ± 18.9% of control). It can be concluded, that high-affinity binding at the CB_1R is almost independent from G-protein binding. In contrast, the CB_2R possesses G-protein independent binding, but to a much lower extent than the CB_1R.

4.3.3 GTPγS binding studies

The hydrolysis-resistant GTP analog [^{35}S]GTPγS has been used to monitor the kinetics of GPCR/G_i-protein interaction and the stoichiometry of GPCR/G-protein coupling (Wenzel-Seifert et al., 1999; Wenzel-Seifert and Seifert, 2000; Seifert and Wenzel-Seifert, 2001).

4.3.3.1 GTPγS time course studies

First, we studied the time course of GTPγS binding (Fig. 19). Overall, GTPγS binding in membranes expressing hCB_1R proceeded much faster than in membranes expressing hCB_2R. In membranes expressing hCB_1R, GTPγS bound to $G\alpha_{i2}$ in the absence of a ligand with a $t_{1/2}$ of 1.0 ± 0.2 min. CP 55,940 increased the maximum extent of GTPγS binding without accelerating $t_{1/2}$ (1.9 ± 0.3 min). In contrast, the inverse hCB_1R agonist AM 251 (Shearman et al., 2003) decreased the maximum extent of GTPγS binding without largely affecting $t_{1/2}$ (0.4 ± 0.3 min). In membranes expressing hCB_2R GTPγS binding under basal conditions proceeded with a $t_{1/2}$ of 55.7 ± 18.4 min. CP 55,940 increased the maximum extent of GTPγS binding and decreased $t_{1/2}$ to 30 ± 6.2 min. The inverse hCB_2R agonist AM 630 (Ross et al., 1999) decreased the maximum extent of GTPγS binding and increased $t_{1/2}$ to 151 ± 90 min.

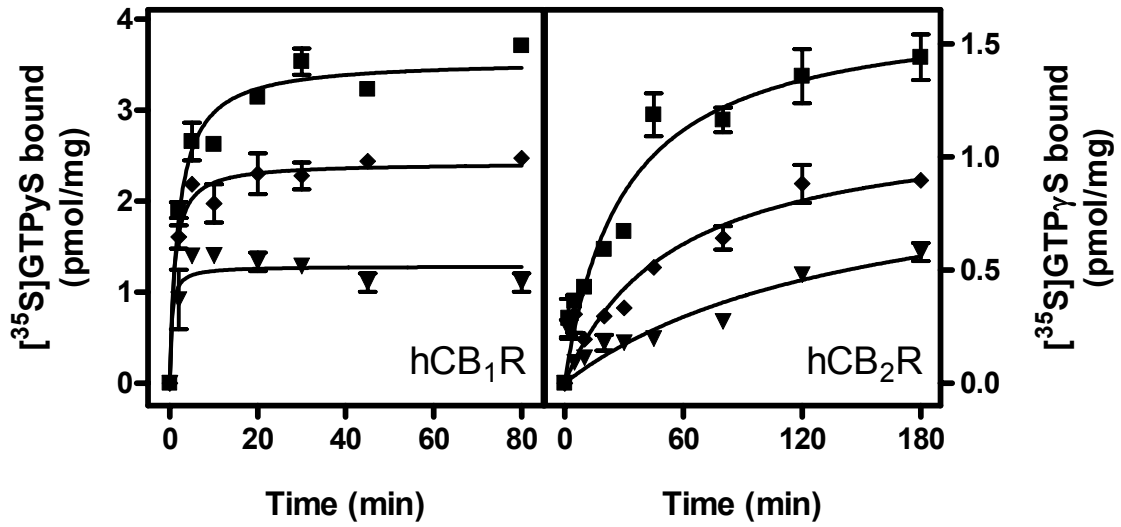

Fig. 19: Time course of GTPγS binding. Time course experiments were performed in Sf9 cells expressing either hCB_1R or hCB_2R in presence 0.6 nM [^{35}S]GTPγS plus 4.4 nM unlabeled GTPγS and 1 µM GDP. Data were analysed by nonlinear regression and best fit to a one-site (monophasic) binding curve. hCB_1R: ♦, basal; ■, 10 µM CP 55,940; ▼, 10 µM AM 251. hCB_2R: ♦, basal; ■, 10 µM CP 55,940; ▼, 10 µM AM 630. Data shown are the means ± S.D. of a representative experiment performed in triplicates. Similar data were obtained in 3 independent experiments.

4.3.3.2 GDP competition binding studies

In order to determine the GDP-affinity of $G\alpha_{i2}$ in membranes expressing hCBRs, GDP competition binding experiments were performed (Fig. 20). GDP competes with [^{35}S]GTPγS for binding to $G\alpha_{i2}$ and, thereby, reduces radioligand binding (Breivogel et al., 1998). In membranes expressing hCB_1R, GDP inhibited [^{35}S]GTPγS binding with an IC_{50} of 190 nM (95% confidence interval 100-340 nM). Agonists decrease GDP-affinity of G-proteins and, as a result, shift the GDP competition curve to the right (Breivogel et al., 1998; Wenzel-Seifert et al., 1999; Wenzel-Seifert and Seifert, 2000; Seifert and Wenzel-Seifert, 2001). In agreement with this concept, CP 55,940 reduced the GDP-affinity of $G\alpha_{i2}$ to 1.14 µM (95% confidence interval 0.71-1.82 µM). In membranes expressing hCB_2R, $G\alpha_{i2}$ exhibited a higher GDP-affinity (IC_{50}, 58 nM; 95% confidence interval, 41-83 nM) than in membranes expressing hCB_1R. In membranes expressing hCB_2R, CP 55,940 reduced GDP-affinity of $G\alpha_{i2}$ to a lesser extent (IC_{50}, 340 nM; 95% confidence interval, 190-610 nM) than in membranes expressing hCB_1R.

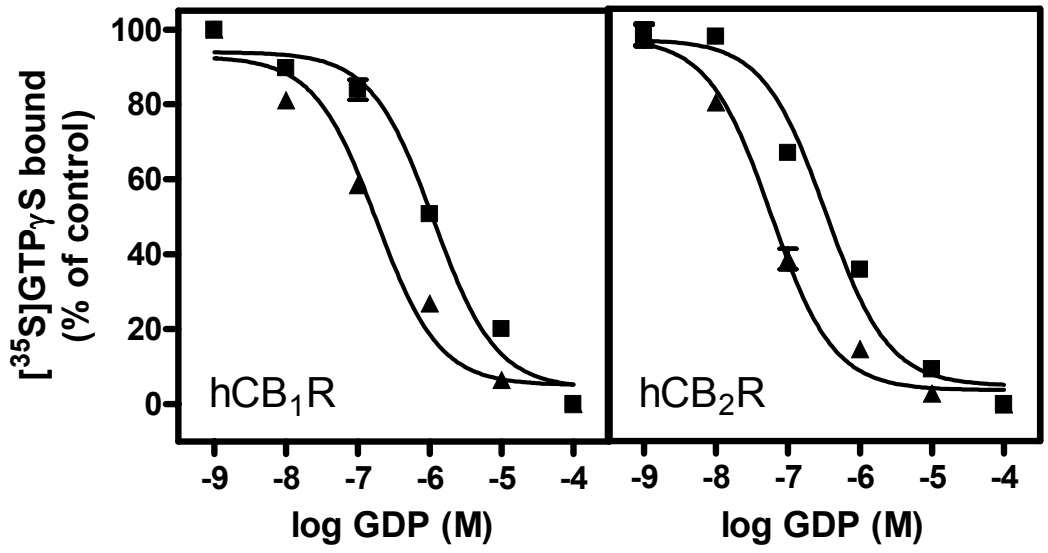

Fig. 20: GDP competition binding assay. GDP competition binding experiments were performed in Sf9 cells expressing either hCB_1R or hCB_2R in the presence of 0.2 nM [^{35}S]GTPγS and varying concentrations of GDP ranging from 1 nM to 10 µM. Data were analysed by nonlinear regression and best fit to a one-site (monophasic) competition curve. Data shown are the means ± S.D. of 3 experiments performed in triplicates.

4.3.3.3 Determination of K_d and B_{max} values by GTPγS binding studies

We also determined the K_d values of agonist-stimulated and inverse agonist-inhibited [^{35}S]GTPγS binding and the B_{max} values of binding in membranes expressing hCB_1R and hCB_2R (Fig. 21). The K_d of CP 55,940-stimulated GTPγS binding in membranes expressing hCB_1R was 5.1 ± 3.3 nM; the corresponding value in membranes expressing hCB_2R was 2.0 ± 1.6 nM. The inverse hCB_1R agonist AM 251 reduced GTPγS affinity to a K_d value of 4.1 ± 0.9 nM; the K_d value of AM 630-inhibited GTPγS binding in membranes expressing hCB_2R was 1.0 ± 0.5 nM. The absolute GTPγS binding values in membranes expressing hCB_1R were considerably larger than in membranes expressing hCB_2R. Additionally, the inhibitory effect of the inverse agonist in membranes expressing hCB_1R was much larger (58.1% of ligand-regulated GTPγS binding) than in membranes expressing hCB_2R (23.8% of ligand-regulated GTPγS binding).

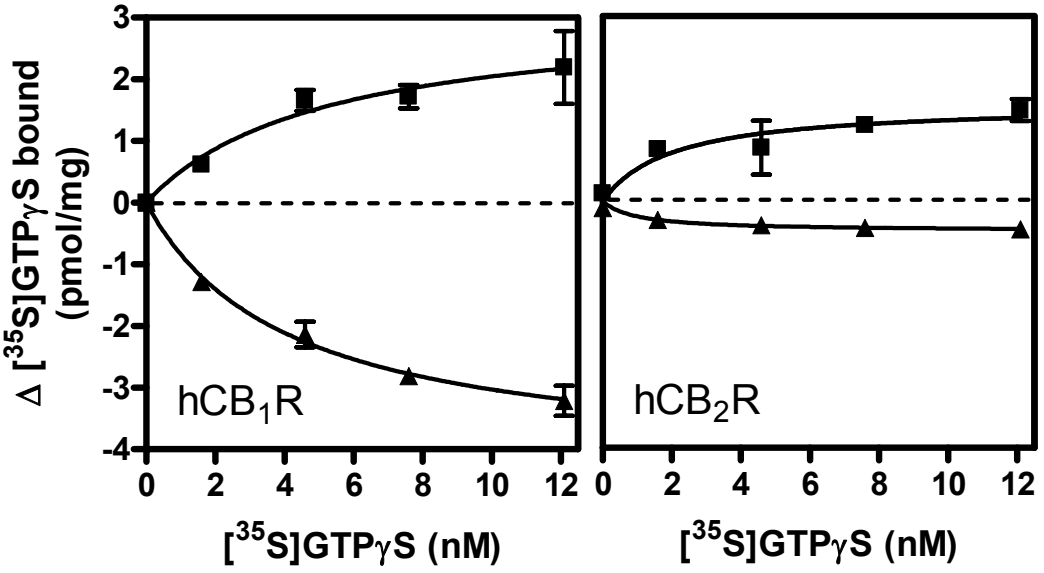

Fig. 21: GTPγS saturation binding assays with agonists and inverse agonists. GTPγS binding assays with membranes expressing hCB_1R and hCB_2R were performed as described under Materials and Methods. Reaction mixtures contained 0.4 nM [^{35}S]GTPγS plus unlabeled GTPγS to yield the final ligand concentrations given on the abscissa. Reaction mixtures contained solvent (basal), 10 µM CP 55,940 or 10 µM AM 251 (hCB_1R) or 10 µM AM 630 (hCB_2R). The differences between CP 55,940-stimulated GTPγS binding and basal GTPγS binding as well as the differences between basal GTPγS binding and GTPγS binding in the presence of AM 251 or AM 630 were calculated. Differences were analysed by nonlinear regression and best fit to a one-site (monophasic) binding curve. hCB_1R: ■, effect of CP 55,940; ▲, effect of AM 251. hCB_2R: ■, effect of CP 55,940; ▲, effect of AM 630. Data shown are the means ± S.D. of a representative experiment performed in triplicates. Similar data were obtained with 4 different membrane preparations.

We also performed GTPγS binding assays with 1.0 nM [^{35}S]GTPγS and cold GTPγS concentrations ranging from 1.6 – 18.6 nM, i.e. much higher final GTPγS concentrations than usually applied (up to 9.8 pmoles), see Fig. 22. Interestingly, we observed a change in the pharmacological profile of CP 55,940. Under the present conditions, CP 55,940, a high-affinity agonist, showed inverse agonist properties at the CB_1R (Fig. 22A). Statistically significance ($p < 0.05$) was demonstrated for a GTPγS concentration of 4.3 pmoles (see Fig. 22A). A switch in ligand profiles from inverse agonism to weak partial agonism has also been described for the G_s-coupled β_2AR expressed in Sf9 cells (Seifert et al., 1999). This effect has also been described for various β_1- and β_2-AR ligands in HEK293S cells (Galandrin and Bouvier, 2006). This switch was not observed for AM 251 at the CB_1R. The agonistic effect of CP 55,940 or the inverse agonistic effect of AM 630 at the CB_2R was not visible any more under the present conditions (Fig. 22B).

The calculated difference between [^{35}S]GTPγS bound in the presence of AM 251 and [^{35}S]GTPγS bound under basal conditions at the CB_1R was ~ 10 pmol/mg protein, although only ~ 6 pmol/mg $G\beta_1\gamma_2$ was expressed in Sf9 cells. This may result of binding of insect cell Gβγ-proteins at the CB_1R instead of mammalian $G\beta_1\gamma_2$-protein.

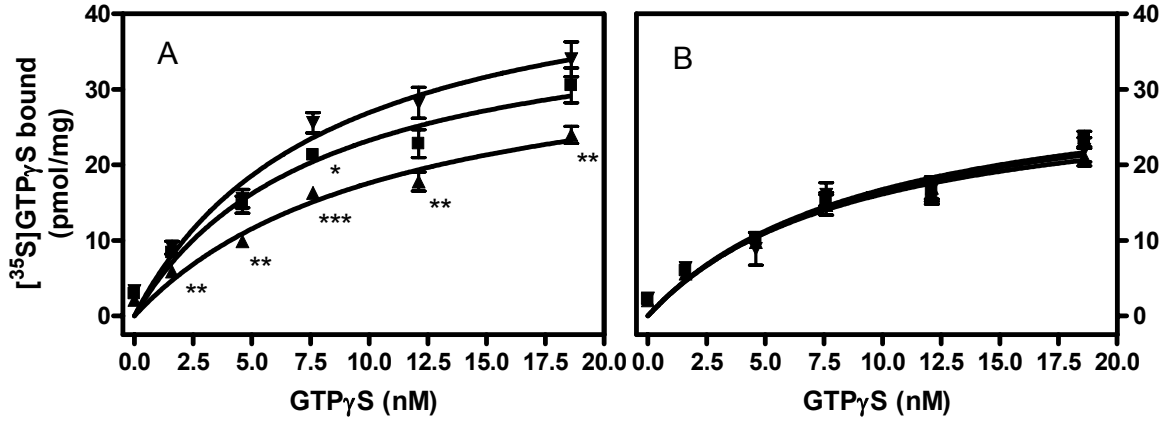

Fig. 22: Agonist/antagonist-switch observed for CP 55,940 at the CB_1R, assessed by GTPγS saturation binding. GTPγS binding assays with membranes expressing hCB_1R and hCB_2R were performed as described under Materials and Methods. Reaction mixtures contained 1.0 nM [^{35}S]GTPγS plus unlabeled GTPγS to yield the final ligand concentrations given on the abscissa. Reaction mixtures contained solvent (basal), 10 µM CP 55,940 or 10 µM AM 251 (hCB_1R) or 10 µM AM 630 (hCB_2R). Data was analysed by nonlinear regression and best fit to a one-site (monophasic) binding curve. **A,** hCB_1R. ■, effect of CP 55,940; ▼, basal; ▲, effect of AM 251. **B**, hCB_2R. ■, effect of CP 55,940; ▼, basal; ▲, effect of AM 630. Data shown are the means ± S.D. of three merged experiments performed in duplicates with different membrane preparations. t-Test analysis was performed in **A** to evaluate the statistical significance of the difference of ligand-stimulated binding and basal binding (* $p < 0.05$, ** $p < 0.01$, *** $p < 0.001$).

4.3.4 Steady-state GTPase activity assay

The GTPase assay assesses GDP/GTP exchange with subsequent GTP hydrolysis under steady-state conditions (Seifert et al., 1999; Wenzel-Seifert et al., 1999). As was the case for GTPγS binding, the absolute GTPase activities were higher for hCB_1R than hCB_2R (Fig. 23 and Table 8). CP 55,940 stimulated GTP hydrolysis at hCB_1R and hCB_2R in a concentration-dependent manner, whereas the inverse agonists AM 251 and AM 630 decreased GTP hydrolysis concentration-dependently.

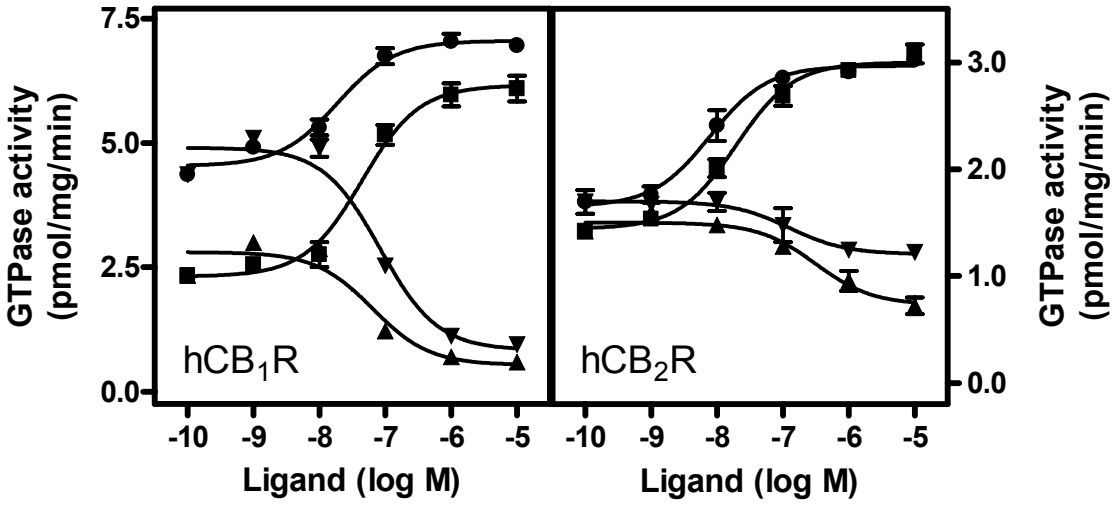

Fig. 23: Regulation of GTPase activity by CBR ligands and NaCl. GTPase activity in Sf9 membranes expressing hCB_1R and hCB_2R was determined as described under Materials and Methods. Reaction mixtures contained solvent (control) or 150 mM NaCl in the presence of CBR ligands at various concentrations. hCB_1R: ●, CP 55,940; ▼, AM 251; ■, CP 55,940 plus 150 mM NaCl; ▲ AM 251 plus 150 mM NaCl. hCB_2R: ●, CP 55,940; ▼, AM 630; ■, CP 55,940 plus 150 mM NaCl; ▲ AM 630 plus 150 mM NaCl. Data were analysed by nonlinear regression and best fit to sigmoidal concentration/response curves. Data shown are the means ± S.D. of 3 independent experiments performed in triplicates.

Na^+ ions act as allosteric inverse agonist at G_i-coupled GPCRs and stabilize the inactive (R) state, thereby reducing constitutive G-protein activation and inverse agonist effects while increasing agonist effects (Seifert and Wenzel-Seifert, 2001; Seifert and Wenzel-Seifert, 2002). In accordance with this paradigm, NaCl (150 mM) reduced basal GTP hydrolysis in membranes expressing hCB_1R by ~50%. Moreover, NaCl reduced the inverse agonistic effect of AM 251 and increased the agonistic effect of CP 55,940 (see Fig. 23). In agreement with the GTPγS binding data (Fig. 21 in Chapter 4.3.3.3) the inverse agonist effect at hCB_2R in the GTPase assay was considerably smaller than the inverse agonist effect at hCB_1R compared to the corresponding agonist effects. In marked contrast to hCB_1R, NaCl did not reduce basal GTPase activity and the inverse agonist effect in membranes expressing hCB_2R, i.e. this GPCR was Na^+-resistant (see Fig. 23).

Table 8. Regulation of GTPase activity in Sf9 membranes expressing hCB_1R and hCB_2R by CBR ligands and NaCl.

Parameter	Control	NaCl (150 mM)
hCB_1R		
EC_{50} CP 55,940 (nM)	19 (9.6-37)	44 (25-78)
IC_{50} AM 251 (nM)	84 (49-144)	64 (25-156)
Δ CP 55,940 (pmol/mg/min)	2.52	3.85
Δ AM 251 (pmol/mg/min)	4.10	2.27
Ligand-regulated GTP hydrolysis (pmol/mg/min)	6.59	6.12
Relative stimulatory effect of CP 55,940 (% of ligand-regulated GTP hydrolysis)	38.2	62.9
Relative inhibitory effect of AM 251 (% of ligand-regulated GTP hydrolysis)	61.8	37.1
hCB_2R		
EC_{50} CP 55,940 (nM)	7.9 (4.3-15)	19 (12-31)
IC_{50} AM 630 (nM)	125 (23-676)	313 (116-851)
Δ CP 55,940 (pmol/mg/min)	1.32	1.59
Δ AM 630 (pmol/mg/min)	0.50	0.77
Ligand-regulated GTP hydrolysis (pmol/mg/min)	1.82	2.33
Relative stimulatory effect of CP 55,940 (% of ligand-regulated GTP hydrolysis)	72.7	66.9
Relative inhibitory effect of AM 630 (% of ligand-regulated GTP hydrolysis)	27.3	33.1

The GTPase data shown in Fig. 23 were used as the basis for the calculations shown in this Table. EC_{50} and IC_{50} values were calculated by non-linear regression analysis. Mean values and 95% confidence intervals are shown. The table also shows the absolute increases in GTP hydrolysis caused by the agonist CP 55,940 and the absolute decreases in GTP hydrolysis caused by the inverse agonists AM 251 and AM 630, respectively. The difference between agonist-stimulated and inverse agonist-inhibited GTP hydrolysis constitutes ligand-regulated GTP hydrolysis. From those values, the relative stimulatory effects of agonists and the relative inhibitory effectof inverse agonists were calculated.

4.3.5 AC assay

$G\alpha_i$-activation of GPCRs is typically associated with an inhibition of AC activity and hence a reduction of generated cAMP. We therefore investigated the effect of CBR ligands on AC activity after pre-stimulating the $G\alpha_{i2}$-subunit with either 10 µM or 100 µM forskolin (Fig. 24). CP 55,940 as an agonist did not reduce forskolin-stimulated AC activity resulting in a decreased formation of cAMP as expected. AM 251 and AM 630, as inverse agonists at the CB_1R or respectively the CB_2R, did not increase AC activity resulting in an increased concentration of cAMP.

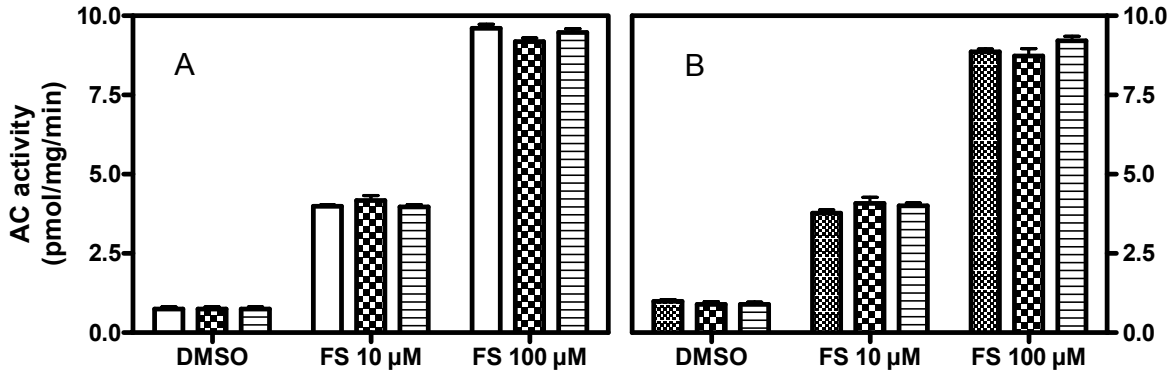

Fig. 24: Effect of CBR ligands on AC activity after stimulation with forskolin. AC activity in Sf9 membranes expressing hCB_1R (**A**) and hCB_2R (**B**) was determined as described under Materials and Methods. Reaction mixtures contained 3% (v/v) DMSO (control) or forskolin (10 µM and 100 µM) in the presence of 10 µM CBR ligands. White bars represent the control, dotted bars the effect of 10 µM CP 55,940 and striped bars the effect of 10 µM AM 251 (**A**) or 10 µM AM 630 (**B**). Data shown are the means ± S.D. of a representative experiment performed in hexaplicates. Similar data were obtained in a second experiment with different membrane preparations.

Cannabinoid receptors are highly constitutive active, as shown in GTPγS binding assays (see Chapter 4.3.3) and in steady-state GTPase assays (see Chapter 4.3.4). However, after activation of $G\alpha_i$-protein the signaling cascade does not seem to be transduced to an inhibition of adenylyl cyclases. Yet, other down-stream effects, such as phoshorylation of proteins via MAP kinases could be influenced.

4.4 Pharmacological analysis of the alkamide dodeca-2*E*,4*E*-dienoic acid isobutylamide and *E. purpurea n*-hexane extract

Echinacea has been used as an immune-stimulatory plant since the 18th century by the Indians of North America (Bauer and Wagner, 1990). Today, preparations of *E. purpurea*, *E. angustifolia* and *E. pallida* are commonly used. Up to now, several compound classes have been discussed as the active principle of *Echinacea*, e.g. caffeic acid derivatives, polysaccharides/glycoproteins and alkamides.

Just a few years ago, the effect of hydrophilic and hydrophobic compounds of *E. purpurea* has been investigated. Only the hydrophobic alkamides showed a significant stimulation of the phagocytic activity of alveolar macrophages in rats (Goel et al., 2002; Goel et al., 2002a). Interestingly, alkamides show structural similarity to the endogenous cannabinoid receptor agonist anandamide (see Fig. 25) and dodeca-2*E*,4*E*-dienoic acid isobutylamide has been described as a high-affinity agonist at CB_2R (Raduner et al., 2006). However, the interaction of dodeca-2*E*,4*E*-dienoic acid isobutylamide with CB_2R was only determined in [^{3}H]CP 55,940 competition binding assays. As this assay is not a functional test system we were interested if the compound would show any agonism or inverse agonism at CBRs in the established functional GTPase assay.

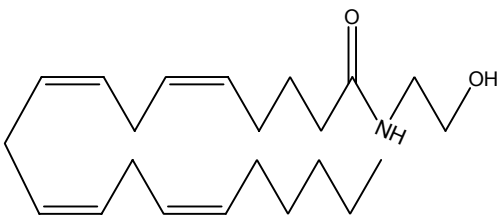

Anandamide

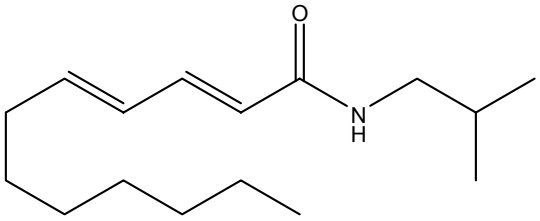

Dodeca-2*E*,4*E*-dienoic acid isobutylamide

Fig. 25: Structures of the endogenous agonist anandamide and dodeca-2*E*,4*E*-dienoic acid isobutylamide. The alkamide dodeca-2*E*,4*E*-dienoic acid isobutylamide has been described as a CB_2R agonist (Raduner, 2006).

4.4.1 [^{3}H]CP 55,940 competition binding of dodeca-2*E*,4*E*-dienoic acid isobutylamide

First, we analysed the alkamide dodeca-2*E*,4*E*-dienoic acid isobutylamide in competition binding assays at CBRs in the presence of 1 nM [^{3}H]CP 55,940.
A 2 mM stock solution of dodeca-2*E*,4*E*-dienoic acid isobutylamide in 100% (m/v) DMSO was dissolved to solutions containing final 3% (v/v) DMSO (1 nM - 10 µM). Unlabeled CP 55,940 (1 nM - 10 µM) was used as a positive control.
A representative competition binding experiment for the CB_2R is depicted in Fig. 26. Unlabeled CP 55,940 potently displaced labeled [^{3}H]CP 55,940 at CB_2R expressed in Sf9 cells (K_i = 6.6 nM), which was comparable to obtained data described in Chapter 4.3.2. However, dodeca-2*E*,4*E*-dienoic acid isobutylamide did not displace the labeled [^{3}H]CP 55,940 at the CB_2R. This finding was surprising, as the alkamide has been reported as CB_2R agonist determined by competition binding (Raduner et al., 2006). We also analysed dodeca-2*E*,4*E*-dienoic acid isobutylamide at the CB_1R, but again no displacement of [^{3}H]CP 55,940 could be observed (data not shown).

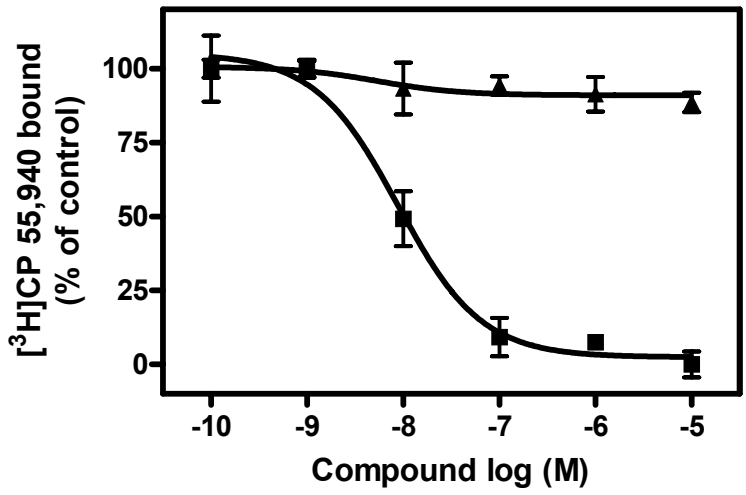

Fig. 26: [^{3}H]CP 55,940 competition binding of dodeca-2E,4E-dienoic acid isobutylamide. Data depicts a representative competition binding experiment obtained for CP 55,940 (■) and dodeca-2*E*,4*E*-dienoic acid isobutylamide (▲) in Sf9 cell membranes coexpressing CB_2R, $G\alpha_{i2}$, $G\beta_1\gamma_2$ and RGS4.

4.4.2 Analysis of dodeca-2*E*,4*E*-dienoic acid isobutylamide and *E. purpurea* extract in the GTPase assay

In general, the analysis of compounds in competition binding assays is not useful for assessing pharmacological efficacy, e.g. agonism and inverse agonism. Hence, we decided to analyse the alkamide dodeca-2*E*,4*E*-dienoic acid isobutylamide and the *n*-hexane *E. purpurea* root extract in the functional GTPase assay.

The 2 mM stock solution of dodeca-2*E*,4*E*-dienoic acid isobutylamide in 100% (m/v) DMSO was dissolved to solutions containing final 3% (v/v) DMSO. The compound was analysed for GTPase activation in a concentration range from 1 nM to 10 µM.

For the establishment of the functional GTPase assay different Gα-subunits and different RGS-proteins were coexpressed with either CB_1R or CB_2R. The most efficient system to measure agonist activity at CBRs was CB_xR + $G\alpha_{i2}$ + $G\beta_1\gamma_2$ + RGS4 (see Chapter 4.1.4). We could also show that this coexpression was suitable for plant derived compounds, such as Δ^9-THC (see Chapter 4.2). To ensure that this system is also the most appropriate system to detect ligands derived from *Echinacea* species, all six constructs were again analysed. Fig. 27 shows a representative graph for dodeca-2*E*,4*E*-dienoic acid isobutylamide at two different systems (CB_2R + $G\alpha_{i2}$ + $G\beta_1\gamma_2$ with and without RGS4). CP 55,940 (10 µM) was used as a positive control. The above described significant increase in GTPase activity by coexpression of RGS4 compared to membranes without RGS-protein could also be shown here for CP 55,940 (see Chapter 4.1.4). Coexpression of RGS4 resulted in an increase of GTPase activity of ~160% compared to ~80% when no RGS4 was present. However, the alkamide dodeca-2*E*,4*E*-dienoic acid isobutylamide failed to activate CB_2R, even in micromolar concentrations. The same outcome was obtained for the other four CB_2R coexpression systems. In addition, no effect at any of the six CB_1R systems could be observed (data not shown).

Analysing the *n*-hexane *E. purpurea* root extract (final concentrations 10 ng/ml – 100 µg/ml) resulted in the same graph as depicted in Fig. 27. Again, 10 µM CP 55,940 as a positive control demonstrated the functionality of receptor protein, but the extract itself did not activate CBRs.

We also performed GTPase assays in the presence of 3 nM CP 55,940 (antagonist-mode) to determine if the compound dodeca-2*E*,4*E*-dienoic acid isobutylamide or the *n*-hexane *E. purpurea* root extract act as antagonists at CBRs. Again, no effect was detected (data not shown).

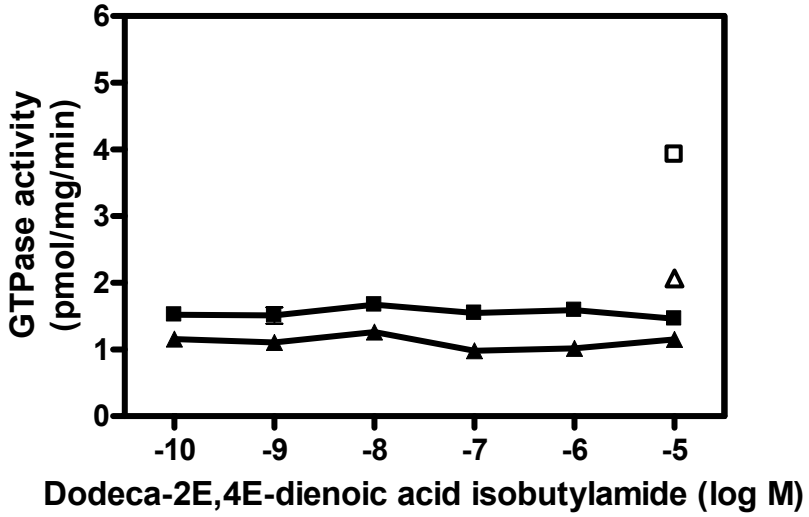

Fig. 27: Effect of dodeca-2*E*,4*E*-dienoic acid isobutylamide on GTPase activity of the CB_2R. Data depicts a representative result obtained in Sf9 cells expressing the CB_2R and $G\alpha_{i2}$ protein (▲), or the CB_2R, $G\alpha_{i2}$ and RGS4 proteins (■). All membranes contained additionally $G\beta_1\gamma_2$ protein. 10 µM CP 55,940 was used as a positive control for the CB_2R and $G\alpha_{i2}$ system (Δ), or the CB_2R, $G\alpha_{i2}$ and RGS4 system (□).

4.4.3 Summary of the pharmacological analysis of dodeca-2*E*,4*E*-dienoic acid isobutylamide and *E. purpurea* extract

An often discussed issue of alkamides is their low solubility in aqueous solutions due to their hydrophobic properties with a long alkyl chain and double bonds (Bauer and Wagner, 1990; Raduner et al., 2006; Raduner et al., 2007). For some alkamides the formation of micelles in aqueous solutions has been reported (Raduner et al., 2007). In the latter publication, the stock solution was prepared in 100% DMSO, yet no comment was made about the further content of DMSO in the assay tubes.

Having performed extensive investigations on the solubility of commercially available CBR ligands (see Chapter 4.1.2 and 4.1.3), we describe for the first time that a DMSO content of 3% (v/v) is necessary for stable and clear CBR ligand solutions. Less than 3% (v/v) DMSO results in unstable and cloudy solutions, which cannot be used for reproducible experiments. As this analysis also included the endogenous agonists, anandamide and 2-AG, as well as the natural agonist, Δ^9-THC, we assume that a content of 3% (v/v) DMSO is also necessary for the class of alkamides.
We therefore suggest that data of alkamides obtained in aqueous solutions should be interpreted with caution. Unstable solutions may be the reason for the contradictory outcome in some publications or biphasic [^{3}H]CP 55,940 competition binding assays (Raduner et al., 2006). Also, in the latter publication binding assays were performed without a positive control, e.g. CP 55,940.

In general, we cannot confirm and explain the reported agonism of alkamides at CB_2R. The alkamide dodeca-2*E*,4*E*-dienoic acid isobutylamide did neither displace [^{3}H]CP 55,940 in competition binding assays nor did it show any activity in a functional test system. The GTPase assay would have detected not only agonism, but also inverse agonism or antagonism at CBRs. Another advantage of the GTPase assay is the point of measurement. We assessed ligand properties directly at the Gα-protein, namely at a very proximal point of the signal cascade of GPCRs. We also can rule out insufficient compound solubility, as depicted in Chapter 4.1.2 and 4.1.3. Furthermore, we assessed the functionality of receptor proteins by positive controls.

However, it is known that endocannabinoids are also ligands at other receptors, e.g. TRPV vanilloid receptors (Zygmunt et al., 1999; Smart et al., 2000). Also, some CBR ligands influence other target proteins, e.g. cyclooxygenases (Mestre et al., 2006). This may reflect the observed long-term effects of alkamides and *E. purpurea* preparations mediated by CBR-independent pathways (Beuscher et al., 1995; Melchart et al., 1998; Goel et al., 2002a; Hostettmann, 2003).

4.5 Pharmacological analysis of *E. pallida* root extract and its lipophilic compounds

4.5.1 Isolation and characterization of pentadec-8*Z*-en-2-one

Alkamides isolated from *E. purpurea* or *E. angustifolia* were previously described as CB_2R agonists (Woelkart et al., 2005; Raduner et al., 2006). However, we show that neither the alkamide dodeca-2*E*,4*E*-dienoic acid isobutylamide nor the *n*-hexane extract of *E. purpurea* are ligands at CBRs (see Chapter 4.4). Interestingly, several *Echinacea* preparations contain only *E. pallida*. The latter shows ketoalkenes and ketoalkynes, a different class of compounds than in *E. purpurea* and *E. angustifolia*. To the best of our knowledge, the pharmacological effects of these compounds at CBRs have never been investigated. Therefore, we were interested if extracts of *E. pallida* or isolated compounds would be ligands at either CB_1 or CB_2 receptors.

The extraction of *E. pallida* roots with ASE, followed by subsequent VLC and RP-18 CC of the VLC fraction A2 (DCM), resulted in the isolation of an oily, chemically pure main compound (31.0 mg). Its EIMS displayed a molecular ion at *m/z* 224 $[M]^+$ indicating, together with the ^{13}C NMR and DEPT data, a molecular formula of $C_{15}H_{28}O$ (Chapter 3.4.3 and 3.4.4). The structure of the compound was elucidated by comprehensive 1D and 2D NMR analyses (^1H, ^{13}C NMR, HSQC and HMBC) and revealed the presence of pentadec-8*Z*-en-2-one (see Fig. 28). The ^1H and ^{13}C NMR data were presented in the experimental part (Chapter 3.4.4) and were identical to literature data (Dickschat et al., 2005). Identity of the isolate was finally confirmed by comparison to authentic reference compound in TLC system ACN : MeOH : H_2O 6 : 3 : 1.25 (R_f = 0.26).

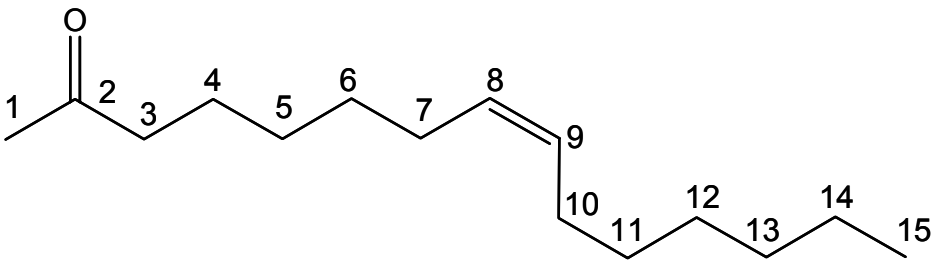

Fig. 28: Pentadec-8*Z*-en-2-one, a ketoalkene isolated of *E. pallida* roots.

Pentadec-8*Z*-en-2-one has been reported as one of the main ketoalkenes in the essential oil from roots of *E. pallida* (Bauer and Wagner, 1990), yet the yield of the isolated compound was relatively low. Unfortunately, the isolation of more compounds of *E. pallida* was not possible due to the small amount of starting material and the presence of multiple minor compounds. However, after CC on RP-18 material as stationary phase the fractions containing more than one compound were merged and analysed by ^{1}H NMR spectroscopy. Fractions showing the functionalities of ketoalkenes or ketoalkynes (double bonds, alkyl chains and CH_3CO) were analysed in the functional GTPase assay at CBRs. None of the obtained fractions showed activity and thus further bio-activity guided isolation of active ligands was not performed.

4.5.2 Pharmacological evaluation of pentadec-8*Z*-en-2-one, fractions from CC on RP-18 material and *n*-hexane *E. pallida* root extract in the functional GTPase assay

Pentadec-8*Z*-en-2-one was dissolved in 100% (m/v) DMSO to prepare a 10 mM stock solution. Then, the stock solution was diluted in a way that all following solutions contained 30% (v/v) DMSO (final 3% (v/v) DMSO in the assay). The final investigated concentrations ranged from 1 nM - 10 µM in the assay. We tested the isolated compound as well as RP-18 CC fractions at Sf9 insect cell systems coexpressing CB_xR, $G\alpha_{i2}$, $G\beta_1\gamma_2$ and RGS4. Among all studied systems, this construct yielded highest GTPase activation when the effect of the agonist CP 55,940 was analysed (see Chapter 4.1.4). We could also show that this construct is suitable for plant derived compounds, such as Δ^9-THC (see Chapter 4.2). CP 55,940 and the endogenous agonist anandamide were used as positive controls to ensure the functionality of the expressed receptor protein (both 10 µM final).
However, pentadec-8*Z*-en-2-one did neither activate the CB_1R nor the CB_2R in the functional GTPase assay. The experiment was repeated twice with different CB_1R and CB_2R membranes, but again, only the positive controls, CP 55,940 and AEA, did increase the GTPase activity at CBRs (data not shown).

Several fractions showed the presence of ketoalkenes and/or ketoalkynes in the recorded ^{1}H NMR spectrums. Also, the crude *n*-hexane extract of *E. pallida* roots was analysed for CBR activation. Stock solutions of fractions and the *n*-hexane root extract (each 10 mg/ml) in DMSO were prepared and diluted to obtain solutions with 3% (v/v) DMSO final. The analysed concentrations in the assay ranged from final 1 ng/ml to 100 µg/ml. However, no activation of GTPase activity at CBRs by any fraction or the *n*-hexane extract of *E. pallida* roots could be detected. Experiments were repeated twice with different Sf9 cell membranes expressing either CB_1R or CB_2R.

4.5.3 Summary of the pharmacological analysis of pentadec-8*Z*-en-2-one and *E. pallida* extract

Several isolation steps (ASE, VLC, RP-18 CC) yielded one completely characterized ketoalkene of *E. pallida*. Extraction of plant material and isolation of compounds is very time- and solvent-consuming and yields only small amounts of compounds. To obtain more compounds or higher yields the extraction process has to be up-scaled to increase the efficacy of isolation of compounds of plant material. Several other fractions contained ketoalkenes after NMR spectroscopy and functional testing in the GTPase assay was performed before separating the compounds by HPLC. However, neither the isolated ketoalkene pentadec-8*Z*-en-2-one nor the analysed RP-18 CC fractions nor the *n*-hexane *E. pallida* root extract did activate CBRs.

4.6 Pharmacological analysis of synthesized constituents of *E. pallida* roots

Cannabinoid receptor agonists can be divided in 4 structural classes. First, the classic cannabinoids, e.g. Δ^9-THC, isolated from *C. sativa*. Second, the non-classic cannabinoids, e.g. CP 55,940, a Pfizer compound derived from Δ^9-THC. In the third class are the endogenous cannabinoids, e.g. anandamide or 2-AG and in the fourth class are the aminoalkylindoles, e.g. WIN 55,212-2. Members of the Department of Organic Chemistry at the University of Regensburg synthesized 14 compounds (for structures and names see Table 2, Fig. 13A and 13B in Chapter 3.4.1). The compounds were plant-derived ketoalkenes (compound **1** and **2**) or non-plant-derived ketoalkenes (compound **3** and **4**). Compound **1** was identical with the isolated compound of *E. pallida*, as described in Chapter 4.5.1. One compound (**5**) was a derivative of the third class, the endogenous cannabinoids. Most of the synthesized compounds were derivated ketoalkenes (compounds **6** - **14**).

Coexpression of CB_xR, $G\alpha_{i2}$, $G\beta_1\gamma_2$ and RGS4 yielded the highest GTPase activation in Sf9 cells (see Chapter 4.1.4). Hence, this system was chosen for the analysis of the agonistic, inverse agonistic or antagonistic potential of the synthesized compounds in the functional GTPase assay. The effect of 2-AG, the most abundant endogenous ligand at CBRs, was defined as 100% stimulation.

Yet, none of the synthesized natural ketoalkenes (**1**, pentadec-8*Z*-en-2-one or **2**, pentadeca-8*Z*,11*Z*-diene-2-one) resulted in an activation of GTPase activity. This is in accordance with our findings in Chapter 4.5.2, where the isolated compound **1**, several fractions and the *n*-hexane extract of *E. pallida* were investigated. However, three of the synthesized compounds acted as agonists at CBRs in the GTPase assay (see Fig. 29 and Table 9).

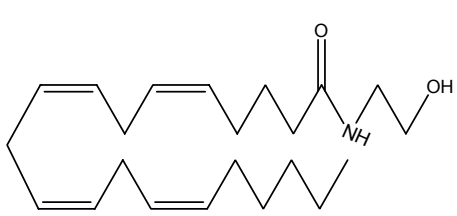

Anandamide

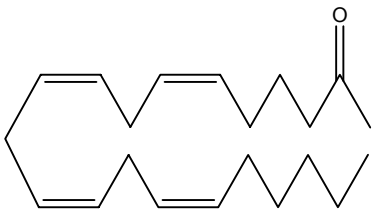

5

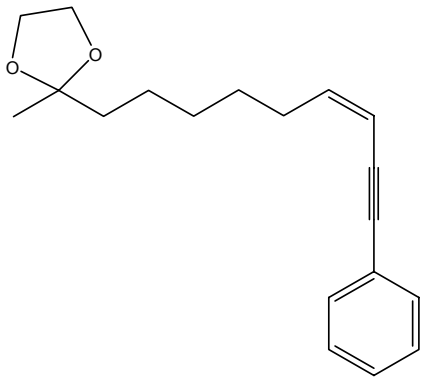

12

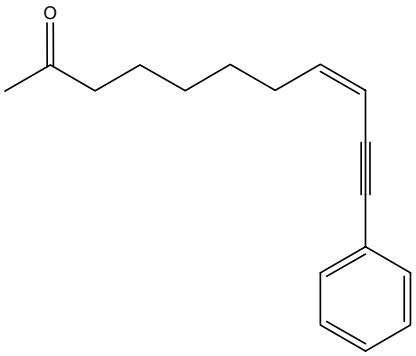

14

Fig. 29: Structure of anandamide and of synthesized compounds that are agonists at CBRs in the functional GTPase assay.

Compound **5**, henicosa-6*Z*,9*Z*,12*Z*,15*Z*-tetraen-2-one, was a full agonist at CB_1R (E_{max}: 99 ± 9%) and a superagonist at CB_2R (E_{max}: 114 ± 9%). This was not surprising, as compound **5** is very similar to the endogenous agonist anandamide by replacing the isobutyl amine at the keto functionality with a methyl group (see Fig. 29). This substitution even led to a much higher efficacy at the CB_2R compared to the endogenous ligand anandamide (E_{max} value 114 ± 9% vs. 66 ± 15%). However, the $logEC_{50}$ values of compound **5** were only in the micromolar range (CB_1R: -5.71 ± 0.44; CB_2R: -5.46 ± 0.29) compared to anandamide (CB_1R: -6.80 ± 0.10; CB_2R: -6.36 ± 0.44) or 2-AG (CB_1R: -6.60 ± 0.12; CB_2R: -6.53 ± 0.51). This finding suggests that substitution of the carboxy group at C1 with a larger or an amine-containing group, e.g. ethanolamine (anandamide) or glycerol (2-AG) is necessary for a high affinity at CBRs.

Compound **12** (2-methyl-2-(9-phenylnon-6*Z*-en-8-ynyl)-1,3-dioxolane) and compound **14** (11-phenylundec-8*Z*-en-10-yn-2-one) were derived from natural ketoalkenynes of *Echinacea* species with a keto group at C2, a *cis*-double bond at C8 and a triple bond at C10. In compound **14**, substitution of the terminal methyl group by a benzyl moiety led to partial agonism at both CBRs (E_{max} at CB_1R: 59 ± 35%, E_{max} at CB_2R: 59 ± 18%) with an affinity in the micromolar range. Protecting the keto group at C2 and substitution at C11 by a benzyl moiety (compound **12**) resulted in a low efficacy at the CB_1R (E_{max}: 21 ± 22%) and partial agonism at the CB_2R (E_{max}: 45 ± 6%). The affinity of compound **12** for CBRs also was in the micromolar range ($logEC_{50}$ at CB_1R: -5.66 ± 0.16, $logEC_{50}$ at CB_2R: -5.23 ± 0.62).

Hence, we identified novel agonists at CBRs derived from natural ketoalkenynes of *Echinacea* as assessed by the GTPase assay. However, the affinity of the compounds at CBRs has to be improved in future studies.

Table 9: Activation of GTPase activity, E_{max} values and $logEC_{50}$ values of 2-AG, anandamide (AEA) and synthesized compounds 5, 12 and 14.

	$CB_1R + G\alpha_{i2} + G\beta_1\gamma_2$ + RGS4			**$CB_2R + G\alpha_{i2} + G\beta_1\gamma_2$ + RGS4**		
	GTPase activation [%]	**E_{max} [%]**	**$logEC_{50}$**	**GTPase activation [%]**	**E_{max} [%]**	**$logEC_{50}$**
2-AG	69 ± 6	100	-6.60 ± 0.12	74 ± 25	100	-6.53 ± 0.51
AEA	80 ± 8	116 ± 19	-6.80 ± 0.10	49 ± 6	66 ± 15	-6.36 ± 0.44
5	68 ± 6	99 ± 9	-5.71 ± 0.44	85 ± 7	114 ± 9	-5.46 ± 0.29
12	15 ± 11[a]	21 ± 22[a]	-5.66 ± 0.16[a]	33 ± 3	45 ± 6	-5.23 ± 0.62
14	41 ± 20	59 ± 35	-5.28 ± 0.27	44 ± 11	59 ± 18	-5.84 ± 0.19

Results are expressed as percentages of mean values ± S.D. compared to basal GTPase activation assessed by 3% (v/v) DMSO. E_{max} values represent the stimulation relative to the endogenous agonist 2-AG (defined as 100% stimulation). Data represents 3 independent experiments ([a] represents 2 experiments) performed with different membrane preparations.

5 Conclusion and Outlook

5.1 Pharmacological test systems for cannabinoid receptors

We established several test systems for cannabinoid receptors using the Sf9 cell/baculovirus transfection system. Sf9 cells offer several advantages to study the function of GPCRs. They are easy to grow and yield high expression levels of GPCRs and G-proteins. Furthermore, Sf9 cells do not express mammalian G-proteins leading to excellent signal-to-noise ratios in experiments.

We investigated the solubility of cannabinoid receptor ligands and show for the first time that a final DMSO assay concentration of 3% (v/v) is necessary for stable solutions. Also, we describe that BSA as a solvent has no advantage over DMSO.

Furthermore, we were interested if different Gα- and RGS-proteins influence GTPase activation. We found that coexpression of cannabinoid receptors with $G\alpha_{i2}$, $G\beta_1\gamma_2$ and RGS4 yielded the most effective system.

We also performed [^{3}H]CP 55,940 competition binding assays to identify new ligands at CBRs. The establishment of GTPγS binding assays and functional GTPase assays allows for the detection of agonists, partial agonists, inverse agonists and antagonists at a very proximal point of the signal cascade of GPCRs.

Further studies should evaluate the effect of other RGS-proteins at $G\alpha_o$-, $G\alpha_{i2}$- or other G-protein subtypes. It would also be of high interest to evaluate the potencies of CBR ligands in mammalian cell lines stably transfected with CBRs.

5.2 Differential coupling of cannabinoid receptors to G-proteins

We were also interested in pharmacological properties of CBRs and decided to focus on the differential coupling of CBRs to $G\alpha_{i2}$-proteins.

The expression levels of CB_1R were approximately two-fold higher than those of CB_2R. This led to higher B_{max} values for the CB_1R in [^{3}H]CP 55,940 competition binding and GTPγS binding assays. GTPγS time course binding studies revealed a much faster activation of the CB_1R after ligand binding. Compared to CB_2R, CB_1R possesses a higher constitutive activity, as assessed in GTPγS saturation binding and in GTPase assays in the presence of NaCl. For the agonist CP 55,940, we also describe for the first time an agonist / inverse agonist switch at CB_1R.

Further studies should investigate other ligands for possible changes in their pharmacological properties, which may depend on assay conditions. Also the coupling of CBRs to $G\alpha_o$-proteins needs to be evaluated in greater detail.

5.3 Alkamides of *E. purpurea*– agonists at CB_2R?

After the establishment of several test systems for CBRs, we reviewed the hypothesis that alkamides from *E. purpurea* are CB_2R agonists.

Although anandamide and 2-AG do possess a very similar structure compared to alkamides, our findings do not support the literature where alkamides have been described as CB_2R ligands. Solubility problems of alkamides due to their amphiphilic structure seem reasonable and micelle formation has been described (Raduner et al., 2007). However, we can rule out insufficient compound solubility, having performed extensive solubility experiments with CBR ligands. Also, the hypothesis that alkamides are high-affinity agonists at CB_2R in the nanomolar range has been reported by only one research group.

We always assessed the functionality of receptor proteins. Furthermore, we analysed the alkamide dodeca-2*E*,4*E*-dienoic acid isobutylamide not only in a competition binding assay, but also in a functional assay at a very proximal point of the signal cascade of GPRCs.

However, the immunomodulatory effects of alkamides and *Echinacea* preparations cannot be explained by activation of cannabinoid receptors. Long-term effects of *Echinacea* preparations may be mediated by different target proteins.

5.4 Ketoalkenes and ketoalkynes of *E. pallida* – the active principle of *Echinacea*?

For the first time, isolated and synthesized compounds as well as a *n*-hexane extract derived from *E. pallida* were analysed for affinity at cannabinoid receptors.
The investigated plant-derived compounds of *E. pallida* are not ligands at cannabinoid receptors. However, we describe new synthesized ligands at CBRs. A compound derived from the endogenous agonists, anandamide and 2-AG, is a full agonist at CB_1R and a superagonist at CB_2R. Also, two more compounds derived from natural ketoalkenynes show partial agonism at CBRs.

Although ketoalkenes and ketoalkynes of *E. pallida* do not show any CBR-affinity, three synthesized compounds derived from ketoalkenynes are ligands at CBRs. Further studies should include structure-activity-relationship investigations to obtain compounds with higher affinities at CBRs.

6 Abstracts and Publications

Prior to submission of this thesis, results were in part published or were presented as posters or short lectures.

Publications:

2008

Nickl K., Gardner E.E., Geiger S., Heilmann J., Seifert R.

"Differential Coupling of the Human Cannabinoid Receptors hCB_1R and hCB_2R to the G-protein $G\alpha_{i2}\beta_1\gamma_2$."

J Neurochem 2008 (in revision)

Poster Presentations and Short Lectures:

2008

Annual Meeting on Frontiers in Medicinal Chemistry

March 2-5, Regensburg/Germany

Nickl K., Gardner E.E., Geiger S., Heilmann J., Seifert R.

"Differential Coupling of Human Cannabinoid Receptors to G-protein $G\alpha_{i2}$."

Poster Contribution

2007

Annual Meeting of the Society for Medicinal Plant Research

September 2-6, Graz/Austria

Nickl K., Schneider E., Seifert R., Heilmann J.

"Establishment of a Sensitive Cannabinoid Receptor Analysis System."

Poster Contribution

3rd Pharmaceutical Sciences World Congress

April 22-25, Amsterdam/Netherlands

Nickl K., Schneider E., Heilmann J., Seifert R.

"Towards a New Cannabinoid Receptor Test System."

Poster Contribution

48. Jahrestagung der Deutschen Gesellschaft für Pharmakologie und Toxikologie

March 13-15, Mainz/Germany

Nickl K., Schneider E., Heilmann J., Seifert R.

“Cannabinoid Receptor Analysis in GTPase and Radioligand-Binding Assays.“

Poster Contribution

2006

Deutsche Pharmazeutische Gesellschaft - Doktorandentagung

September 6-8, Nürnberg-Heroldsberg/Germany

“A Model System for the Analysis of Cannabinoid Receptors and Screening of Natural Ligands.”

Short Lecture

7 References

Addy C, Li S, Agrawal N, Stone J, Majumdar A, Zhong L, Li H, Yuan J, Maes A, Rothenberg P, Cote J, Rosko K, Cummings C, Warrington S, Boyce M, Gottesdiener K, Stoch A and Wagner J (2008) Safety, tolerability, pharmacokinetics, and pharmacodynamic properties of taranabant, a novel selective cannabinoid-1 receptor inverse agonist, for the treatment of obesity: results from a double-blind, placebo-controlled, single oral dose study in healthy volunteers. *J Clin Pharmacol* **48**:418-427.

Addy C, Wright H, Van Laere K, Gantz I, Erondu N, Musser BJ, Lu K, Yuan J, Sanabria-Bohorquez SM, Stoch A, Stevens C, Fong TM, De Lepeleire I, Cilissen C, Cote J, Rosko K, Gendrano IN, 3rd, Nguyen AM, Gumbiner B, Rothenberg P, de Hoon J, Bormans G, Depre M, Eng WS, Ravussin E, Klein S, Blundell J, Herman GA, Burns HD, Hargreaves RJ, Wagner J, Gottesdiener K, Amatruda JM and Heymsfield SB (2008a) The acyclic CB1R inverse agonist taranabant mediates weight loss by increasing energy expenditure and decreasing caloric intake. *Cell Metab* **7**:68-78.

Andersson H, D'Antona AM, Kendall DA, Von Heijne G and Chin CN (2003) Membrane assembly of the cannabinoid receptor 1: impact of a long N-terminal tail. *Mol Pharmacol* **64**:570-577.

Ashton CH (2001) Pharmacology and effects of cannabis: a brief review. *Br J Psychiatry* **178**:101-106.

Baker D, Pryce G, Davies WL and Hiley CR (2006) In silico patent searching reveals a new cannabinoid receptor. *Trends Pharmacol Sci* **27**:1-4.

Bauer R (1999) Chemistry, analysis and immunological investigations of *Echinacea* phytopharmaceuticals, in *Immunomodulatory Agents for Plants* (Wagner H ed), Birkhäuser Verlag, Berlin, Germany.

Bauer R and Wagner H eds (1990) *Echinacea - Handbuch für Ärzte, Apotheker und andere Naturwissenschaftler*. Wissenschaftliche Verlagsgesellschaft mbH, Stuttgart, Germany.

Bensaid M, Gary-Bobo M, Esclangon A, Maffrand JP, Le Fur G, Oury-Donat F and Soubrie P (2003) The cannabinoid CB1 receptor antagonist SR141716

increases Acrp30 mRNA expression in adipose tissue of obese fa/fa rats and in cultured adipocyte cells. *Mol Pharmacol* **63**:908-914.

Berman DM and Gilman AG (1998) Mammalian RGS proteins: barbarians at the gate. *J Biol Chem* **273**:1269-1272.

Berman DM, Wilkie TM and Gilman AG (1996) GAIP and RGS4 are GTPase-activating proteins for the Gi subfamily of G protein alpha subunits. *Cell* **86**:445-452.

Beuscher N, Bodinet C, Willigmann I and Egert D (1995) Immunmodulierende Eigenschaften von Wurzelextrakten verschiedener *Echinacea*-Arten. *Zeitschrift für Phytotherapie* **16**:157-166.

Binns SE, Hudson J, Merali S and Arnason JT (2002) Antiviral activity of characterized extracts from echinacea spp. (Heliantheae: Asteraceae) against herpes simplex virus (HSV-I). *Planta Med* **68**:780-783.

Binns SE, Livesey JF, Arnason JT and Baum BR (2002a) Phytochemical variation in echinacea from roots and flowerheads of wild and cultivated populations. *J Agric Food Chem* **50**:3673-3687.

Breivogel C (2006) Cannabinoid receptor binding to membrane homogenates and cannabinoid-stimulated [^{35}S]GTPgammaS binding to membrane homogenates or intact cultured cells, in *Methods in Molecular Medicine: Marijuana and Cannabinoid Research: Methods and Protocols* (Onaivi ES ed), Humana Press Inc., Totowa, NJ, USA.

Breivogel CS, Selley DE and Childers SR (1998) Cannabinoid receptor agonist efficacy for stimulating [35S]GTPgammaS binding to rat cerebellar membranes correlates with agonist-induced decreases in GDP affinity. *J Biol Chem* **273**:16865-16873.

Centonze D, Finazzi-Agro A, Bernardi G and Maccarrone M (2007) The endocannabinoid system in targeting inflammatory neurodegenerative diseases. *Trends Pharmacol Sci* **28**:180-187.

Chang YH, Lee ST and Lin WW (2001) Effects of cannabinoids on LPS-stimulated inflammatory mediator release from macrophages: involvement of eicosanoids. *J Cell Biochem* **81**:715-723.

Classen B, Csavas M, Borbas A, Dingermann T and Zundorf I (2004) Monoclonal antibodies against an arabinogalactan-protein from pressed juice of Echinacea purpurea. *Planta Med* **70**:861-865.

Cosenza M, Gifford AN, Gatley SJ, Pyatt B, Liu Q, Makriyannis A and Volkow ND (2000) Locomotor activity and occupancy of brain cannabinoid CB1 receptors by the antagonist/inverse agonist AM281. *Synapse* **38**:477-482.

Cota D, Marsicano G, Tschop M, Grubler Y, Flachskamm C, Schubert M, Auer D, Yassouridis A, Thone-Reineke C, Ortmann S, Tomassoni F, Cervino C, Nisoli E, Linthorst AC, Pasquali R, Lutz B, Stalla GK and Pagotto U (2003) The endogenous cannabinoid system affects energy balance via central orexigenic drive and peripheral lipogenesis. *J Clin Invest* **112**:423-431.

De Petrocellis L, Cascio MG and Di Marzo V (2004) The endocannabinoid system: a general view and latest additions. *Br J Pharmacol* **141**:765-774.

De Vries L, Mousli M, Wurmser A and Farquhar MG (1995) GAIP, a protein that specifically interacts with the trimeric G protein G alpha i3, is a member of a protein family with a highly conserved core domain. *Proc Natl Acad Sci U S A* **92**:11916-11920.

Devane WA, Hanus L, Breuer A, Pertwee RG, Stevenson LA, Griffin G, Gibson D, Mandelbaum A, Etinger A and Mechoulam R (1992) Isolation and structure of a brain constituent that binds to the cannabinoid receptor. *Science* **258**:1946-1949.

Di Marzo V, Bifulco M and De Petrocellis L (2004) The endocannabinoid system and its therapeutic exploitation. *Nat Rev Drug Discov* **3**:771-784.

Dickschat JS, Helmke E and Schulz S (2005) Volatile organic compounds from arctic bacteria of the Cytophaga-Flavobacterium-Bacteroides group: a retrobiosynthetic approach in chemotaxonomic investigations. *Chem Biodivers* **2**:318-353.

Felder CC and Glass M (1998) Cannabinoid receptors and their endogenous agonists. *Annu Rev Pharmacol Toxicol* **38**:179-200.

Felder CC, Joyce KE, Briley EM, Mansouri J, Mackie K, Blond O, Lai Y, Ma AL and Mitchell RL (1995) Comparison of the pharmacology and signal transduction of the human cannabinoid CB1 and CB2 receptors. *Mol Pharmacol* **48**:443-450.

Felder CC, Nielsen A, Briley EM, Palkovits M, Priller J, Axelrod J, Nguyen DN, Richardson JM, Riggin RM, Koppel GA, Paul SM and Becker GW (1996) Isolation and measurement of the endogenous cannabinoid receptor agonist,

anandamide, in brain and peripheral tissues of human and rat. *FEBS Lett* **393**:231-235.

Filppula S, Yaddanapudi S, Mercier R, Xu W, Pavlopoulos S and Makriyannis A (2004) Purification and mass spectroscopic analysis of human CB2 cannabinoid receptor expressed in the baculovirus system. *J Pept Res* **64**:225-236.

Fong TM, Guan XM, Marsh DJ, Shen CP, Stribling DS, Rosko KM, Lao J, Yu H, Feng Y, Xiao JC, Van der Ploeg LH, Goulet MT, Hagmann WK, Lin LS, Lanza TJ, Jr., Jewell JP, Liu P, Shah SK, Qi H, Tong X, Wang J, Xu SS, Francis B, Strack AM, MacIntyre DE and Shearman LP (2007) Antiobesity efficacy of a novel cannabinoid-1 receptor inverse agonist, N-[(1S,2S)-3-(4-chlorophenyl)-2-(3-cyanophenyl)-1-methylpropyl]-2-methyl-2 -[[5-(trifluoromethyl)pyridin-2-yl]oxy]propanamide (MK-0364), in rodents. *J Pharmacol Exp Ther* **321**:1013-1022.

Galandrin S and Bouvier M (2006) Distinct signaling profiles of beta1 and beta2 adrenergic receptor ligands toward adenylyl cyclase and mitogen-activated protein kinase reveals the pluridimensionality of efficacy. *Mol Pharmacol* **70**:1575-1584.

Gertsch J, Schoop R, Kuenzle U and Suter A (2004) Echinacea alkylamides modulate TNF-alpha gene expression via cannabinoid receptor CB2 and multiple signal transduction pathways. *FEBS Lett* **577**:563-569.

Goel V, Chang C, Slama J, Barton R, Bauer R, Gahler R and Basu T (2002a) Echinacea stimulates macrophage function in the lung and spleen of normal rats. *J Nutr Biochem* **13**:487.

Goel V, Chang C, Slama JV, Barton R, Bauer R, Gahler R and Basu TK (2002) Alkylamides of Echinacea purpurea stimulate alveolar macrophage function in normal rats. *Int Immunopharmacol* **2**:381-387.

Goel V, Lovlin R, Barton R, Lyon MR, Bauer R, Lee TD and Basu TK (2004) Efficacy of a standardized echinacea preparation (Echinilin) for the treatment of the common cold: a randomized, double-blind, placebo-controlled trial. *J Clin Pharm Ther* **29**:75-83.

Gong JP, Onaivi ES, Ishiguro H, Liu QR, Tagliaferro PA, Brusco A and Uhl GR (2006) Cannabinoid CB2 receptors: immunohistochemical localization in rat brain. *Brain Res* **1071**:10-23.

Griffin G, Atkinson PJ, Showalter VM, Martin BR and Abood ME (1998) Evaluation of cannabinoid receptor agonists and antagonists using the guanosine-5'-O-(3-[35S]thio)-triphosphate binding assay in rat cerebellar membranes. *J Pharmacol Exp Ther* **285**:553-560.

Harrison C and Traynor JR (2003) The [^{35}S]GTPgammaS binding assay: approaches and applications in pharmacology. *Life Sci* **74**:489-508.

Heilmann J, Calis I, Kirmizibekmez H, Schuhly W, Harput S and Sticher O (2000) Radical scavenger activity of phenylethanoid glycosides in FMLP stimulated human polymorphonuclear leukocytes: structure-activity relationships. *Planta Med* **66**:746-748.

Hostettmann K (2003) [History of a plant: the example of Echinacea]. *Forsch Komplementarmed Klass Naturheilkd* **10 Suppl 1**:9-12.

Howlett AC (2005) Cannabinoid receptor signaling, in *Handb Exp Pharmacol* (Pertwee RG ed) pp 53-79, Springer-Verlag, Berlin.

Howlett AC, Barth F, Bonner TI, Cabral G, Casellas P, Devane WA, Felder CC, Herkenham M, Mackie K, Martin BR, Mechoulam R and Pertwee RG (2002) International Union of Pharmacology. XXVII. Classification of cannabinoid receptors. *Pharmacol Rev* **54**:161-202.

Ibrahim MM, Deng H, Zvonok A, Cockayne DA, Kwan J, Mata HP, Vanderah TW, Lai J, Porreca F, Makriyannis A and Malan TP, Jr. (2003) Activation of CB2 cannabinoid receptors by AM1241 inhibits experimental neuropathic pain: pain inhibition by receptors not present in the CNS. *Proc Natl Acad Sci U S A* **100**:10529-10533.

Jhaveri MD, Richardson D and Chapman V (2007) Endocannabinoid metabolism and uptake: novel targets for neuropathic and inflammatory pain. *Br J Pharmacol* **152**:624-632.

Johns DG, Behm DJ, Walker DJ, Ao Z, Shapland EM, Daniels DA, Riddick M, Dowell S, Staton PC, Green P, Shabon U, Bao W, Aiyar N, Yue TL, Brown AJ, Morrison AD and Douglas SA (2007) The novel endocannabinoid receptor GPR55 is activated by atypical cannabinoids but does not mediate their vasodilator effects. *Br J Pharmacol* **152**:825-831.

Justinova Z, Goldberg SR, Heishman SJ and Tanda G (2005) Self-administration of cannabinoids by experimental animals and human marijuana smokers. *Pharmacol Biochem Behav* **81**:285-299.

Klein TW, Newton C, Larsen K, Lu L, Perkins I, Nong L and Friedman H (2003) The cannabinoid system and immune modulation. *J Leukoc Biol* **74**:486-496.

Leff P (1995) The two-state model of receptor activation. *Trends Pharmacol Sci* **16**:89-97.

Lever IJ and Rice AS (2007) Cannabinoids and pain, in *Handb Exp Pharmacol* pp 265-306, Springer-Verlag, Berlin.

Mackie K, Lai Y, Westenbroek R and Mitchell R (1995) Cannabinoids activate an inwardly rectifying potassium conductance and inhibit Q-type calcium currents in AtT20 cells transfected with rat brain cannabinoid receptor. *J Neurosci* **15**:6552-6561.

MacLennan SJ, Reynen PH, Kwan J and Bonhaus DW (1998) Evidence for inverse agonism of SR141716A at human recombinant cannabinoid CB1 and CB2 receptors. *Br J Pharmacol* **124**:619-622.

Malan TP, Jr., Ibrahim MM, Lai J, Vanderah TW, Makriyannis A and Porreca F (2003) CB2 cannabinoid receptor agonists: pain relief without psychoactive effects? *Curr Opin Pharmacol* **3**:62-67.

Maldonado R (2002) Study of cannabinoid dependence in animals. *Pharmacol Ther* **95**:153-164.

Marsicano G, Goodenough S, Monory K, Hermann H, Eder M, Cannich A, Azad SC, Cascio MG, Gutierrez SO, van der Stelt M, Lopez-Rodriguez ML, Casanova E, Schutz G, Zieglgansberger W, Di Marzo V, Behl C and Lutz B (2003) CB1 cannabinoid receptors and on-demand defense against excitotoxicity. *Science* **302**:84-88.

Matsuda LA, Lolait SJ, Brownstein MJ, Young AC and Bonner TI (1990) Structure of a cannabinoid receptor and functional expression of the cloned cDNA. *Nature* **346**:561-564.

McPartland JM and Glass M (2003) Functional mapping of cannabinoid receptor homologs in mammals, other vertebrates, and invertebrates. *Gene* **312**:297-303.

Mechoulam R, Ben-Shabat S, Hanus L, Ligumsky M, Kaminski NE, Schatz AR, Gopher A, Almog S, Martin BR, Compton DR and et al. (1995) Identification of an endogenous 2-monoglyceride, present in canine gut, that binds to cannabinoid receptors. *Biochem Pharmacol* **50**:83-90.

Mechoulam R and Gaoni Y (1965) A Total Synthesis Of Dl-Delta-1-Tetrahydrocannabinol, The Active Constituent Of Hashish. *J Am Chem Soc* **87**:3273-3275.

Melchart D, Linde K, Worku F, Sarkady L, Holzmann M, Jurcic K and Wagner H (1995) Results of five randomized studies on the immunomodulatory activity of preparations of Echinacea. *J Altern Complement Med* **1**:145-160.

Melchart D, Walther E, Linde K, Brandmaier R and Lersch C (1998) Echinacea root extracts for the prevention of upper respiratory tract infections: a double-blind, placebo-controlled randomized trial. *Arch Fam Med* **7**:541-545.

Meschler JP, Kraichely DM, Wilken GH and Howlett AC (2000) Inverse agonist properties of N-(piperidin-1-yl)-5-(4-chlorophenyl)-1-(2, 4-dichlorophenyl)-4-methyl-1H-pyrazole-3-carboxamide HCl (SR141716A) and 1-(2-chlorophenyl)-4-cyano-5-(4-methoxyphenyl)-1H-pyrazole-3-carboxyl ic acid phenylamide (CP-272871) for the CB(1) cannabinoid receptor. *Biochem Pharmacol* **60**:1315-1323.

Mestre L, Correa F, Docagne F, Clemente D and Guaza C (2006) The synthetic cannabinoid WIN 55,212-2 increases COX-2 expression and PGE2 release in murine brain-derived endothelial cells following Theiler's virus infection. *Biochem Pharmacol* **72**:869-880.

Müller-Jakic B, Breu W, Pröbstle A, Redl K, Greger H and Bauer R (1994) In vitro inhibition of cyclooxygenase and 5`-lipoxygenase by alkamides from *Echinacea* and *Achillea* species. *Planta Med* **60**:37-40.

Munro S, Thomas KL and Abu-Shaar M (1993) Molecular characterization of a peripheral receptor for cannabinoids. *Nature* **365**:61-65.

Nambi P and Aiyar N (2003) G protein-coupled receptors in drug discovery. *Assay Drug Dev Technol* **1**:305-310.

Osowski S, Rostock M, Bartsch HH and Massing U (2000) [Pharmaceutical comparability of different therapeutic Echinacea preperations]. *Forsch Komplementarmed Klass Naturheilkd* **7**:294-300.

Pagotto U, Marsicano G, Cota D, Lutz B and Pasquali R (2006) The emerging role of the endocannabinoid system in endocrine regulation and energy balance. *Endocr Rev* **27**:73-100.

Panikashvili D, Simeonidou C, Ben-Shabat S, Hanus L, Breuer A, Mechoulam R and Shohami E (2001) An endogenous cannabinoid (2-AG) is neuroprotective after brain injury. *Nature* **413**:527-531.

Pertwee RG (1997) Pharmacology of cannabinoid CB1 and CB2 receptors. *Pharmacol Ther* **74**:129-180.

Pertwee RG (2008) The diverse CB1 and CB2 receptor pharmacology of three plant cannabinoids: delta9-tetrahydrocannabinol, cannabidiol and delta9-tetrahydrocannabivarin. *Br J Pharmacol* **153**:199-215.

Preuss H, Ghorai P, Kraus A, Dove S, Buschauer A and Seifert R (2007) Constitutive activity and ligand selectivity of human, guinea pig, rat, and canine histamine H2 receptors. *J Pharmacol Exp Ther* **321**:983-995.

Raduner S, Bisson W, Abagyan R, Altmann KH and Gertsch J (2007) Self-assembling cannabinomimetics: supramolecular structures of N-alkyl amides. *J Nat Prod* **70**:1010-1015.

Raduner S, Majewska A, Chen JZ, Xie XQ, Hamon J, Faller B, Altmann KH and Gertsch J (2006) Alkylamides from Echinacea are a new class of cannabinomimetics. Cannabinoid type 2 receptor-dependent and -independent immunomodulatory effects. *J Biol Chem* **281**:14192-14206.

Rinaldi-Carmona M, Barth F, Heaulme M, Shire D, Calandra B, Congy C, Martinez S, Maruani J, Neliat G, Caput D and et al. (1994) SR141716A, a potent and selective antagonist of the brain cannabinoid receptor. *FEBS Lett* **350**:240-244.

Ross RA, Brockie HC, Stevenson LA, Murphy VL, Templeton F, Makriyannis A and Pertwee RG (1999) Agonist-inverse agonist characterization at CB1 and CB2 cannabinoid receptors of L759633, L759656, and AM630. *Br J Pharmacol* **126**:665-672.

Ryberg E, Larsson N, Sjogren S, Hjorth S, Hermansson NO, Leonova J, Elebring T, Nilsson K, Drmota T and Greasley PJ (2007) The orphan receptor GPR55 is a novel cannabinoid receptor. *Br J Pharmacol* **152**:1092-1101.

Schwarz E, Parlesak A, Henneicke-von Zepelin HH, Bode JC and Bode C (2005) Effect of oral administration of freshly pressed juice of Echinacea purpurea on the number of various subpopulations of B- and T-lymphocytes in healthy volunteers: results of a double-blind, placebo-controlled cross-over study. *Phytomedicine* **12**:625-631.

Seifert R, Gether U, Wenzel-Seifert K and Kobilka BK (1999) Effects of guanine, inosine, and xanthine nucleotides on beta(2)-adrenergic receptor/G(s) interactions: evidence for multiple receptor conformations. *Mol Pharmacol* **56**:348-358.

Seifert R, Lee TW, Lam VT and Kobilka BK (1998) Reconstitution of beta2-adrenoceptor-GTP-binding-protein interaction in Sf9 cells--high coupling efficiency in a beta2-adrenoceptor-G(s alpha) fusion protein. *Eur J Biochem* **255**:369-382.

Seifert R and Wenzel-Seifert K (2001) Unmasking different constitutive activity of four chemoattractant receptors using Na+ as universal stabilizer of the inactive (R) state. *Receptors Channels* **7**:357-369.

Seifert R and Wenzel-Seifert K (2002) Constitutive activity of G-protein-coupled receptors: cause of disease and common property of wild-type receptors. *Naunyn Schmiedebergs Arch Pharmacol* **366**:381-416.

Seifert R and Wenzel-Seifert K (2003) The human formyl peptide receptor as model system for constitutively active G-protein-coupled receptors. *Life Sci* **73**:2263-2280.

Shah SA, Sander S, White CM, Rinaldi M and Coleman CI (2007) Evaluation of echinacea for the prevention and treatment of the common cold: a meta-analysis. *Lancet Infect Dis* **7**:473-480.

Shearman LP, Rosko KM, Fleischer R, Wang J, Xu S, Tong XS and Rocha BA (2003) Antidepressant-like and anorectic effects of the cannabinoid CB1 receptor inverse agonist AM251 in mice. *Behav Pharmacol* **14**:573-582.

Smart D, Gunthorpe MJ, Jerman JC, Nasir S, Gray J, Muir AI, Chambers JK, Randall AD and Davis JB (2000) The endogenous lipid anandamide is a full agonist at the human vanilloid receptor (hVR1). *Br J Pharmacol* **129**:227-230.

Song ZH, Slowey CA, Hurst DP and Reggio PH (1999) The difference between the CB(1) and CB(2) cannabinoid receptors at position 5.46 is crucial for the selectivity of WIN55212-2 for CB(2). *Mol Pharmacol* **56**:834-840.

Srinivasa SP, Watson N, Overton MC and Blumer KJ (1998) Mechanism of RGS4, a GTPase-activating protein for G protein alpha subunits. *J Biol Chem* **273**:1529-1533.

Sugiura T, Kishimoto S, Oka S and Gokoh M (2006) Biochemistry, pharmacology and physiology of 2-arachidonoylglycerol, an endogenous cannabinoid receptor ligand. *Prog Lipid Res* **45**:405-446.

Sugiura T, Kondo S, Sukagawa A, Nakane S, Shinoda A, Itoh K, Yamashita A and Waku K (1995) 2-Arachidonoylglycerol: a possible endogenous cannabinoid receptor ligand in brain. *Biochem Biophys Res Commun* **215**:89-97.

Sutkowski EM and Catterall WA (1990) Beta 1 subunits of sodium channels. Studies with subunit-specific antibodies. *J Biol Chem* **265**:12393-12399.

Traynor JR and Neubig RR (2005) Regulators of G protein signaling & drugs of abuse. *Mol Interv* **5**:30-41.

Twitchell W, Brown S and Mackie K (1997) Cannabinoids inhibit N- and P/Q-type calcium channels in cultured rat hippocampal neurons. *J Neurophysiol* **78**:43-50.

Van Sickle MD, Duncan M, Kingsley PJ, Mouihate A, Urbani P, Mackie K, Stella N, Makriyannis A, Piomelli D, Davison JS, Marnett LJ, Di Marzo V, Pittman QJ, Patel KD and Sharkey KA (2005) Identification and functional characterization of brainstem cannabinoid CB2 receptors. *Science* **310**:329-332.

Wagner H, Proksch A, Riess-Maurer I, Vollmar A, Odenthal S, Stuppner H, Jurcic K, Le Turdu M and Fang JN (1985) [Immunostimulating action of polysaccharides (heteroglycans) from higher plants]. *Arzneimittelforschung* **35**:1069-1075.

Wenzel-Seifert K, Arthur JM, Liu HY and Seifert R (1999) Quantitative analysis of formyl peptide receptor coupling to g(i)alpha(1), g(i)alpha(2), and g(i)alpha(3). *J Biol Chem* **274**:33259-33266.

Wenzel-Seifert K and Seifert R (2000) Molecular analysis of beta(2)-adrenoceptor coupling to G(s)-, G(i)-, and G(q)-proteins. *Mol Pharmacol* **58**:954-966.

Wenzel-Seifert K and Seifert R (2003) Critical role of N-terminal N-glycosylation for proper folding of the human formyl peptide receptor. *Biochem Biophys Res Commun* **301**:693-698.

Woelkart K, Xu W, Pei Y, Makriyannis A, Picone RP and Bauer R (2005) The endocannabinoid system as a target for alkamides from Echinacea angustifolia roots. *Planta Med* **71**:701-705.

Xiong Q, Kadota S, Tani T and Namba T (1996) Antioxidative effects of phenylethanoids from Cistanche deserticola. *Biol Pharm Bull* **19**:1580-1585.

Xiong Q, Tezuka Y, Kaneko T, Li H, Tran LQ, Hase K, Namba T and Kadota S (2000) Inhibition of nitric oxide by phenylethanoids in activated macrophages. *Eur J Pharmacol* **400**:137-144.

Xu W, Filppula SA, Mercier R, Yaddanapudi S, Pavlopoulos S, Cai J, Pierce WM and Makriyannis A (2005) Purification and mass spectroscopic analysis of human CB1 cannabinoid receptor functionally expressed using the baculovirus system. *J Pept Res* **66**:138-150.

Zygmunt PM, Petersson J, Andersson DA, Chuang H, Sorgard M, Di Marzo V, Julius D and Hogestatt ED (1999) Vanilloid receptors on sensory nerves mediate the vasodilator action of anandamide. *Nature* **400**:452-457.

Lebenslauf

Persönliche Daten

Name:	Kathrin Nickl
Geburtsdatum:	01. März 1979
Geburtsort:	Bayreuth

Beruflicher Werdegang

01/2005 – heute	Universität Regensburg, Institut für Pharmazie, Doktorandin
09 – 10/2004	University of Canterbury, Christchurch, Neuseeland, Forschungsaufenthalt
06/2004	3. Abschnitt der pharmazeutischen Prüfung
11/2003 – 04/2004	Heumann Pharma, Nürnberg
05/2003 – 10/2003	Dom-Apotheke, Regensburg

Universitärer Werdegang

04/2003	Abschluss: 2. Abschnitt der pharmazeutischen Prüfung
11/1998 – 04/2003	Universität Regensburg, Studium der Pharmazie
10/2001 – 02/2002	ETH Zürich, Lehrstuhl Angewandte Biowissenschaften – Pharmazeutische Technologie, Auslandssemester

Schulischer Werdegang

1989 – 1998	Luisenburg-Gymnasium in Wunsiedel
1985 – 1989	Grundschule Fichtelberg-Mehlmeisel

Eidesstattliche Erklärung

Ich erkläre hiermit an Eides statt, dass ich die vorliegende Arbeit ohne unzulässige Hilfe Dritter und ohne Benutzung anderer als der angegebenen Hilfsmittel angefertigt habe; die aus anderen Quellen direkt oder indirekt übernommenen Daten und Konzepte sind unter Angabe des Literaturzitats gekennzeichnet.

Weitere Personen waren an der inhaltlich-materiellen Herstellung der vorliegenden Arbeit nicht beteiligt. Insbesondere habe ich hierfür nicht die entgeltliche Hilfe eines Promotionsberaters oder anderer Personen in Anspruch genommen. Niemand hat von mir weder unmittelbar noch mittelbar geldwerte Leistungen für Arbeiten erhalten, die im Zusammenhang mit dem Inhalt der vorgelegten Dissertation stehen.

Die Arbeit wurde bisher weder im In- noch im Ausland in gleicher oder ähnlicher Form einer anderen Prüfungsbehörde vorgelegt.

Regensburg, den _____ _____

Kathrin Nickl